SAPIENZA
UNIVERSITÀ DI ROMA

MOLECULAR MECHANISM OF THE Ca^{2+}-DEPENDENT ACTIVATION OF SORCIN (SOLUBLE RESISTANCE-RELATED CALCIUM BINDING PROTEIN). A STUDY WITH SITE-SPECIFIC MUTANTS.

DOTTORATO DI RICERCA IN BIOCHIMICA (XVIII Ciclo)

DOTTORANDA
MANUELA MELLA

DOCENTE GUIDA
Prof.ssa EMILIA CHIANCONE

COORDINATORE
Prof. PAOLO SARTI

ABSTRACT

Sorcin is a two-domain protein belonging to the penta-EF-hand family that traslocates reversibly from cytosol to membranes through a Ca^{2+}-dependent interaction with protein targets. Although EF1, EF2, EF3 are potentially able to bind calcium at micromolar concentrations, binding of two Ca^{2+}/monomer activates sorcin and triggers translocation. To identify the functional pair, the conserved bidentate –Z glutamate in these EF-hands was mutated to yield E53Q-, E94A-, E124A-sorcin, respectively. The behavior of the three site-specific sorcin mutants shows that the EF3 hand is the site endowed with the highest affinity for calcium and that EF2 and EF3 that are not paired structurally are the functional EF-hand pair. Information of Ca^{2+} binding to EF3 was proposed to be transferred to the rest of the molecule by means of the long and rigid D-helix that is shared by EF2 and EF3. To establish whether this helix is instrumental in sorcin activation, two D-helix residues were mutated into glycine: W105 involved in the network of interaction around the helix itself, and W99, which faces solvent. The substitution of W105 almost abolishes the capacity of sorcin to interact with its molecular targets while mutation of W99 has little effect. Disruption of the interaction network around the D-helix, therefore, inhibits information transfer from the EF3 hand demonstrating the central role of the D-helix in the Ca^{2+}-dependent activation of sorcin.

INDEX

1. INTRODUCTION

1.1 CALCIUM AS A MESSENGER

Cellular signalling mechanisms are designed to transmit information from the cell surface to specific targets within the cell by means of intracellular messenger among these the calcium ion has a major role. Ca^{2+} operates in all cell types - from bacteria to specialized neurons - and is responsible for controlling numerous cellular processes, such as fertilization, proliferation, development, learning and memory. This simple ion can control all these processes due to the enormous versatility of Ca^{2+} signals. For example, Ca^{2+} can operate within small cellular compartments, it can act globally in the cytoplasm, or penetrate specific organelles, such as mitochondria and the nucleus. Moreover, Ca^{2+} signals can have variable durations ranging from microseconds to hours.

Unlike many other second-messenger molecules, prolonged high intracellular Ca^{2+} levels lead to cell death: calcium can not be metabolized and, in order to prevent its cytotoxic effects, the cells need to regulate its homeostasis very tightly.

Ca^{2+} concentration is maintained at ~ 100 nM in a cell at rest, but is significantly higher (~ 1000 nM) in the extracellular compartement and in the lumen of the endoplasmic reticulum. The existence of such a marked electrochemical gradient allows a cell to increase rapidly the cytoplasmatic calcium concentration in response to a variety of external stimuli. Ca^{2+} may enter the cell across the plasma membrane or can be released into the cytoplasm from the endoplasmic reticulum. In both instances Ca^{2+} entry takes place through finely regulated calcium channels.

To control the possible cytotoxic effect of Ca^{2+}, two groups of intracellular calcium binding proteins have evolved: buffer and sensor proteins (Heizmann and Hunzinker, 1991). Buffer proteins, such as calsequestrin, bind calcium when its concentration within a cell or organelle increases over the submicromolar level. These molecules are essential to the homeostasis of the cation, as they contribute to reducing its ionic concentration to non cytotoxic levels (Carafoli, 2005).

Sensor proteins, enable the cell to detect any change in Ca^{2+} concentration which is then transformed into a variety of cellular processes that often require a rapid response (from Silva and Williams, 1991). At a molecular level, sensor proteins, such as calmodulin, when activated upon Ca^{2+} binding, amplify the initial signal in the cytoplasm and thereby

modulate a great variety of molecular targets (e. g. enzymes and ion channels).

The different function of sensor and buffer proteins is reflected in the equilibrium and kinetic features of the Ca^{2+} binding reaction. Buffer proteins are characterized by higher calcium affinity constants than sensor proteins, which in turn, have higher kinetic association rate constant. Thus, in the presence of a rapid increase of cytoplasmic Ca^{2+} concentration, sensor proteins will interact with the cation and activate the appropriate molecular target.

From a structural view point sensor proteins are of importance as they revealed the existence of the Ca^{2+} binding motif named EF-hand.

1.2 EF-HAND Ca^{2+}-BINDING PROTEINS

The EF-hand structural motif was first discovered in the crystal structure of parvalbumin, a protein involved in the relaxation process of muscle cells (Kretsinger et al., 1973), but turned out to be very widespread (Ikura et al., 1996). It consists of two perpendicularly oriented α-helices (helices E and F in parvalbumin) and an interhelical loop involved directly in calcium binding. The helices are disposed as the index finger and the thumb of the right hand (Fig. 1).

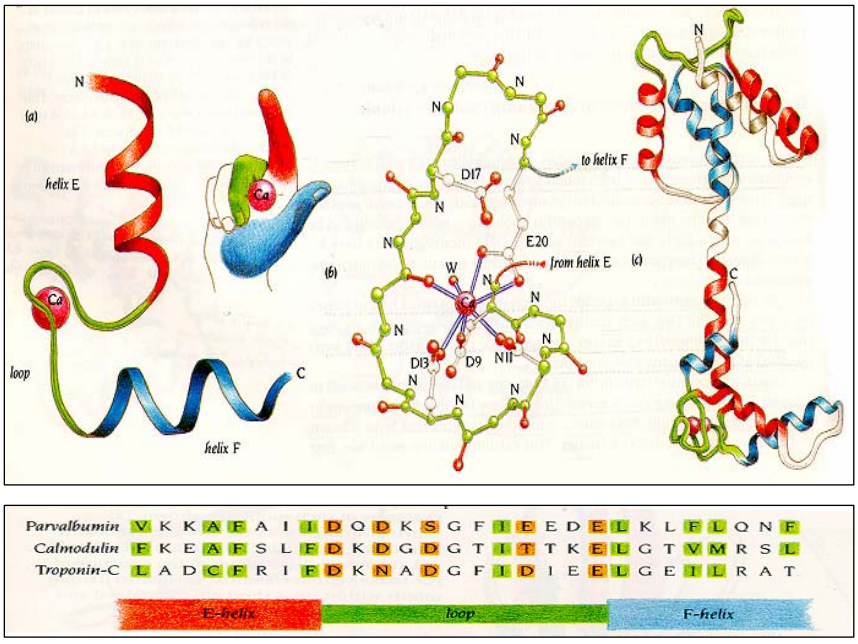

Fig. 1 – Calmodulin EF-hand site. (a) Site structure; (b) Ca^{2+} coordination complex; (c) Calmodulin structure; (d) Canonical sequence of a canonical EF-hand site: the brown residue are the amino-acids that bind calcium, the green residues belong to the hydrophobic core.

The canonical EF-hand motif is composed by 29 residues: the first ten are organized in the E helix, the twelve following ones constitute the Ca^{2+} binding loop and the last form the F helix. In the loop, calcium is bound by seven ligands at the vertices of a pentagonal bipyramid (Kawasaki and Kretsinger, 1994) (Fig. 2).

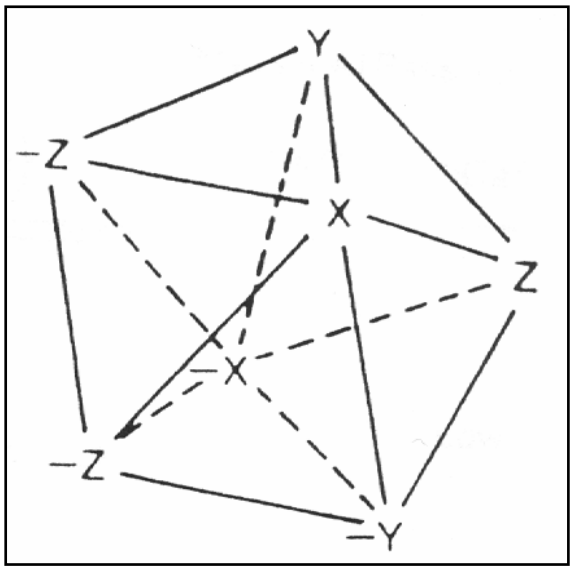

Fig. 2 – EF-hand site: Calcium is bound by seven ligands at the vertices of a pentagonal bipyramid.

The residues involved in metal coordination in particular are: 1(X), 3 (Y), 5 (Z), 7 (-Y), 9 (-X) and 12 (-Z). The five equatorial Ca^{2+} ligands lie close to a plane that includes the calcium ion and are contributed by the side chains of two acidic residues (position Y and –Z), the latter providing two ligands, one polar group (Ser/Thr, position Z), and one main chain carbonyl oxygen (position –Y). The two apical ligands are furnished by the side chain of an acidic group (position X) and by a water molecule (position –X). In position –Z the bidentate interaction with the metal is established by a glutamate residue, which is favoured with respect to aspartate because the longer side chain allows the carboxylic group to be positioned optimally for calcium coordination. The residues in position 2, 5, 6, 9, 17, 22, 25, 26 and 29 are hydrophobic and interact with analogous amino acids of another EF-hand motif, forming a hydrophobic protein core (see below).

The canonical sequence of the EF-hand motif has been detected in small proteins (e.g. calmodulin or S100) and within domains of much larger,

complex proteins (e.g. myosin or calpain) (Fig. 3). EF-hand motifs have been identified also in proteins in which they were not expected, such as cholinesterases (Tsigelny et al., 2000).

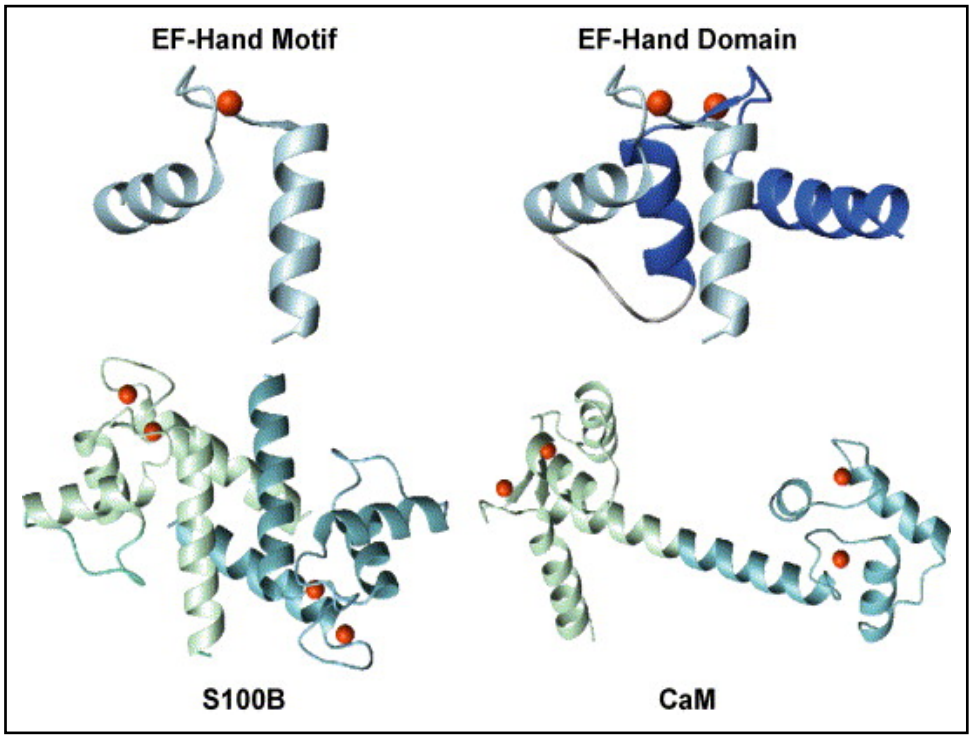

Fig. 3 – Basic structural features of the EF-hand Ca2+-binding proteins.

The basic structural-functional unit is formed by EF-hand pairs, rather than by single sites in most known cases. The EF-hand motifs are matched structurally and functionally; their pairing stabilizes the protein conformation and results in cooperativity in Ca^{2+} -binding. Tipically, a pair of EF-hand motifs forms a globular domain, such that a protein containing four EF-hands is organized in two Ca^{2+} binding domains that can be either structurally independent, e.g. calmodulin (Kretsinger, 1986), and troponin C (Herzberg, 1988), or be well packed together, as in recoverin (Flaherty, 1993).

The Ca^{2+} affinities of EF-hand proteins vary greatly ($K_d = 10^{-4} – 10^{-9}$ M) and are amino acid sequence-dependent, especially with regard to the 12-residue consensus loop that provides all the Ca^{2+} ligating amino acids (Ikura et al. 1996). Ca^{2+} affinity is influenced also by the length of the loop since this can alter the geometry of metal coordination (Linse and Forsén, 1995).

Ca^{2+} binding proteins involved in calcium signalling undergo Ca^{2+} dependent structural rearrangements that modulate directly their functionality. A number of structural studies on different EF-hand domains have revealed substantial differences in the extent of the Ca^{2+}-induced conformational changes (Fig. 4).

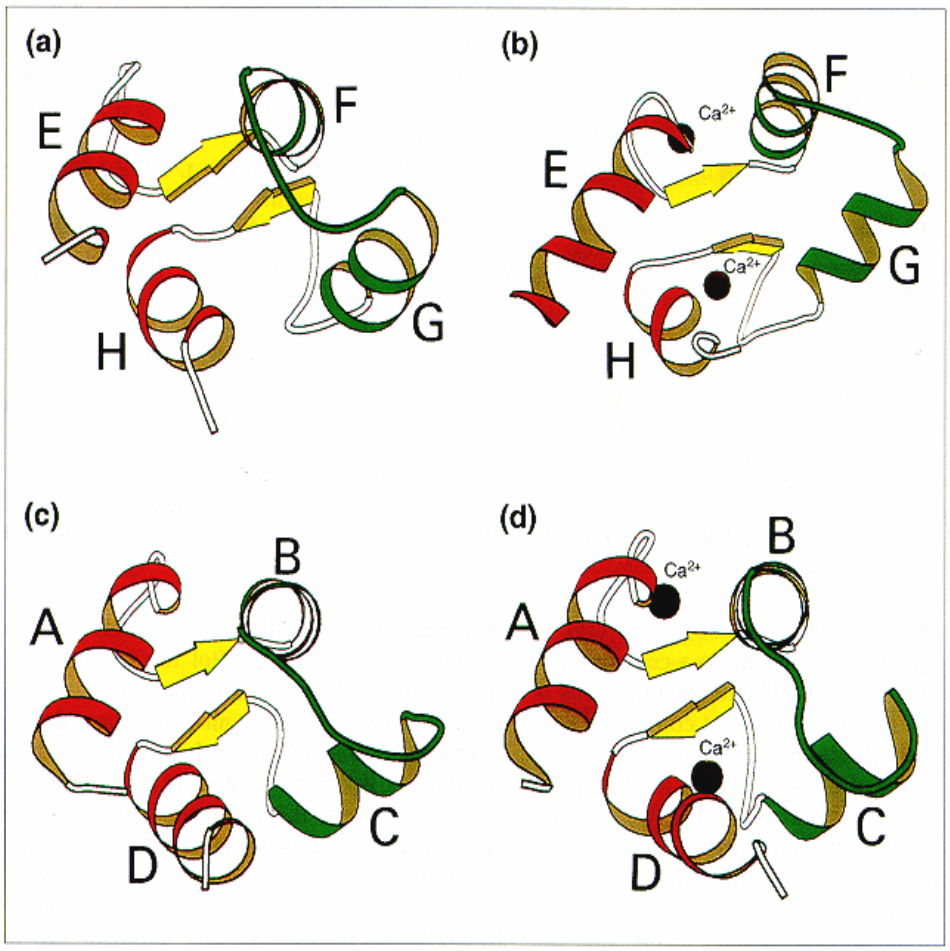

Fig. 4 – Conformational changes induced by Ca^{2+} -binding to a pair of EF-hands. The two α-helices are displayed in red and in green. The C-terminal domain of calmodulin **(a)** in the "closed" Ca^{2+} -free state and **(b)** in the "open" Ca^{2+} -bound state. Calbindin D_{9k} **(c)** in the "closed" Ca^{2+} -free state and **(d)** in the "closed" Ca^{2+} -bound state (from Ikura, 1996).

Thus in calmodulin both the carboxy- and the amino-terminal domains of the protein undergo significant structural rearrangements from a "closed" conformation, pertaining to the apoprotein, where the two helices of each EF hands are almost anti-parallel to an "open" conformation, characteristic of the Ca^{2+}-bound form, where the two helices are almost perpendicular (Zhang et al., 1995; Finn et al., 1995). By contrast, the buffer protein calbindin D_{9K} retains the calcium free "closed" conformation even after binding of Ca^{2+} (Finn et al., 1995).

The different extent of structural rearrangements can be compared quantitatively by analyzing the changes in interhelical angle of various EF-hand proteins upon Ca^{2+}-binding (Table 1). The analysis brings out that domains undergoing large conformational changes are typical of sensor proteins. In buffer proteins, where small conformational changes suffice to ensure protein structural and functional stability, extended conformational changes are not observed (Nelson and Chazin,1998).

	Interhelical angle change (°)			
	A/B	C/D	E/F	G/H
Calmodulin	34	34	39	36
Troponin C	40	56		
Recoverin	61	7	16	1
Calbindin D9k	12	1		

Table 1 – Interhelical angle changes of various EF-hand proteins upon Ca^{2+} binding.

The large Ca^{2+}-induced structural changes that take place in sensor proteins enable them to respond to the specific Ca^{2+}-transmitted stimulus by interacting with specific molecular targets. This interaction can take place in a variety of manners.

In calmodulin, for example, the significant conformational change of the two EF-hand domains and of the central helical linker leads

to the exposure of a large, sticky, hydrophobic surface ideally suited for target interaction (Fig. 5).

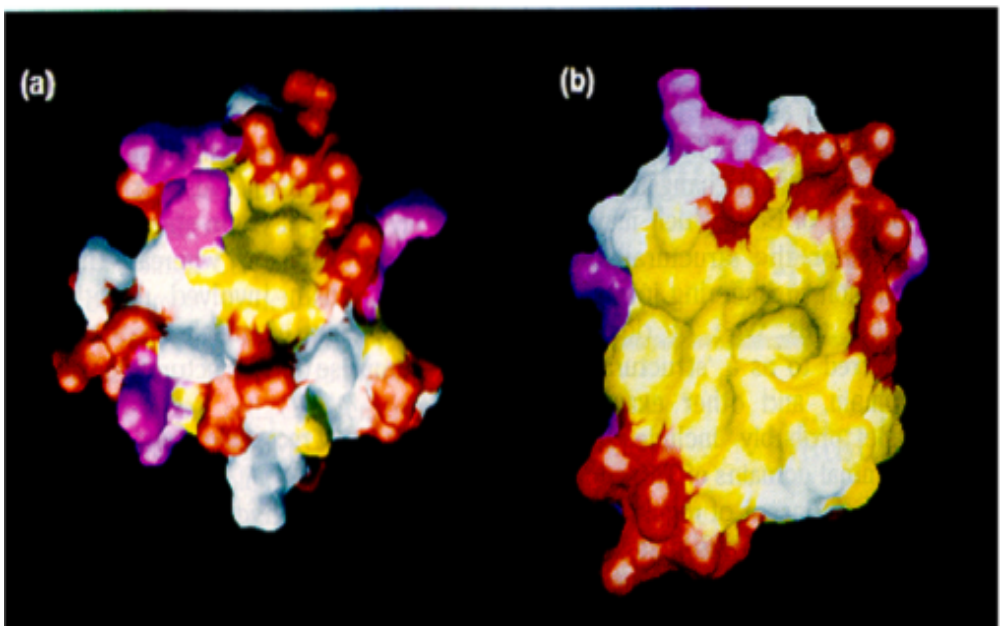

Fig. 5 – The molecular surface of the C-terminal domain of calmodulin, (a) in the Ca2+-free state and (b) in the Ca2+-bound state. Hydrophobic residues are shown in yellow, acidic residues in red, and basic residues in purple (from Ikura, 1996).

1.3 PENTA-EF-HAND PROTEIN FAMILY

As mentioned above, the EF-hand motifs in the various proteins are usually repeated tandemly, with a number of repeats ranging from two to eight. The presence of uneven EF-hand motifs in a Ca^{2+}-binding protein was not recognized until the X-ray crystallographic analyses of the Ca^{2+}-binding domains in calpain small subunits revealed an unsuspected EF hand motif named EF1 in addition to four canonical ones (Blanchard et al. 1997; Lin et al 1997). The novel motif has an 11 aminoacid residues long loop sequence and an alanine residue in place of the canonical aspartic acid in the calcium-coordination position designated X.

This finding prompted a re-evaluation of the primary structures of multiple-EF-hand proteins in the literature and in DNA databases and led to the identification by Maki et al. 1997 of a new protein family, named “penta-EF-hand” (PEF) which comprises calpains light and heavy chains (Blanchard et al., 1997; Lin et al. 1997) sorcin (Meyers et al., 1995a; Zamparelli et al.,1997), grancalcin, ALG-2, peflin (Kitaura et al. 1999) and the hypothetical yeast protein YG25 (Fig. 6).

```
                          x y z-y -x -z
                          | | | |  |  |
EF-1                      |  Loop  |  |
                 _Helix A__| | | |  |__Helix B__
Sorcin           DPLYGYFASVAG-QDGQI DADELQRCLTQS---GIAGGYK  33- 68
Grancalcin       DSVYTYFSAVAG-QDGEV DAEELQRCLTQS---GINGTYS  52- 87
CDVI             RQFRRLFAQLAG-DDMEV SATELMNILNKVVTRHPDLKTD  97-135
CDIV             ENFKALFRQLAG-EDMEI SVRELRTILNRIISKHKDLRTK 545-583
ALG-2            SFLWNVFQRVDKDRSGVI SDTELQQALSNG-------TWT  26- 58
Peflin           PEAYSWFQSVDSDHSGYI SMKELKQALVN-------CNWS  66- 98

EF-2
                   __Helix C__           __Helix D__
Sorcin       PFNLETCRLMVSMLDRDMSGTM GFNEFKELWAVL           69-102
Grancalcin   PFSLETCRIMIAMLDRDHTGKM GFNAFKELWAAL           88-121
CDVI         GFGIDTCRSMVAVMDSDTTGKL GFEEFKYLWNNI          136-169
CDIV         GFSLESCRSMVNLMDRDGNGKL GLVEFNILWNRI          584-617
ALG-2        PFNPVTVRSIISMFDRENKAGV NFSEFTGVWKYI           59- 92
Peflin       SFNDETCLMMINMFDKTKSGRI DVYGFSALWKFI           99-132

EF-3
                 _Helix D__            __Helix E_
Sorcin           NGWRQHFISFDSDRSGTV DPQELQKALTTMGFRLN      103-137
Grancalcin       NAWKENFMTVDQDGSGTV EHHELRQAIGLMGYRLS      122-156
CDVI             KKWQAIYKQFDVDRSGTI GSSELPGAFEAAGFHLN      170-204
CDIV             RNYLSIFRKFDLDKSGSM SAYEMRMAIESAGFKLN      618-652
ALG-2            TDWQNVFRTYDRDNSGMI DKNELKQALSGFGYRLS       93-127
Peflin           QQWKNLFQQYDRDRSGSI SYTELQQALSQMGYNLS      133-167

EF-4
                 _Helix F__            __Helix G_
Sorcin           PQTVNSIAKRY-S-TSGKI TFDDYIACCVK           138-165
Grancalcin       PQTLTTIVKRY-S-KNGRI FFDDYVACCVK           157-184
CDVI             EHLYSMIIRRY-SDEGGNM DFDNFISCLVR           205-233
CDIV             KKLFELIITRY-SEPDLAV DFDNFVCCLVR           653-681
ALG-2            DQFHDILIRKFDRQGRGQI AFDDFIQGCIV           128-157
Peflin           PQFTQLLVSRYCPRSANPAMQLDRFIQVCTQ           168-198

EF-5
                 ___Helix G_            __Helix H_
Sorcin           LRALTDSFRRRDSAQQGMV NFSYDDFIQCVMTV        166-198
Grancalcin       LRALTDFFRKRDHLQQGSA NFIYDDFLQGTMAI        185-217
CDVI             LDAMFRAFKSLDKDGTGQI QVNIQEWLQLTMYS        234-266
CDIV             LETMFRFFKTLDTDLDGVV TFDLFKWLQLTMFA        682-714
ALG-2            LQRLTDIFRRYDTDQDGWI QVSYEQYLSMVFSIV       158-191
Peflin           LQVLTEAFREKDTAVQGNI RLSFEDFVTMTASRML      199-233
```

Fig. 6 – Sequence alignment of the calcium binding domains of penta-EF proteins. The residues involved in calcium ion coordination are indicated by x, y, z,-y, -x, -z. Identical or similar residues are indicated in boldface.

In PEF proteins the polypeptide chain is organized in two domains: the N-terminal one is rich in glycine and proline residues and therefore is highly flexible and not visible in the available crystal structures of the whole proteins (Blanchard et al., 1997; Jia J. et al., 2001; Xie et al., 2001).

The C-terminal domain contains all the EF-hands and is characterized by a very similar compact fold in all PEF proteins. An intriguing peculiarity of the Ca^{2+} -binding domain is the unusual presence of two long (six-turns) α-helices that are shared by EF2 and EF3 (D-helix) and by EF4 and EF5 (G-helix). EF hands 1-2 and 3-4 display the canonical EF-hand pairing, whereas the uneven EF5 does not have a partner. The presence of the uneven EF-hand, EF5, however, does not contradict the rule that EF-hands occur in structural and functional pairs. PEF proteins are dimeric in nature and in the dimer the uneven EF5 site pairs with the corresponding motif of the other subunit, thereby contributing to dimer stabilization. PEF proteins can form both homodimers and heterodimers in solution (Teahan et al., 1992; Hamada et al., 1988; Maki et al., 1998; Missotten et al., 1999), in turn, dimerization is essential for their function (Kitaura et al., 2002; Yoshizawa et al.,1995; Graham et al., 1994; Meyers et al.,1996; Arthur et al., 2000).

In those member of the family in which the identification of the physiological EF hands has been attempted, EF3 appears to be the site endowed with the highest affinity for the metal. In grancalcin, EF2 cannot bind Ca^{2+} (in position −Z alanine is in place of the canonical glutamate which typically provides two oxygen ligands to the calcium ion); in the crystals Ca^{2+} is bound to EF3 in one subunit only (Jia et al., 2000). In ALG-2, studies on site-specific mutants point to EF1 (which in this protein has the canonical 12 residue interhelical loop) and EF3 as the functionally relevant Ca^{2+} binding sites (Lo et al., 1999, Jia et al., 2001). In calpain dVI crystals grown in 1 mM Ca^{2+}, EF1, EF2, EF3 are saturated with Ca^{2+} (Blanchard et al., 1997; Lin et al., 1997); studies with site-specific mutants suggest that all these EF-hands contribute to calpain activation, but that EF3 has the highest Ca^{2+} affinity (Dutt et al., 2000).

In turn, the functional coupling of EF3 to EF1 and /or EF2 requires a novel mechanism of information transfer to be operative since the above mentioned sites are not coupled structurally.

The binding of calcium to PEF proteins increases the overall hydrophobicity and leads to their translocation from the cytoplasm to cell membranes where PEF proteins interact with specific protein targets and thereby participate in a variety of Ca^{2+} mediated

signalling processes (Vito et al., 1999; Meyers et al., 1995a; Lollike et al., 2001). Complex formation with the target can take place via either the N- or C-terminal domain (Maki et al., 1997; Kitaura et al., 1999). However, the molecular events that are triggered by Ca^{2+} binding and lead to the change in subcellular localization through the specific interaction with protein targets are still obscure. Ca^{2+} induced conformational changes as manifest in the X-ray crystal structures are unexpectedly small and are limited to the EF1 region (Lin et al., 1997; Blanchard et al., 1997; Jia et al., 2000; Strobl et al., 2000). It is not known how the small changes apparent in the crystal structures are amplified to the extent required for target protein recognition. Moreover, EF3, which is the site with the highest Ca^{2+} affinity is not paired in the canonical manner with EF2, another functionally relevant Ca^{2+} binding site (Jia et al., 2001; Subramanian et al., 2004; Jia et al., 2000). At least in principle, the D-helix which is highly conserved and is shared by EF3 and EF2 may represent the natural means for transferring functional information between them.

1.4 SORCIN

Sorcin (SOluble Resistance-related Calcium binding proteIN), a 21.6 kDa protein isolated from the cytosol of multidrug-resistant cells, but expressed also in several normal tissues including skeletal muscle, heart and brain, albeit at lower levels, is a typical PEF protein. (Meyers and Biedler, 1981 ; Polotskaja et al., 1983; Meyers et al., 1985; Koch et al., 1986; Shen et al., 1986; Meyers et al., 1987; Hamada et al., 1988; Van der Bliek et al., 1988; Roberts et al., 1989; Wang et al., 1995, Meyers et al., 1995).

The polipeptide chain has a two-domain organization with an extremely flexible N-terminal domain and a compact calcium-binding C-terminal domain. In solution sorcin forms stable dimers when Ca^{2+}-free, but has a strong tendency to precipitate in the Ca^{2+}-bound form due to the increased overall hydrophobicity (Zamparelli et al., 1997). In turn, the latter feature permits the Ca^{2+}-dependent interaction with protein targets that leads to translocation from the cytoplasm to cell membranes and induces the specific cellular response. Two calcium ions bind to sorcin with micromolar affinity and trigger the conformational change that underlies the traslocation process as indicated by titration of sorcin with calcium in the analytical ultracentrifuge (Fig. 7).

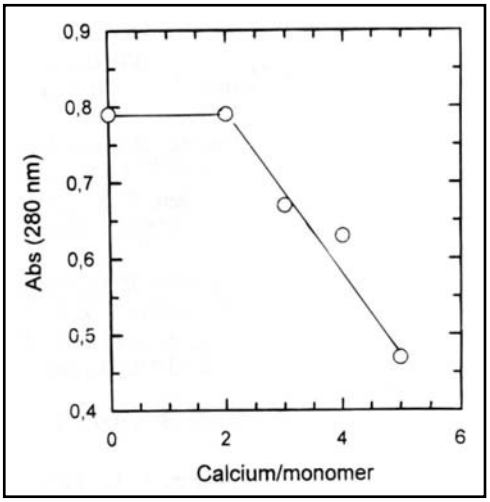

Fig. 7 – Titration of sorcin with calcium in the analytical ultracentrifuge. Different amounts of calcium were added just before the sedimentation velocity experiment. The absorbance in the plateau region is plotted as a function of the Ca^{2+}: monomer molar ratio.

In addition to the typical properties of the PEF family, sorcin has two interesting features. First, sorcin is the only PEF protein which contains a cAMP-dependent protein kinase (PKA) phosphorylation site (Van der Bliek et al, 1986, Ilari et al., 2002, Matsumoto et al., 2005). Indeed phosphorylation has been shown modulate the interaction of sorcin with its targets such as the ryanodine receptor and sarcoplasmic reticulum (SR) Ca^{2+}-ATPase pump (SERCA) (see below) (Lokuta et al., 1997; Matsumoto et al., 2005). Second, sorcin, though a stable dimer at neutral pH, forms tetramers at slightly acid pH values (Zamparelli et al., 1997) that are thought to occur near membranes.

1.4.1 STRUCTURE

The first attempts to crystallize the full-length protein did not yield crystals diffracting at high resolution due to the high flexibility of the N-terminal domain.

In contrast, the Ca^{2+}-free form of the sorcin C-terminal domain (Sorcin Calcium Binding Domain, SCBD: residues 33-198) yielded X-ray quality crystals that diffracted at 2,2 Å resolution (Ilari et al., 2002) (Fig. 8).

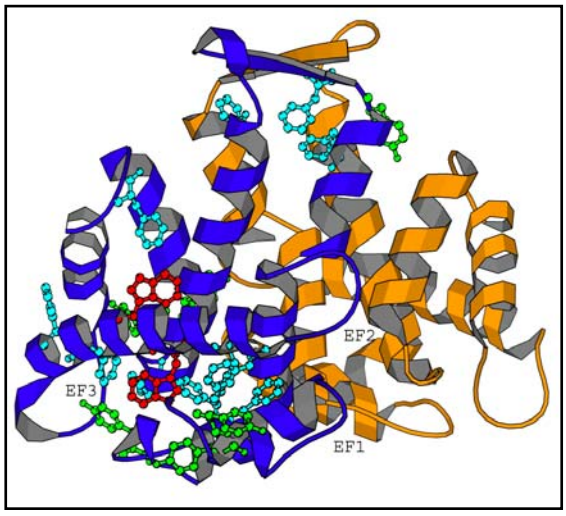

Fig. 8 – Crystal structure of the sorcin C-terminal Ca^{2+} binding domain (SCBD) The two chains in the homodimer are in blue and orange. EF1, EF2 and EF3 are indicated, as well as the D-helix connecting EF2 and EF3.

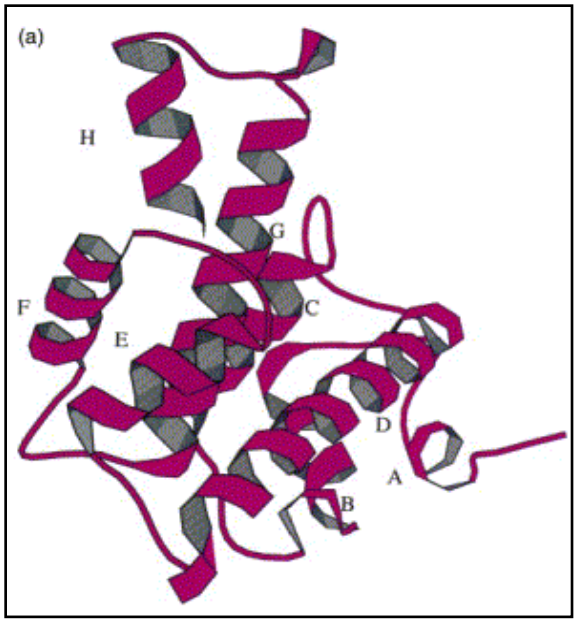

The SCBD fold resembles that of known PEF proteins and confirms the general characteristics of the family disclosed by the structures of calpain dVI, grancalcin and ALG-2 (Blanchard et al., 1997; Lin et al., 1997; Jia et al., 2000; Jia et al., 2001) (Fig. 9). Thus, the SCBD contains eight α-helices (A-H) organised in five calcium binding motifs (EF1-EF5). Two long α-helices contribute to two consecutive EF hands: helix D is common to EF2 and EF3, while helix G is common to EF4 and EF5.

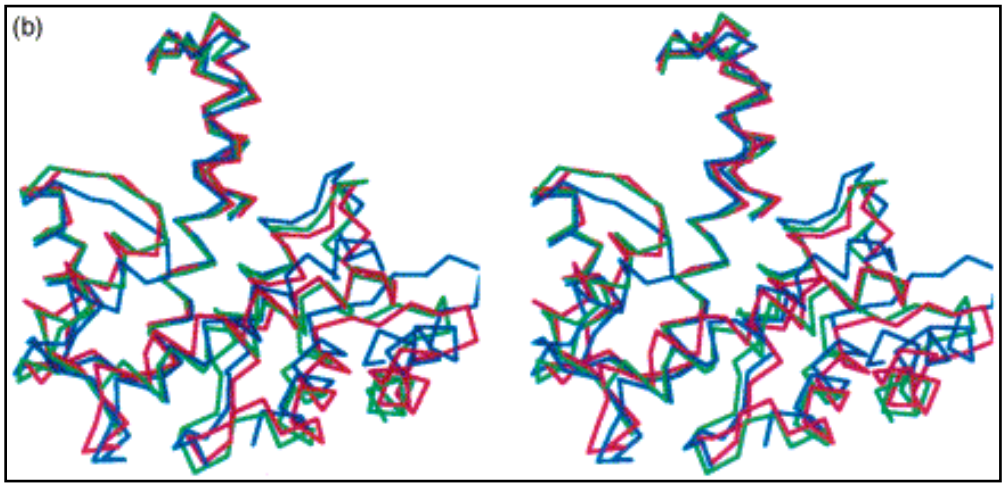

Fig. 9 – Sorcin calcium-binding domain (SCBD) monomer. In (a) the eight α-helices are labelled. In (b) a comparison with the grancalcin and calpain monomers in the apo-form is shown. SCBD is coloured red, grancalcin green and calpain blue (adapted from Ilari et al.,2002).

As for the other PEF proteins, the EF1 motif is coupled structurally with EF2 and EF3 pairs with EF4, while the EF5 site is left unpaired in the monomer but pairs with the EF5 of a second monomer in the dimer

forming the subunit interface (Fig. 10); the EF-hands associate through a short two-stranded β-sheet arrangement.

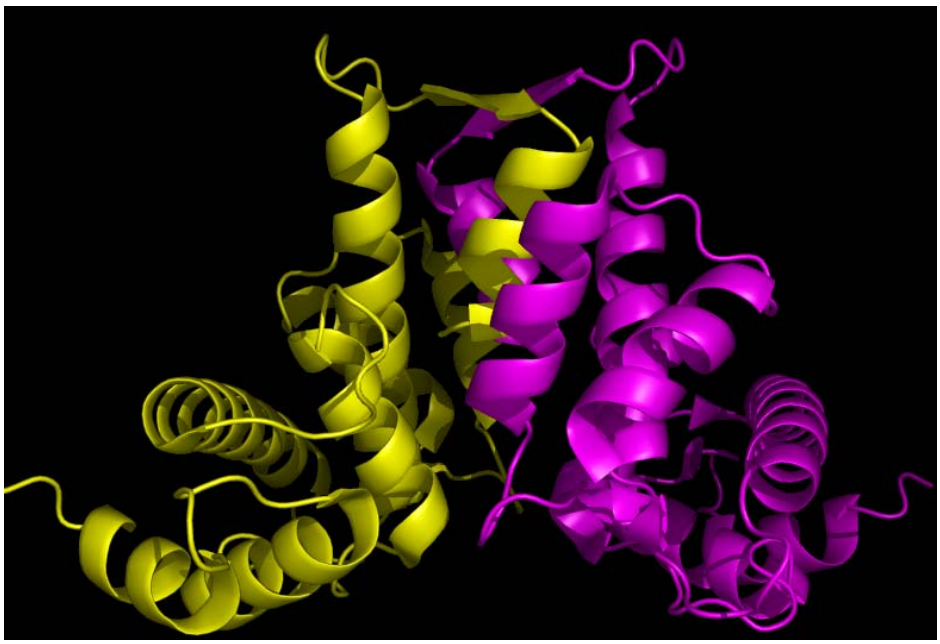

Fig. 10 – SCBD dimer.

1.4.2 *MODEL OF THE Ca^{2+}-DEPENDENT ACTIVATION*

Fluorescence and circular dichroism studies of sorcin and SCBD suggested that in the full-length protein the Ca^{2+}-dependent conformational changes involve a reorientation of the N- and C-terminal domains with no significant change in the structure of the Ca^{2+} binding domain itself. In particular, solely a Ca^{2+}-induced shift of the flexible N-terminal region relative to SCBD could explain the observation that the intrinsic fluorescence of the two tryptophan residues (Trp99 and Trp105, both located in the D helix) is unaffected by Ca^{2+} binding in SCBD, but is quenched in the native protein (Zamparelli et al., 2000). In turn, the Ca^{2+}-induced increase in overall hydrophobicity is apparent in hydrophobic chromatography experiments (Zamparelli et al., 1997).

This detailed knowledge of the solution properties of sorcin and the availability of the ALG2 structure enabled Ilari et al., (2002) to propose a model of full-length sorcin. The ALG-2 structure was found to contain an 11 residue stretch of the N-terminal domain, thought to have been removed by proteolytic cleavage, in contact with

residues of the D-helix, the EF loop, the G-helix and the GH loop of the Ca^{2+} binding domain (Fig. 11a) (Jia et al., 2001).

Fig. 11a – Ribbon-style view of the ALG-2 structure. The A, G, H helices and C terminus are labelled for reference. The bound N-terminal peptide (residues Pro8-Ala18) is depicted as bond and atom style as are also contact residues Trp95, Tyr124, and Ala166. A red curved line connecting residue Ala18 with Leu22 depicts the three missing residues between the N-terminal peptide and the Ca^{2+} binding domain. (a) was constructed using Ribbons. (taken from Ilari et al., 2002)

The sorcin N-terminus contains a very similar proline/glycine-rich stretch, with Tyr18 as the only critical difference, at the same linear distance in sequence from the Ca^{2+} binding domain (Fig. 11b).

SCBD (struct.seq.)					32 MDPLYGYFASV
Sorcin(prot.seq.)	8	GAGGGYY	**PGGYGGAPGGP**	SFP	GQTQGPLYGYFASV
ALG2 (prot.seq.)	1	MAAYSYR	**PGPGGGPGPAA**	GAA	LPDQSFLWNVFQRV
ALG2 (struct.seq.)		8	**PGPGGGPGPAA**	---	LPDQSFLWNVFQRV

Fig. 11b – Sequence of ALG-2 and sorcin showing the bound peptide in the ALG-2 structure and the corresponding one in sorcin. The bound peptide in the ALG-2 structure is comprised of residues 8 to 18 (boldface). There follows a three residue gap (GlyAlaAla) and the structure begins again with Leu22. The residues Gln25 and Val35 have a "structural equivalence" with the corresponding residues in the SCBD structure as determined by superposition using SEQUOIA (Carson, 1997). (taken from Ilari et al., 2002).

On the basis of this similarity, a model of the SCBD with the ALG-2 peptide bound between the D-helix and the EF loop was constructed (Ilari et al., 2002). It mimics the Ca^{2+}-free form of full-length sorcin where the flexible N-terminal and the C-terminal domains tend to interact with each other. Thus, the N-terminal domain positioned as in Fig. 11c buries the two tryptophan residues on the D helix, as indicated by the fluorescence and CD data, and covers a large hydrophobic surface as indicated by the hydrophobic chromatography experiments (Zamparelli et al., 1997). The model also explains the observed twofold decrease in the rate of phosphorylation of full-length sorcin compared to that of SCBD (Ilari et al., 2002). According to the model, the N-terminal domain physically hinders access of PKA to the phosphorylation site in intact sorcin.

Ilari et al., (2002) also proposed that calcium binding causes structural rearrangements that lead to loosening of the interactions between the two sorcin domains such that a large hydrophobic surface (comprising the D-helix and the EF loop) is exposed on SCBD and both domains become available for interaction with the respective target proteins.

Fig. 11c – Ribbon-style view of SCBD superposed onto the ALG-2 monomer depicted in (a). SCBD was divided into two parts (residues 33–117 and 118–198) which were superposed separately using SEQUOIA. The bound peptide is as in (a). Three residues of SCBD analogous to those in (a) are shown in bond and atom style, Trp105, Phe134, and Arg174. Also shown is a bound sulphate ion near Ser172; two residues which stabilize the bound sulphate ion, Arg175 and Arg176, and the putative phosphorylation site Ser178. (c) was constructed using Ribbons. (taken from Ilari et al., 2002)

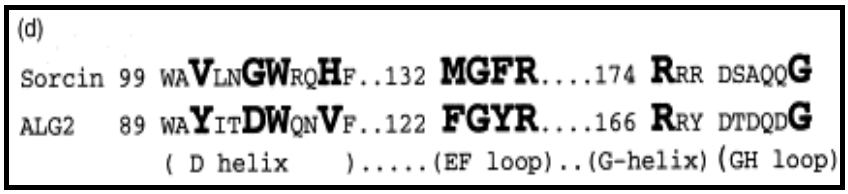

Fig. 11d – Residues from the Ca^{2+}-binding domains of ALG-2 and the SCBD model which contact the bound N-terminal peptide depicted in (a) are shown in boldface and larger type. The side-chains of the ALG-2 residues Trp95, Tyr124 and Arg166 are depicted in (a). The corresponding residues of SCBD are shown in (c). Tyr90 and Asp93 make side-chain to side-chain contacts with Pro16 imide ring. Gly174 makes a side-chain H polar (perpendicular) contact with Pro10 imide ring. Trp95 forms main-chain polar contacts with Pro16. Phe122 and Arg125 form main-chain polar contacts with Pro14 to Gly9. Arg166 makes a very interesting side-chain to main-chain contact with the carbonyl oxygen atoms of Gly11 and Gly12 of the peptide. (taken from Ilari et al., 2002)

1.4.3 PROTEIN TARGETS

Different sorcin targets have been identified in different tissues.

Annexin VII (synexin) was the first to be recognized (Brownawell and Creutz, 1997). The interaction involves the N-terminal domains of both proteins. It takes place in adrenal medulla and leads to inhibition of the synexin-mediated aggregation of chromaffin granules (Brownawell and Creutz, 1997). Interaction between sorcin and annexin VII occurs also in differentiating myoblasts (Clemen et al., 1999) and in vesicles from erythrocytes (Salzer et al., 2002).

In the brain, sorcin was found to interact with the N-methyl-D-aspartate receptor 1 in the caudate putamen nucleus (Gracy et al.,1999) and with presenilin 2, an integral membrane protein localized predominantly to the endoplasmic reticulum and the Golgi apparatus in brain tissues, whose mutations is linked to familial Alzheimer's disease (Pack-Chung et al., 2000). In muscle tissues, sorcin interacts with several channels involved in cell contraction: the pore-forming α_1 subunit of voltage-dependent L-type Ca^{2+} channels, the ryanodine receptor, the Na^{+}-Ca^{2+} exchanger and the

sarcoplasmic reticulum ATPase SERCA2a (Meyers et al., 1995; Meyers et al., 1998, Farrell et al., 2003; Matsumoto et al., 2005). The interactions taking place in muscle have received special attention in view of the role played by Ca^{2+} in the contraction and relaxation processes.

These processes will be described briefly for a better understanding of the role played by sorcin.

1.4.4 CALCIUM AND CARDIAC EXCITATION-CONTRACTION-RELAXATION PROCESSES

The human heart proceeds from a relaxed state (diastole) to a fully contracted state (systole) and recovery in 600 ms. The contractile-relaxation (E-C) cycle is tightly coupled to Ca^{2+} transients. This ubiquitous second messenger is the direct activator of the myofilaments and causes contraction.

During the cardiac action potential, Ca^{2+} enters the cell through depolarization-activated Ca^{2+} channels as an inward Ca^{2+} current (I_{Ca}), which contributes to the action potential plateau (Fig. 12), Ca^{2+} entry triggers Ca^{2+} release from the sarcoplasmic reticulum (SR).

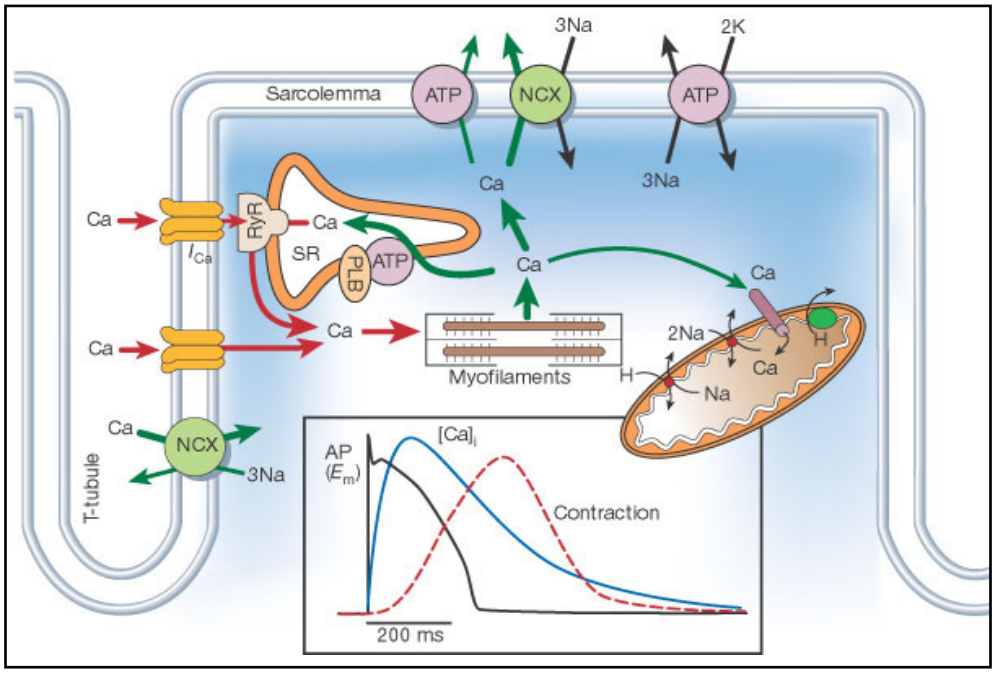

Fig. 12 – Ca^{2+} transport in ventricular myocytes. The red arrows show the activation of contraction, the green arrows the relaxation process. Inset shows the time course of an action potential, Ca^{2+} transient and contraction measured in a rabbit ventricular myocyte at 37°C. SR, sarcoplasmic reticulum; NCX, Na^{+}/Ca^{2+} exchange; ATP, SR and sarcolemmal ATPases; PLB, phospholamban (from Bers, 2002).

The combination of Ca^{2+} influx and release raises the free intracellular Ca^{2+} concentration ($[Ca^{2+}]_i$), allowing Ca^{2+} to bind to the myofilament protein troponin C, which switches the contractile machinery. For relaxation to occur, $[Ca^{2+}]_i$ must decline, thereby, allowing Ca^{2+} to dissociate from troponin. This requires Ca^{2+} transport out of the cytosol by at least four pathways involving the sarcoplasmic reticulum (SR) Ca^{2+}-ATPase, the sarcolemmal Na^+/Ca^{2+} exchanger, the sarcolemmal Ca^{2+}-ATPase or the mitochondrial Ca^{2+} uniport (Bers, 2002).

The amount of total cytosolic $[Ca^{2+}]$ ($[Ca^{2+}]_{Tot}$ = $[Ca^{2+}]_i$ plus bound Ca^{2+}) that must be supplied to and removed from the cytosol during each cardiac beat is shown in Figure 13. Half-maximal activation of contraction requires roughly 70 µmol of Ca^{2+} per litre of cytosol, which would raise $[Ca^{2+}]_i$ to 600 nM. The local Ca^{2+} concentration, subsarcolemmal or at the cleft ($[Ca]_{sm}$; $[Ca]_{cleft}$), may rise up to several tens of micromolar (Bers, 2001; Langer and Peskoff, 1996; Trafford et al., 1995).

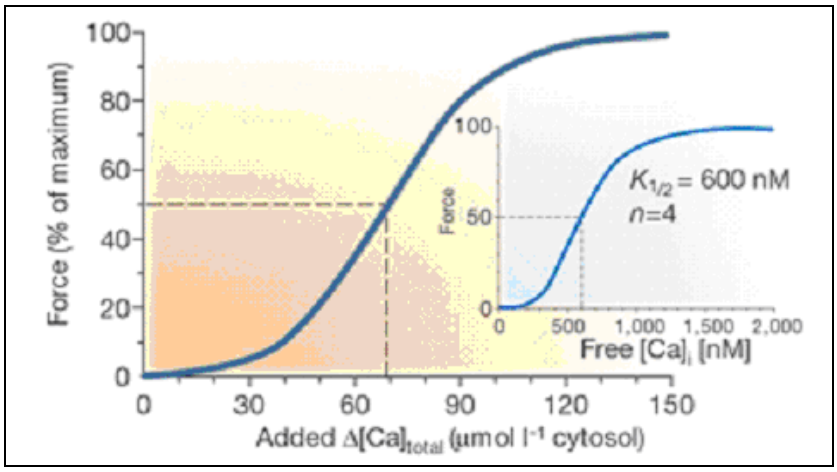

Fig. 13 – Amount of Ca^{2+} required for contractile activation, assuming a diastolic intracellular Ca^{2+} concentration ($[Ca^{2+}]_i$) of 150 nM and cytosolic Ca^{2+} buffers including troponin C (Ca^{2+} and Ca^{2+}/Mg^{2+} sites), myosin, SR Ca^{2+}-ATPase, calmodulin, ATP, creatine phosphate and sarcolemmal sites. Inset shows force as a function of $[Ca^{2+}]_i$ (that is, force is equal to $100/(1+\{600/[Ca^{2+}]_i\}$(adapted from Bers, 2002).

Upon membrane depolarization, the large electrochemical $[Ca^{2+}]$ gradient drives Ca^{2+} into resting myocytes mainly through two classes of voltage-dependent Ca^{2+} channels (L- and T-type). Ca^{2+} influx via sarcolemmal L-type Ca^{2+} channels (or dihydropyridine receptors, DHPRs) triggers the release of Ca^{2+} from the sarcoplasmic reticulum via

ryanodine receptors (RyR). This released Ca^{2+} is the major fraction of Ca^{2+} involved in the activation of the myofilaments to produce contraction. RyR is the main SR Ca^{2+}-release channel in striated muscle, and as such plays a critical role in cardiac E-C coupling. In all cardiac myocytes the SR and sarcolemmal membranes come into very close apposition at periodic regions along the surface membrane, and in ventricular myocytes also in the transverse tubules (T-tubules); about 20–50% of the T-tubules is involved in such junctions. At each junctional cleft, a cluster of about 100 individual RyRs are close to 10–25 DHPRs forming a local SR Ca^{2+}-release unit called a couplon. During E-C coupling each of the about 10000 couplons in a ventricular myocyte are activated independently by Ca^{2+} influx from the juxtaposed sarcolemmal Ca^{2+} channels. These local SR Ca^{2+}-release events (Ca^{2+} sparks) are the fundamental units of SR Ca^{2+} release both at rest (rare, stochastic events) and during excitation-contraction coupling. However, during excitation-contraction coupling several thousand Ca^{2+} sparks in each cell are synchronized by the action potential, such that the local rises in $[Ca^{2+}]_i$ are completely overlapping in time and space, such that the Ca^{2+} transients appear as spatially uniform (Franzini-Armstrong et al., 1999; Scriven et al., 2000; Bers, 2002).

The Ca^{2+}-induced Ca^{2+}-release is inherently a positive-feedback mechanism, but its turn-off is essential for diastolic relaxation and refilling of the myocytes. The cardiac RyR isoform (RyR2) interacts with a series of proteins that regulate its function. These include FK-506 binding protein (FKBP 12.6; which may stabilize RyR gating and also couple the gating of both individual and adjacent RyR tetramers), cAMP-dependent protein kinase (which can alter RyR and I_{Ca} gating), phosphatases 1 and 2A, and in particular calmodulin and sorcin, both of which decrease RyR opening in a Ca^{2+}- dependent fashion, thereby contributing to the shut-off of SR Ca^{2+}-release (Meyers et al., 1998; Fruen et al., 2000; Marx et al., 2000; Marx et al., 2001).

Ca^{2+} must be removed from the cytosol to lower $[Ca^{2+}]_i$ and allow relaxation. This is achieved by several routes, the quantitative importance of which varies between species. In rabbit ventricular myocytes, the SR Ca^{2+}-ATPase pump (SERCA) removes 70% of the activator Ca^{2+}, and the Na^+/Ca^{2+} exchanger removes 28%, leaving only about 1% each to be removed by the sarcolemmal Ca^{2+}-ATPase and mitochondrial Ca^{2+} uniporter. The amount of Ca^{2+} extruded from the cell during relaxation must be the same as the amount of Ca^{2+} entry for each beat, otherwise the cell would gain or lose Ca^{2+} and would not be in steady state (Bassani et al., 1994; Bers, 2002).

The Na^+/Ca^{2+} exchanger (NCX) can work in both directions, depending on local electrochemical potential, with a stoichiometry of three Na^+ ions to one Ca^{2+} that produces an ionic current ($I_{Na/Ca}$). Na^+/Ca^{2+} exchange can extrude Ca^{2+} (as an inward $I_{Na/Ca}$) or bring Ca^{2+} into the cell (as outward $I_{Na/Ca}$); high $[Ca^{2+}]_i$ favours Ca^{2+} efflux (inward $I_{Na/Ca}$), whereas positive membrane potential (E_m) and high $[Na^+]_i$ favour outward $I_{Na/Ca}$. Fig. 14 shows possible time courses for $[Ca^{2+}]_{sm}$ and $[Na^+]_{sm}$ that may be sensed by the Na^+/Ca^{2+} exchanger during normal excitation−contraction coupling. Although NCX participates in the entry of calcium in the very first milliseconds of the action potential, under physiological conditions Na^+/Ca^{2+} exchange works mainly in the Ca^{2+} extrusion mode, driven mostly by the Ca^{2+} transient (Hinata and Kimura, 2004; Bers and Despa, 2006).

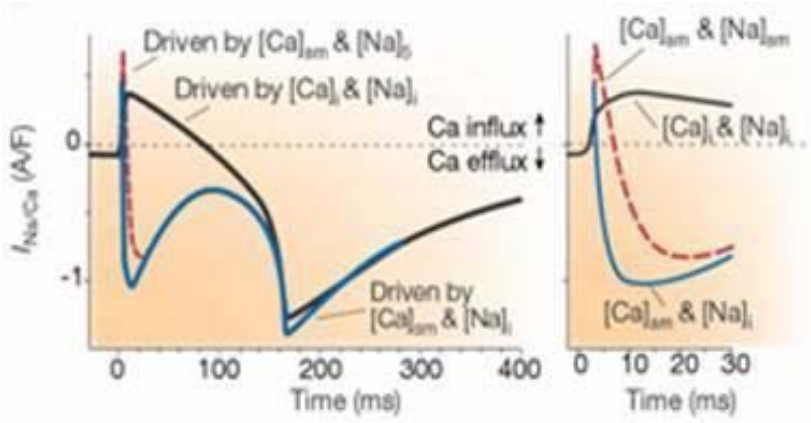

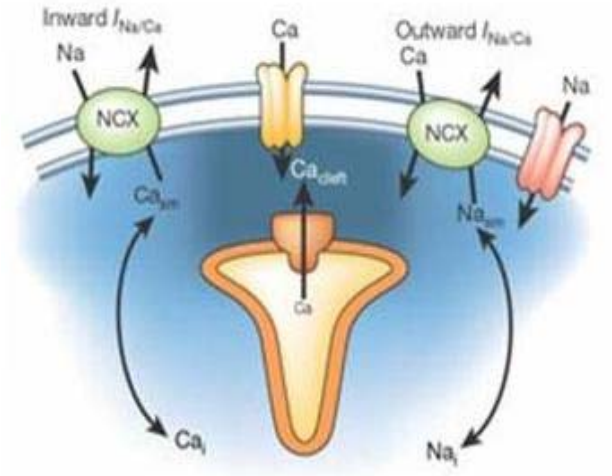

Fig. 14 – Na^+/Ca^{2+} exchange during an action potential. $I_{Na/Ca}$ calculated as a function of E_m (action potential) and the indicated concentrations of Ca^{2+} and Na^+. The red curve represents the global ionic current. Right panel is expanded in time. Geometry of junctional and submembrane spaces (adapted from Bers, 2002).

1.4.5 EMERGING ROLE OF SORCIN IN SKELETAL AND CARDIAC MUSCLE

Sorcin binds to the cytoplasmic side of both L-type calcium channels and RyRs in skeletal and cardiac muscle, participating in channel gating (Meyers et al., 1995b, Meyers et al., 1998). Binding has been evaluated by co-immunoprecipitation of metabolically labelled cardiac myocyte proteins and by several types of *in vitro* binding studies. In the cardiac L-type calcium channel calcium-bound sorcin binds to the cytoplasmically-oriented carboxy-terminal domain of the pore-forming 1C subunit, either at or near the calmodulin binding region, participating in channel inactivation (Meyers et al., 1998).

The interaction of sorcin with RyR takes place with high affinity. Thus, sorcin completely inhibits open cardiac RyRs (RyR2) from being incorporated into planar lipid bilayers and depresses ryanodine-binding. The concentration for half-maximal inhibition is as low as 480 nM. This inhibitory effect is relieved by phosphorylation of sorcin with the catalytic subunit of PKA (Lokuta et al., 1997; Farrell et al. 2003).

In cardiac myocytes, sorcin significantly inhibits both the spontaneous activity of RyRs in quiescent cells (calcium sparks) and the inward calcium current-triggered activity that gives rise to intracellular transients. Sorcin decreases spark efficiency and amplitude, and the dynamic interaction with RyRs occurs at a rate that would allow for modulation of the channel on a beat-to-beat basis. Kinetically, the rapid and reversible effect of sorcin on RyR2 closure is capable of playing a role in terminating the positive feedback loop of calcium-induced calcium release (Farrell et al., 2003; Seidler et al., 2003).

The functional effects of sorcin on RyR2 and the L-type calcium channel suggest that sorcin may play a role in interchannel communication. In addition, sorcin increases NCX activity in sorcin-overexpressing rabbit cardiac myocytes (Farrell et al., 2003), while reduced cellular sorcin expression depresses NCX activity in an animal model of left ventricular dysfunction (Smith et al., 2006).

In turn, the interaction between sorcin and SERCA that takes place in cardiac myocytes is able to modulate the SR Ca^{2+} uptake function. In a normal heart, PKA-phosphorylation of sorcin allows it to translocate to the SR fraction, while in a failing heart condition, hyperphosphorylation of sorcin by PKA promotes its Ca^{2+}-dependent translocation from the cytosol to the SR membrane. This translocation to the SR results in an activation of Ca^{2+} uptake through SERCA2a (Matsumoto et al., 2005).

Immmunoprecipitation analysis showed that presenilin 2 (PS2), sorcin, and RyR2 interact with each other in HEK-293 cells overexpressing these proteins or in mouse hearts. Immunohistochemistry of heart muscle indicated that PS2 colocalizes with RyR2 and sorcin at the Z-lines. High Ca^{2+} concentrations increase the association of sorcin with PS2, and attenuate the association of RyR2 with PS2 (Pack-Chung et al., 2000; Takeda et al., 2005).
The body of these studies points to sorcin as an important player in the diastolic function. In particular, sorcin inhibits calcium release from the sarcoplasmic reticulum by RyR2, increases cation uptake from the SR by SERCA and its sarcolemmal extrusion by NCX. Hence, sorcin participates in the relaxation processes that follow cardiac contraction, contributing to both the shut-off of SR Ca^{2+}-release and the lowering of calcium cytosolic content.

1.5 AIM OF THE WORK

The research activity described in the present thesis is based on the recognition that the molecular mechanism that permits activation of PEF proteins and leads to their interaction with specific protein targets on cell membranes is still largely obscure. Sorcin appeared as a good candidate to unveil the underlying processes in view of the fairly thorough characterization of its solution properties and of the ongoing determination of its X-ray crystal structure.

The titration of sorcin with calcium in the analytical ultracentrifuge had shown that the Ca^{2+}-induced conformational change is triggered upon saturation of only two EF-hands out of the three predicted to have affinities in the micromolar range, namely EF1, EF2 and EF3 (Zamparelli et al., 2000). Thus, the first aim of the study has been to identify the functional EF-hand pair. The strategy employed has been to mutate the conserved glutamate in position –Z of the EF1, EF2 and EF3 sites because it establishes a bidentate interaction with the metal ion (Fig. 15). The respective site-specific mutants E53Q, E94A and E124A were expressed and characterized structurally and functionally. Determination of their affinity for calcium and of their ability to interact with two sorcin targets, annexin VII and the ryanodine receptor, indicated that EF3 and EF2 are the physiologically relevant sites and that the former is endowed with the highest affinity for the metal.

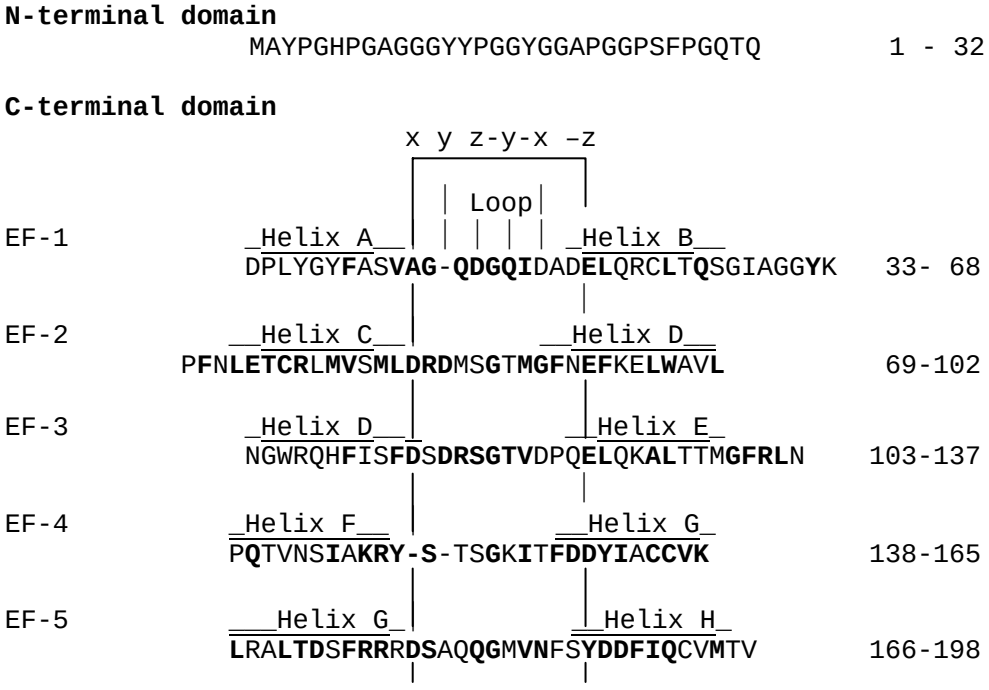

Fig. 15 – Amino acid sequences of the sorcin five EF-hands, the residues conserved in all the member of the PEF family are in bold.

These findings taken together with the X-ray crystal structure of the Ca^{2+}-binding domain determined meanwhile, led to the proposal that the D helix which connects the two physiologically active Ca^{2+}-binding sites transmits the conformational change occurring after binding of the metal from EF3 to EF2 and therefrom to the rest of the sorcin molecule.

On this basis, the second objective of the present study has been to establish whether the D-helix is instrumental in sorcin activation. To this end, the only two tryptophan residues of the polypeptide chain, W99 and W105, that are both located on the D helix, were substituted by glycine (Fig. 16). W105 is involved in the network of interaction around the D-helix, while W99 faces solvent. The different location of the tryptophan residues along the D-helix and the different type of interactions they establish suggest that their substitution may affect differently sorcin activation and the interaction with its targets. To verify this contention, the site-specific mutants W99G and W105G were produced and their functional properties characterized in terms of the interaction with molecular targets.

The results obtained are of relevance in understanding the role of sorcin in the excitation-contraction-relaxation cycle of cardiac muscle.

A

N-terminal domain

MAYPGHPGAGGGYY**PGGYGGAPGGP**SFPGQTQ 1-32

C-terminal domain (SCBD)

Helix A *EF1* *Helix B* *Helix C* *EF2*
DPLYGYFASVAGQDGQIDADELQRCLTQSGIAGGYKPFNLETCRLMVSMLDRDMSGTMG 33-91

Helix D *EF3* *Helix E* *Helix F*
FNEFKELWAVLNGWRQHFISFDSDRSGTVDPQELQKALTTMGFRLNPQTVNSIAKR 92-147

EF4 *Helix G* *EF5* *Helix H*
YSTSGKITFDDYIACCVKLRALTDSFRRRDSAQQGMVNFSYDDFIQCVMTV 148-198

B

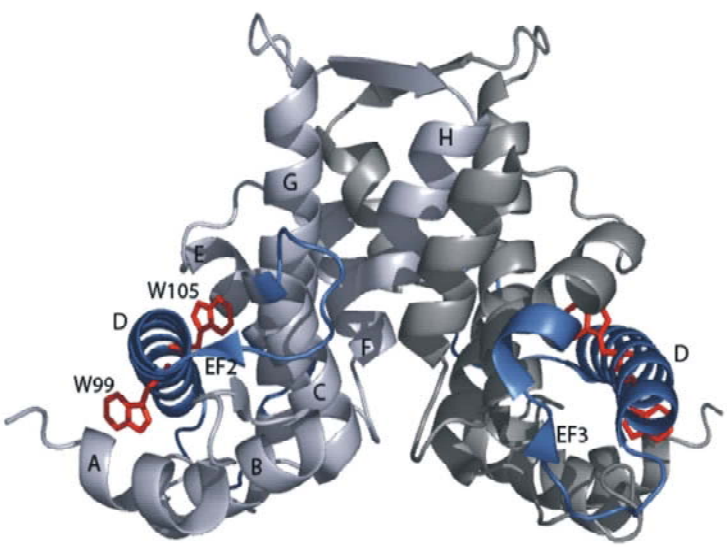

Fig. 16 – Sorcin sequence (A) and structure of the Ca^{2+}-binding domain, SCBD (B). In A, the 11 aminoacids which interact with SCBD in the model of Ilari et al. are in boldface. In B, the two monomers are depicted in different colours. The D helix and the physiologically relevant EF2 and EF3 hands are in blue; the two tryptophan residues, W99 and W105, are in red.

2. MATERIALS AND METHODS

2.1 CLONING OF THE EF-HANDS AND D-HELIX MUTANTS E53Q, E94A, E124A, W105G AND W99G

The cDNA of chinese hamster ovary sorcin, kindly provided by Dr M. B. Meyers (New York University School of Medicine, New York, USA), was amplified by PCR using two oligonucleotides, one of which was designed to generate a novel NdeI restriction site at the 5'end at the place of NcoI without altering the sequence within the gene. The amplified DNA thus obtained was digested with restriction enzymes NdeI and Hind III and was inserted subsequently in a pET22 expression vector previously digested with the same enzymes (Fig. 17).

Fig. 17 – Properties and characteristics of the expression vector used: Pet 22.

The digestion was performed at 37°C for 4 hours using 2 µl of each enzyme at the concentration of 10 U/µl; the enzymes were then inactivated at 80°C for 20 minutes.

Site–directed mutagenesis was carried out by the PCR overlap extension mutagenesis method (Higugi et al., 1988), using for each mutant two external oligonucleotides (N forward, C reverse) and two internal complementary primers of 25-30 nucleotides containing the desired mutation (Fig. 18).

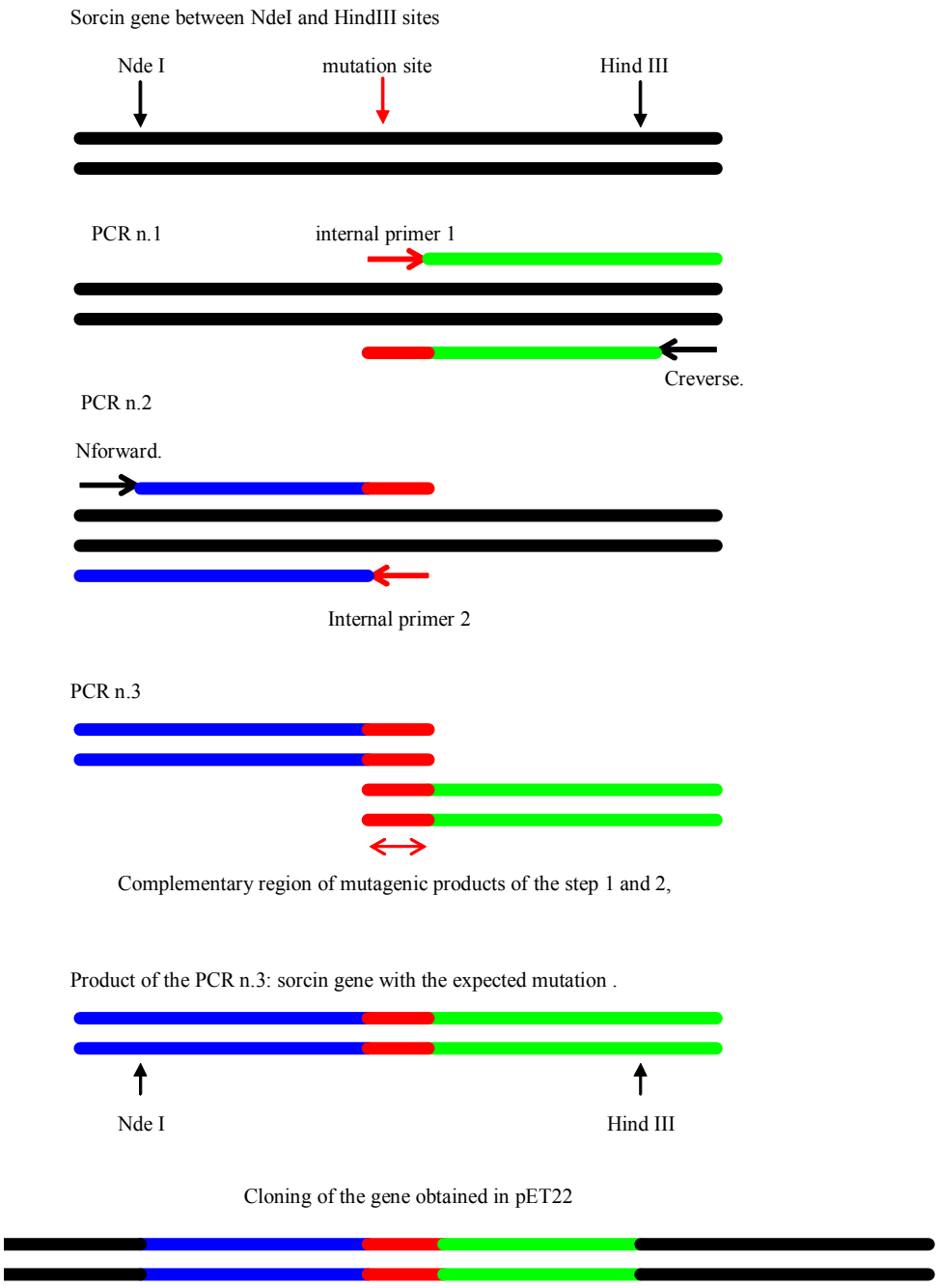

Fig. 18 – Cloning of sorcin variants E53Q, E94A, E124A, W105G and W99G.

The following oligonucleotides were used:

N forward: 5'-GCGAAATTAATACGACTCACTATAGGG- 3',
C reverse: 5'-CAAGCTTTTAGACGGTCATGACAC- 3',
E53Q forward: 5'-CAAATTGATGCTGATCAGTTGCAGAGATGACA- 3',
E53Q reverse: 5'-GTTAGACATCTCTGCAACTGATCAGCATCAATTTG- 3',
E94A forward: 5'-CACCATGGGATTCAATGCATTTAAAGAGCT- 3',
E94A reverse : 5'-GAGCTCTTTAAATGCATTGAATCCCATGGTG- 3',
E124A forward: 5' -GGAACGGTGGATCCCCAGGCACTGCAGAAGGCTCTG- 3',
E124A reverse: 5' -CGTCAGAGCCTTCTGCAGTGCCTGGGGATCCACCGT- 3',
W99G forward: 5'-GAATTTAAAGAGCTCGGCGCTGTGCTGAATGG- 3',
W99G reverse: 5'-CCATTCAGCACAGCGCCGAGCTCTTTAAATTC- 3',
W105G forward: 5'-CTGTGCTGAATGGCGGCAGACAACACTTCATC- 3',
W105G reverse: 5'-GATGAAGTGTTGTCTGCCGCCATTCAGCACAG- 3'.

For each mutant two PCR reactions were performed using one of the two external primers and the corresponding internal one. The PCR was carried out under the following conditions: amplification cycles, 30; annealing temperature, 60°C, extending step, 5 seconds at 72°C. The length and the purity of the PCR products were checked by electrophoresis carried out on agarose 1% gel in TBE (90 mM Tris-borate, 2 mM EDTA, pH 8,0). The amplification products were purified using the DNA purification kit (Qiagen). They correspond to the N-terminal and C-terminal regions of the sorcin gene and are complementary in the central region which contains the desired mutation. The second PCR reaction was performed under the following conditions: amplification cycles, 30; annealing temperature, 60°C; extension cycle, 40 seconds at 72°C. The length and the purity of the PCR products were checked by on agarose gel electrophoresis in TBE as above. The amplification products were purified using the DNA purification kit (Qiagen). The genes thus obtained were digested with restriction enzymes NdeI and Hind III and were inserted into a pET22 expression vector previously digested with the same enzymes.

Fresh competent *E. coli*- BL21(DE3) cells were prepared from a single colony grown for 16-20 hours at 37°C in 5 ml of LB broth (10 g/l tryptone, 5 g/l yeast extract and 5 g/l NaCl) and then transferred into 100 ml of the same medium. The culture was incubated for ≈3 hours at 37°C with vigorous shaking until the OD_{600} was ≈ 0.3, thereafter the cells were cooled to 0°C by storing the samples on ice for 10 minutes. The culture was centrifuged at 4000 rpm for 10 minutes at 4°C and the pellet was resuspended in 10 ml of ice-cold 0.1 M $CaCl_2$ and stored on ice for 10 minutes. The cells

were recovered by centrifugation at 4000 rpm for 10 minutes at 4°C and resuspended in 2ml of ice-cold 0.1 M $CaCl_2$.

The recombinant plasmids obtained as described above were used to transform competent *E. coli* BL21(DE3) cells which were then plated on bacterial LB agar plates containing 0.1 mg/ml ampicillin. Transformants were screened for the proper insert by PCR. Agarose electrophoresis was performed on the PCR products, plasmid DNA was isolated, and the sorcin cDNA sequenced.

2.2 EXPRESSION AND PURIFICATION OF WILD TYPE SORCIN AND ITS MUTANTS

The same expression and purification procedure was used for the sorcin and all the site-specific mutants under investigation. The purification step takes advantage of the ability of sorcin to translocate from cytosol to membranes when Ca^{2+}-bound. This process takes place also in *E. coli* cells (Meyers et al., 1995a).

Transformed bacteria were inoculated into 5 ml of standard LB broth containing 5 mM $CaCl_2$ and 0.1 mg/ml ampicillin. Cells were grown for 5-6 h at 37°C and were transferred to 1 l of the same medium for overnight growth at 37°C. Cells were grown to mid-log phase (A_{600nm} = 1). Protein expression was induced by addition of 1 mM isopropyl-*β*-D-thiogalactopyranoside (IPTG), a molecule able to activate the lac promoter. After addition of IPTG the cells were grown at 37°C for 1.30 h; cytotoxic effects were apparent for longer periods of growth. Bacteria were harvested and suspended in 10 ml of sonication buffer (10 mM Tris-HCl at pH 7.4, 10 mM NaCl, 1 mM phenylmethyl sulfonyl fluoride, 1 mM dithiothreitol). Cells were sonicated on ice using MSE Soniprep 15, and centrifuged at 14000 x g for 20 min. The recovered pellet was resuspended with 10 ml sonication buffer containing 0.2 μg DNase and 5 mM $MgCl_2$ and was incubated at room temperature for 30 min. The suspension was centrifuged at 15000 x g for 20 min. In order to remove contaminant DNA, the pellet was washed repeatedly with sonication buffer. The removal of DNA was checked by following the progressive decrease of the typical nucleic acids absorbance at 260 nm. The recovered pellet was resuspended in sonication buffer containing 10 mM ethylene glycol-bis(2-ammino-ethylether)-tetra-acetic acid, EGTA. Under physiological conditions (pH 7.5 and 100 mM ionic strength) the Ca^{2+} affinity constant of EGTA is 2×10^7 M^{-1}.

Sorcin and its mutants were extracted from the membranes by resuspending the pellets in 10 ml of sonication buffer containing 5 mM EGTA. After 10 min incubation at 25°C, the sample was centrifuged at 15000 x g for 20 min. The optical spectrum of the supernatant has the typical protein absorbance maximum at 280 nm (fig. 19). Analysis of the sample by SDS-PAGE according to Laemmli (1970) shows that this step yields a 70-80% pure proteint. Further purification was achieved using an anionic exchanger at pH 7.5 since the predicted isoelectric point of sorcin is about 5.7.). The sample was dialyzed against 10 mM Tris-HCl, pH 7.5 and applied to a Mono-Q FPLC column equilibrated with the same buffer. A linear gradient of NaCl between 0 and 0.5 M was used to recover sorcin which elutes at 0.25 M NaCl. Protein concentration was determined spectrophotometrically at 280 nm. The molar extinction coefficient, calculated according to Edelhoch (1967), was 29.400 for wt sorcin and for E53Q, E94A, E124A; 22.640 for W99G and for W105G.

2.3 CIRCULAR DICHROISM SPECTRA

Circular dichroism (CD) spectroscopy measures differences in the absorption of left-handed polarized (L) versus right-handed polarized light (R) of an optically active compound. The absence of regular structure results in zero CD intensity, while an ordered structure results in a spectrum which can contain both positive and negative signals. Circular dichroism spectroscopy is suitable for determining protein folding and in particular its secondary and tertiary structure. Secondary structure can be determined by CD spectroscopy in the far UV spectral region (190-250 nm). At these wavelengths the cromophore is the peptide bond, and the signal arises when it is located in a regular environment. Alpha-helix, beta-sheet, and random coil structures each give rise to a characteristic shape and magnitude of the CD spectrum. The CD spectrum of a protein in the near UV spectral region (250-350 nm) is sensitive to protein tertiary structure.

CD spectra were recorded on a Jasco J-710 spectropolarimeter in the far UV (200-250 nm) and in the near UV (250-350 nm) regions. The experiments were carried out at 20°C in 100 mM Tris-HCl at pH 7.5. The α-helical content was calculated from the ellipticity value at 222 nm and with the Selcon3 program (srs.dl.ac.uk/VUV/CD/selcon.html).

2.4 FLUORESCENCE SPECTRA

Fluorescence is the phenomenon in which absorption of light of a given wavelength by a fluorescent molecule is followed by the emission of light at longer wavelengths. The distribution of wavelength-dependent intensity that causes fluorescence is known as the fluorescence excitation spectrum, and the distribution of wavelength-dependent intensity of emitted energy is known as the fluorescence emission spectrum. Because the magnitude and the position of the emission peak depend on the local environment of the cromophore, fluorescence can be used to study local changes in protein structure.

Intrinsic fluorescence was measured in a Fluoromax spectrofluorimeter at 25°C, in 100 mM Tris-HCl at pH 7.5 using an excitation wavelength of 280 nm and a slit width of 0.5 nm. The emission signal was followed between 300 and 400 nm.

2.5 DETERMINATION OF Ca^{2+} AFFINITY

The affinity of sorcin for calcium could not be determined in direct fluorescence experiment because the binding of calcium leads to precipitation of the protein. Ca^{2+} binding constants were assessed in indirect fluorescence titration experiments in the presence of the fluorescent calcium chelator Quin2 (2-metil-8-nitroquinoline) that binds calcium with a dissociation constant $K_D = 1.2 \times 10^7$ M at pH 7.5 (Bryant, 1985).

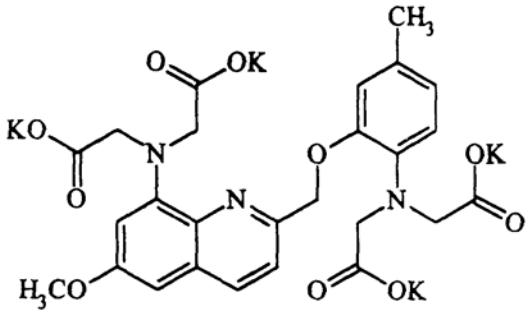

The concentration of Quin 2 was determined from the absorbance of the Ca^{2+} complex at 240 nm (ε_M 42000 M^{-1} cm^{-1}).

In a standard experiment, all solutions were prepared in 100 mM Tris-HCl at pH 7.5 using doubly distilled water and were stored in plastic flasks containing a dialysis bag with Chelex 100.

To reduce Ca^{2+} contamination to 0.5 – 1 μM, the glassware was treated with Chelex 100 as recommended by André and Linse (2002). The concentration of Quin2 and sorcin or its mutants were around 25 μM (total volume 2 ml); the calcium solution (10 mM) was added in aliquots of a few μl. The experiments were carried out at 25°C in a Fluoromax spectrofluorimeter; excitation wavelength was at 339 nm (slit width 0.5 nm). The increment of fluorescence emission due to Ca^{2+} binding to Quin2 was followed at 492 nm (slit width 0.5 nm). Control experiment were performed on Quin 2 alone. A the end of each titration, the fluorescence intensity corresponding to nominally zero free Ca^{2+} concentration was determined by addition of 5 mM EGTA. The fluorescence intensity of Quin2 at high Ca^{2+} concentrations was taken as the higher asymptote. The binding constants were assessed by fitting the experimental data to the model [2 Ca^{2+} sites + chelator] with the program CaLigator (André and Linse, 2002) .

2.6 OVERLAY ASSAY EXPERIMENTS

Aliquots of purified wild-type sorcin and of the mutants were subjected to electrophoresis on a 15% polyacrylamide gel under denaturing conditions (Laemmli, 1970) and transferred to polyvinyldifluoride membranes (PVDF) in transfer buffer (25 mM Tris-HCl, 192 mM glycine, 20% methanol, pH 8.3) at 100 mA for 45 min.

To monitor the interaction of wild-type sorcin and its mutants with annexin VII, the PVDF membranes were incubated at room temperature with annexin VII (5 μg/ml) in 1% gelatin in TBST buffer (20 mM Tris-HCl, 0.5 M NaCl, 0.05% Tween 20, pH 7.5), containing EGTA or different $CaCl_2$ concentrations. Subsequently, the membranes were incubated with anti-annexin VII polyclonal antibody (dilution 1:3000) in 1% gelatin in TBST buffer.

To monitor the interaction of wild-type sorcin and its mutants with RyR, the PVDF membranes were incubated at room temperature with terminal cisternae vesicles from rabbit skeletal muscle enriched in RyR (5μg/ml), prepared according to Saito et al., 1984). In brief, the skeletal muscles were ground in a meat grinder and then homogenized and centrifuged at 16000 rpm for 30 min. The supernatant was layered onto a gradient of 45%, 38%, 32% and 27% sucrose in 5 mM imidazole-HCl pH 7.4 and centrifuged at 20000 rpm overnight. The membrane fractions located at the interfaces of the gradient steps were collected and examined

by electron microscopy; fractions enriched in terminal cisternae of sarcoplasmic reticulum were present at the interface 38% - 45% sucrose.

The incubation of the PVDF membranes was carried out in TBST buffer containing 10 μM or 500 μM CaCl2. Subsequently, the membranes were incubated with either anti-annexin VII antibody (dilution 1:3000) or anti-RyR monoclonal antibody (dilution 1:1000) in 1% gelatin in TBST buffer. The blots were developed by incubation with alkaline phosphatase conjugate monoclonal anti-mouse IgG (dilution 1:3000) in 1% gelatin in TBST.

Control experiments ruled out the existence of cross-reactivity between the sorcin and its mutants and anti-annexin VII or the anti-RyR antibody.

2.7 SURFACE PLASMON RESONANCE EXPERIMENTS

The surface plasmon resonance-based biosensor technology allows the real time detection and assessment of biomolecular binding events.

The SPR phenomenon occurs when polarized light, under conditions of total internal reflection, strikes an electrically conducting gold layer at the interface between media of different refractive index: the glass of a sensor surface and a water solution.

The angle of incident light at which SPR occurs (named Resonance Angle) is strongly dependent on the refractive indices of all the boundary media, including the gold film, the bulk solution and additional layers such as interacting molecules.

In a typical experiment, one of the interacting molecule is bound to the biosensor surface, whereas the other is delivered to the surface in a continuous flow. Binding to the immobilized ligand is monitored by changes of resonance angle which are directly proportional to the mass of molecules that bind to the sensor surface.

SPR experiments were carried out using a BIACORE X system (BIAcore AB, Uppsala, Sweden).

The N-terminal peptide of annexin VII was synthesized by SIGMA-Genosys (Cambridge, UK); in order to improve peptide solubility and binding to the sensor chip, three lysine residues were added N-terminal to the 20 first amino acids (MSYPGYPPTGYPPFPGYPPA). The peptide purity was checked by MALDI-TOF mass spectrometry.

The sensor chip (CM5, Biacore AB) was activated chemically by injection of 35 μl of a 1:1 mixture of *N*-ethyl-*N′*-(3-dimethylaminopropyl)carbodiimide (200 mM) and *N*-hydroxysuccinimide (50 mM) at a flow rate of 5 μl/min.

The N-terminal peptide of annexin VII was immobilized on the activated sensor chip via amine coupling. The reaction was carried out in 20 mM sodium acetate at pH 6.0; the remaining ester groups were blocked by injecting 1 M ethanolamine hydrochloride (35 µl). In control experiments, the sensor chip was treated as described above in the absence of peptide.

The interaction of the immobilized annexin VII peptide with sorcin and its mutants was detected through mass concentration-dependent changes of the refractive index on the sensor chip surface. Such changes are expressed as resonance units (RU). A response change of 1000 RU typically corresponds to a change in the protein concentration on the sensor chip of about 1 ng per mm^2 .

The experiments were carried out at 25 °C in 10 mM HEPES at pH 7.4, 150 mM NaCl, and 0.005% surfactant P-20. The buffer was treated with Chelex 100 to eliminate Ca^{2+} contaminations and degassed. In the experiments carried out as a function of Ca^{2+} concentration, calcium chloride or EGTA were added to the buffer; protein concentration was 300 nM. Measurements were performed at a flow rate of 20 µl/min with an immobilization level of the annexin VII N-terminal peptide corresponding to 100-900 RU.

Values of the plateau signal at steady state (R_{eq}) were calculated from the sensorgrams using the BIAevaluation 3.0 software.

To assess the dissociation constant, the dependence of the SPR signal at steady state (R_{eq}) on the concentration of wt sorcin was analysed in terms of a Scatchard plot.

2.8 MEASUREMENT OF Ca^{2+} SPARK CHARACTERISTICS IN ISOLATED HEART CELLS

These experiments were carried out by Prof. G.L. Smith, University of Glasgow (UK) in the framework of a collaboration with the Dept. of Biochemical Sciences.

As mentioned in the Introduction (1.4.4) Ca^{2+}sparks reflect RyR activation in cardiomyocytes. However, the investigation of the effect of sorcin on Ca^{2+} sparks in intact rabbit cardiomyocytes is complicated by the parallel effects on the sarcolemmal extrusion of intracellular Ca^{2+}. For this reason, sarcolemmal fluxes are bypassed by the acute permeabilization of the sarcolemma with ß-escin, a permeabilizing agent. Under such experimental conditions, single cardiomyocytes can be superfused using standardized Ca^{2+} concentration and pH in the presence of ATP and creatine phosphate. Ca^{2+} spark activity is monitored

by the inclusion of 10 μM Fluo-3 in the perfusing solution. In this study isolated rabbit ventricular cardiomyocytes were initially suspended in a mock intracellular solution with the following composition (mM): KCl 100, Na_2ATP 5, Na_2CrP 10, $MgCl_2$ 5.5, HEPES 25, K_2EGTA 1, pH 7.0 with no added Ca^{2+} (20-21^{o}C) and permeabilized using β-escin (0.1 mg/ml for 0.5-1 min). Confocal line-scan images of single cardiomyocytes were recorded using a BioRad Radiance 2000 confocal system. Permeabilized cells were perfused with a mock intracellular solution containing 0.05 mM EGTA. Fluo-3 (10 μM) in the perfusing solution was excited at 488 nm (Kr laser line) and measured above 515 nm using epifluorescence optics of a Nikon Eclipse inverted microscope with a 60X/1.2 NA water-immersion objective lens (Plan Apochromat, Nikon, UK). In all experiments included in the analysis, the Ca^{2+} concentration in the test solution was 155-165 nM. Ca^{2+} sparks were quantified using an automatic detection and measurement algorithm.

3. RESULTS

3.1 SITE-SPECIFIC MUTANTS OF EF-HANDS 1, 2 AND 3 (E53Q, E94A, E124A)

3.1.1 CLONING, EXPRESSION AND PURIFICATION

The site-specific mutants E53Q, E94A and E124A were obtained as described under Materials and Methods. The sorcin c-DNA was mutated in order to replace the conserved bidentate glutamate, in position –Z of the EF-hand site, with a glutammine residue in the EF1 site (mutant E53Q) and with an alanine residue in the EF2 and EF3 sites (mutants E94A and E124A, respectively). The length and the purity of the genes were checked by electrophoresis on agarose 1% gel in TBE: the length of the final DNA products was of 620 base pairs as expected.

The DNA fragments were sequenced to verify the introduction of the desired mutation and thereafter were inserted in a recombinant plasmid suitable for protein expression (Pet22).

The recombinant plasmids were used to transform competent E.coli BL21(DE3) cells: the recombinant proteins were expressed and purified following the procedures detailed under Materials and Methods. The expression level was good although lower than for wt-sorcin. Importantly the protein purification procedure, that takes advantage of the reversible translocation of sorcin from cytoplasm to membranes upon calcium binding, resulted suitable also for its site-specific mutants. In brief the procedure entails washing the cell membranes with sonication buffer to eliminate contaminant DNA; as expected, the spectra of the supernatants show a progressive decrease of the absorbance at 260 nm typical of nucleic acids. After elimination of nucleic acids, extraction of the mutants was achieved by resuspending the membranes in sonication buffer containing the calcium chelator EGTA (5 mM). The optical absorption spectra of the mutants thus obtained are shown in Fig. 19.

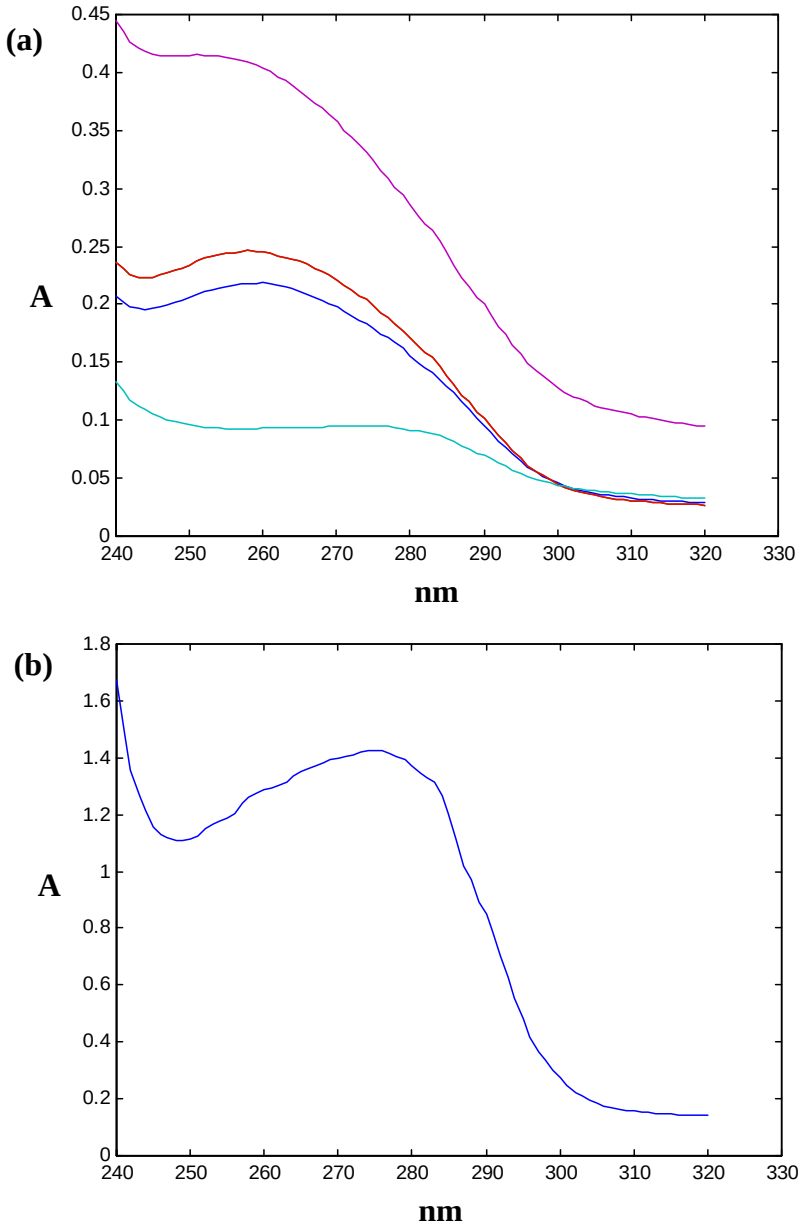

Fig. 19 – Purification procedure of sorcin and its site-specific mutants.

(a): Optical spectra of the supernatants yielded by washing repeatedly the cell membranes to eliminate DNA;

(b): Optical spectrum of the supernatant obtained resuspending the membranes in the sonication buffer containing EGTA.

The SDS polyacrylamide gel electrophoresis patterns presented in Fig. 20 exemplify this part of the purification procedure. Sorcin is associated with the membrane fraction of cells lysed in the presence of contaminating Ca^{2+} (lane P_1) and is released in to the supernatant upon repeated treatment of the membrane fraction with EGTA (lane S_2; lane $S^{\bullet}_2$).

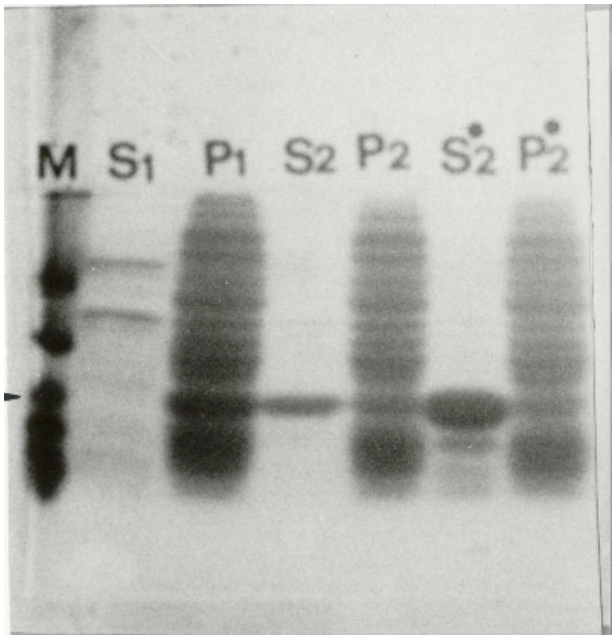

Fig. 20 – SDS PAGE of samples obtained in different steps of the purification procedure of sorcin. M: molecular weight markers (46 kDa, 30 kDa, 21,5 kDa, 14,3 kDa e 6,5 kDa); The arrow indicates the band corresponding to sorcin (Mr 21.5 kDa).
S_1 e **P_1**: supernatant and pellet obtained after centrifugation of the cellular lysate.
S_2, **P_2**, **$S_2^{\bullet}$**, **$P_2^{\bullet}$**: supernatants and pellets yielded in two subsequent extractions with EGTA 5mM.

The final purification step was achieved by means of a Mono-Q anion-exchanger column. The yield of purified site-specific mutants is about 4-5 mg/l of culture, two-three time lower with respect of wild type sorcin.

3.1.2 STRUCTURAL CHARACTERIZATION

Far and near UV CD spectroscopy was used to assess the possible occurrence of structural changes in the mutated apoproteins with respect to wt sorcin.

The experiments were carried out at pH 7.5 and at pH 6.0 since the X-ray crystal structure of the Ca^{2+}-binding domain was obtained at the latter pH value (Ilari et al., 2002).

The far UV CD spectra of all the site-specific mutants, measured at 20°C in the absence of calcium, are indistinguishable from that of wt sorcin at both pH values. The α-helical content, calculated from the ellipticity value at 222 nm, is about 60% for all the proteins analysed (sorcin, E53Q, E94A, E124A) in accordance with the crystallographic structure of SCBD. The spectra in the far UV region were measured at 20°C in the absence of calcium, because previous experiments had shown that calcium–binding does not alter the secondary structure of sorcin (Zamparelli et al., 1997).

In the near UV-CD region the spectrum of wild-type sorcin is negative and is characterized by two sharp bands at 262 and 268 nm attributed to phenylalanines, by a weaker band at 283 nm due to tyrosyl fine structure, and by a fairly intense, well resolved peak at 292 nm due to tryptophan residues. The spectra of the site-specific mutants are very similar to those of the wild-type protein at both pH values with the exception of E124A. Thus, in the E124A variant, the phenylalanine bands are unchanged, whereas the bands of tyrosine and tryptophan residues occur at the same wavelength as in the wild-type protein but have a smaller amplitude at both pH values (Fig. 21).

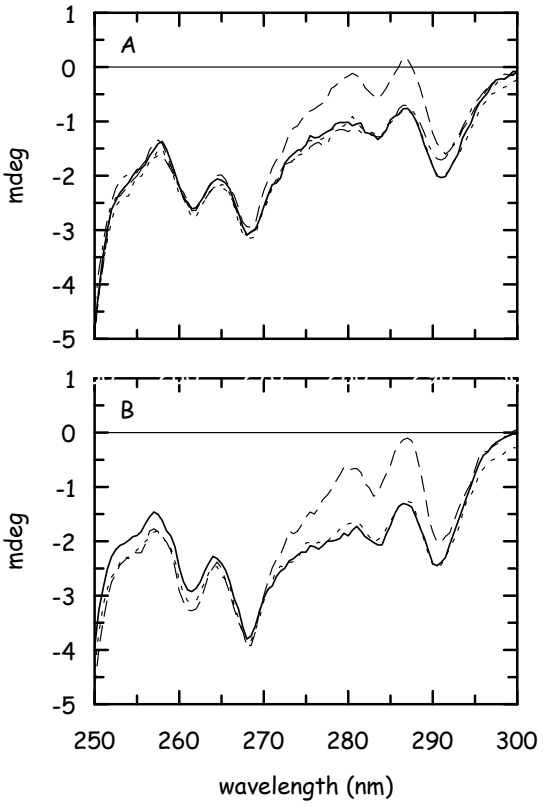

Fig. 21 – Near UV circular dichroism spectra of wild type sorcin and of the E53Q, E94A, and E124A mutants. Wild-type sorcin (—), E53Q (····), E94A(-), E124A (---) were at concentration of 50 μM. A, 0,1 M sodium acetate buffer, pH 6.0, 40°C. B, 0.1M Tris-HCl buffer, pH 7.5, 25°C.

The effect of calcium on the near UV CD spectra was not studied because, at the protein concentration employed, sorcin and its variants precipitate upon binding of 2 Ca^{2+}/monomer in the absence of target proteins due to the exposure of hydrophobic surfaces.

3.1.3 FUNCTIONAL CHARACTERIZATION

3.1.3.1 Determination of calcium affinity

The affinity for calcium of sorcin variants could not be determined in direct fluorescence experiments since the fluorescence intensity is practically unchanged upon binding of 2 eq of Ca^{2+}/monomer, as for the wild-type protein, and higher amounts of calcium lead to precipitation.

Therefore, calcium affinities were determined in indirect fluorescence experiments in the presence of Quin2, a chelator that binds calcium with K_D 0.06 μM at pH 7.5. Sorcin and its variants compete effectively with Quin 2 for the binding of calcium. This competition causes a shift to the right of the titration curve of the chelator; from the extent of the shift it is possible to calculate the Ca^{2+} affinity constants of the different proteins. The titrations were performed in Tris 100 mM, pH 7.5 at 25°C and the increment of fluorescent emission intensity at 492 nm due to calcium binding to Quin2 followed. The titration curves of wild type sorcin and its variants are presented in Fig. 22 in terms of the degree of saturation of Quin 2 as a function of total calcium concentration. Simple inspection of the data indicates that in the mutants calcium affinity decreases with respect to the wild-type protein in the order E53Q > E94A > E124A.

For the analysis of the titration data a mathematical model that simulates the competition between the chelator and the protein for the binding of $Ca^{2+}$was used. Due to the occurrence of precipitation upon saturation of sorcin with 2 eq Ca^{2+}/ monomer, higher Ca^{2+}/ protein ratios cannot be scrutinized; hence, one is forced to analyze the titration data in terms of a two site model. On the basis of the statistical parameters obtained from the fitting procedure, the behaviour of the wild type protein can be described with two dissociation constants in the micromolar range namely $K_1 = 0.42 \pm 0.05 \times 10^{-6}$ M and $K_2 = 6.3 \pm 4.1 \times 10^{-6}$ M using a dissociation constant for the chelator of 60 nM at pH 7.5, 20°C. The titration curves of the site-specific mutants can be fitted by a single binding constant: $0.48 \pm 0.13 \times 10^{-6}$ M in E53Q, $0.71 \pm 0.14 \times 10^{-6}$ M in E94A and $1.10 \pm 0.27 \times 10^{-6}$ M in E124A. The second constant cannot be determined with accuracy because it is below the resolution limits of the technique (about 1×10^{-5} M).

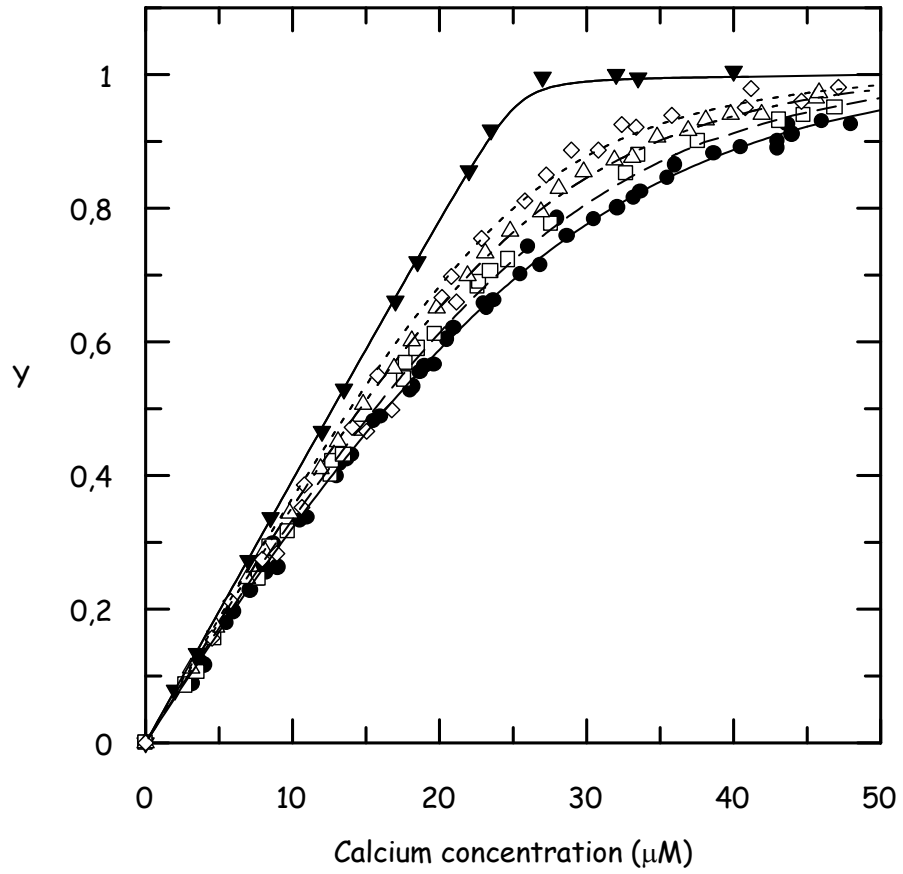

Fig. 22 – Fluorescence titration of wild type sorcin and of the E53Q, E94A, and E124A mutants with calcium in the presence of the calcium chelator Quin2. The degree of saturation of Quin2 (y) is plotted as a function of total calcium concentration. Wild type sorcin (•), E53Q (□), E94A (Δ), E124A (◊) at a concentration of 25 μM were titrated with calcium in the presence of 25 μM Quin2 in 0.1 M Tris-HCl at pH 7.5 and 25°C. The titration of Quin2 alone (▼) is also shown.

The titration data bring out that the E124 variant (mutated EF3 site) is characterized by the largest change in the dissociation constant relative to wild type sorcin while E53Q and E94A mutants (mutated EF1 and EF2 sites, respectively) behave similarly to the native protein. It follows that the site endowed with the highest affinity for $Ca^{2+}$is EF3. The underlying assumption is that the site-specific mutations studied introduce only local structural perturbations, that are limited to the immediate environment of the mutated residue

3.1.3.2 Interaction with annexin VII and the ryanodine receptor monitored in immunoblot and Surface Plasmon Resonance (SPR) experiments.

The determination of Ca^{2+} affinity of the different variants shows that mutation of the EF3 site has the largest effect on this property of sorcin and in turn suggests that the EF3 hand is more important than the EF2 and EF1 hands in determining the conformational change that permits interaction with target proteins. To prove this hypothesis, interaction of the site-specific mutants with two physiological sorcin targets was assessed, namely annexin VII and RyR which are known to interact with N- and C-terminal sorcin domains respectively (Verzili et al., 2000; Zamparelli et al., 2000).

In a first set of experiment wild-type sorcin and its mutants were subjected to electrophoresis, transferred to polyvinyldifluoride membranes and then incubated with annexin VII at pH 7.5 in buffer containing 10 or 500 μM calcium. Complex formation was detected by incubation with polyclonal anti-annexin VII antisera and thereafter with alkaline phosphatase conjugate monoclonal anti-mouse IgG. Figure 23a shows the immunoblot obtained in the presence of 10 μM calcium while Figure 23b displays those in 500 μM calcium. At the lower calcium concentration, E53Q and E94A interact with annexin VII similarly to wild type sorcin, whereas no interaction is detected for the E124 mutant. At the higher calcium concentration, all the proteins interact with annexin VII in a similar way.

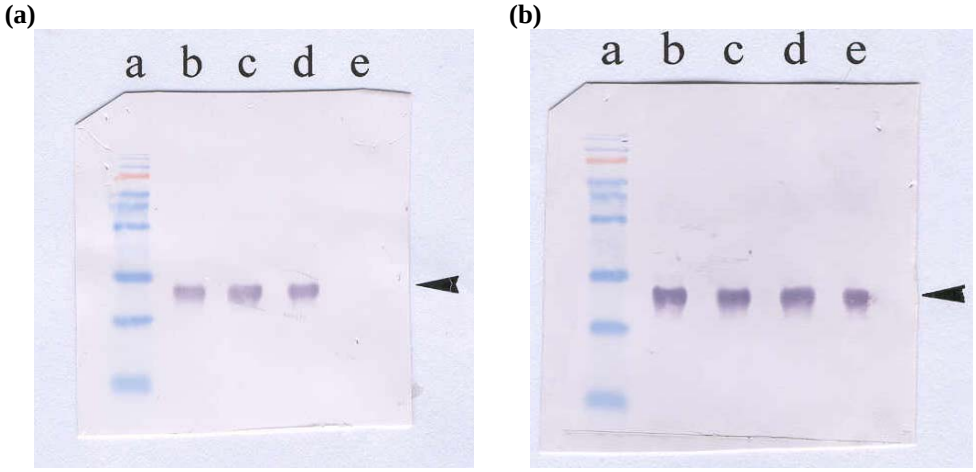

Fig. 23 – Interaction of wild-type sorcin and of the E53Q, E94A and E124A mutants with annexin VII in the presence of 10 μM $CaCl_2$ (a) or 500 μM $CaCl_2$ (b). a, molecular weight markers (180, 130, 100, 73, 54, 50, 35, 24, 16, and 10kDa). b, wild-type sorcin; c, E53Q; d, E94A; e, E124A subjected to SDS-PAGE and transferred to PVDF membranes. The arrow indicates the band corresponding to sorcin (M_r 21.5 kDa).

In a second set of overlay assay experiments, the interaction between the site-specific sorcin mutants and RyR was monitored. Wild-type sorcin and the E53Q, E94A and E124A proteins were transferred to PVDF membranes and incubated with RyR-enriched terminal cisternae vesicles extracted from rabbit skeletal muscle in buffer containing 10 or 500 μM calcium (Fig. 24a and 24b, respectively). The interaction was detected using monoclonal anti-RyR antibody and alkaline phosphatase conjugate monoclonal anti-mouse IgG. As for annexin VII, at 10 μM calcium wild type sorcin, E53Q and E94A interact with RyR whereas no interaction occurs in the case of the E124A mutant; at the higher calcium concentration all the proteins interact with RyR to a similar extent. In control experiments carried out in EGTA-containing buffer no interaction of sorcin and its mutants with annexin VIII or with RyR was observed (data not shown).

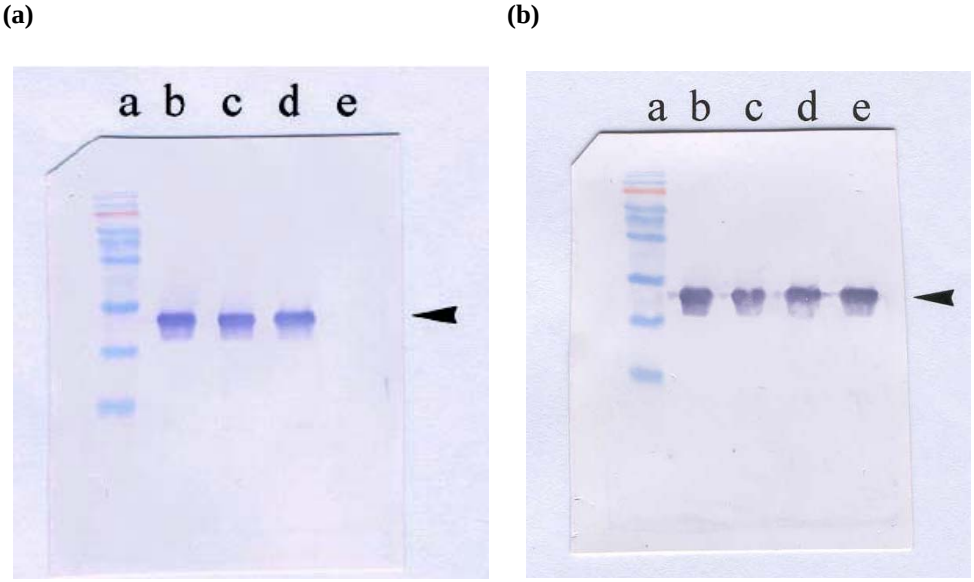

Fig. 24 – Interaction of wild-type sorcin and of the E53Q, E94A and E124A mutants with the ryanodine receptor in the presence of 10 μM $CaCl_2$ (a) or 500 μM $CaCl_2$ (b). a, molecular weight markers (180, 130, 100, 73, 54, 50, 35, 24, 16, and 10kDa). b, wild-type sorcin; c, E53Q; d, E94A; e, E124A subjected to SDS-PAGE and transferred to PVDF membranes. The arrow indicates the band corresponding to sorcin (M_r 21.5 kDa).

Surface Plasmon Resonance was used to obtain quantitative information on the interaction between sorcin and its site-specific (E53Q, E94A, E124A) mutants with annexin VII, an interaction known to involve the N-terminal domain of both proteins (Brownawell and Creutz, 1997).

The experiments were performed by immobilizing on the chip a synthetic peptide corresponding to the annexin VII N-terminus (amino-acids 1-20) extended by the addition of three lysine residues before amino acid 1 in order to increase peptide solubility and to favour its binding to the sensor chip via amine coupling. The use of the annexin VII N-terminus presents several advantages over immobilization of the entire protein. It increases the lifetime of the chip and simplifies the experimental picture because the peptide does not bind calcium. Under same conditions the immobilized annexin VII N-terminus yields apparent K_D values in good agreement with the results obtained with the full-length protein, thus this peptide was chosen for the systematic study of the interaction with sorcin and its mutants.

A typical sensorgram display three phases; the increase in RU from the baseline upon sample injection corresponds to association of sorcin or its mutants to the immobilized annexin peptide, the plateau represents the steady-state phase of the interaction, and the decrease in RU corresponds to the dissociation phase during buffer flow at the end of the sample injection.

The Ca^{2+}-dependence of the interaction with the annexin VII N-terminus was assessed at constant (300 nM) concentration of native or mutant sorcin. The sensorgrams are shown in Fig. 25 A-D. In Fig. 25 E the values of the plateau signal at steady state (R_{eq}), obtained from the data depicted in Fig. 25 A-D and in an independent set of experiments, are plotted as a function of calcium concentration. Analysis of the sensorgrams shows that the k_{on} and k_{off} values of the mutants increase with respect to native sorcin while the RU values in the plateau region (R_{eq}), and hence the amount of bound analyte, decrease at all calcium concentrations. As expected for any given protein, the R_{eq} values increase when the calcium concentration in the medium increases. The R_{eq} values show that the affinity for the annexin VII N-terminus decreases in the order wild-type sorcin > E53Q > E94A > E124A and thus confirm that mutation of EF3 has the highest effect on the ability of sorcin to interact with annexin VII.

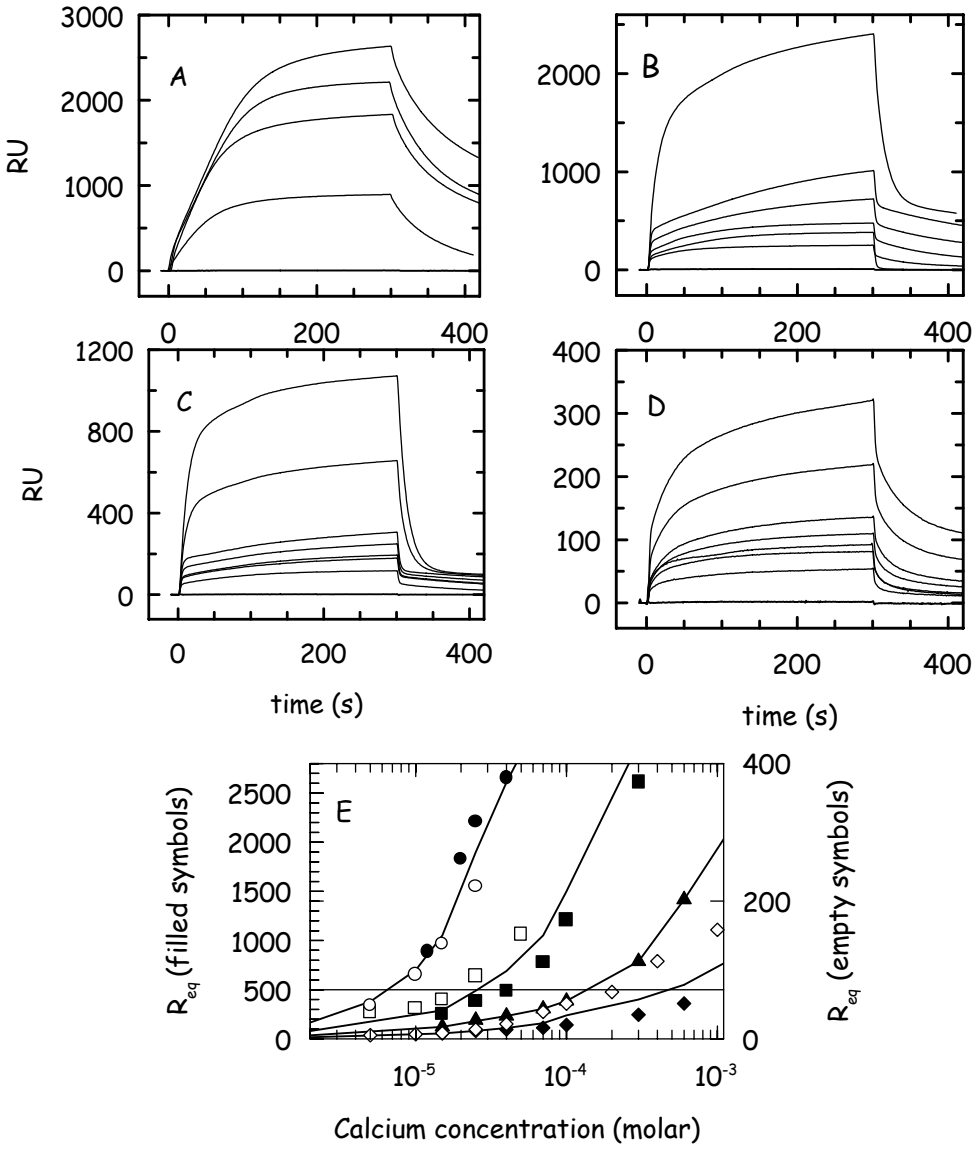

Fig. 25 – SPR experiments on the binding of sorcin or its E53Q, E94A, and E124A mutants to the immobilized N-terminal peptide of annexin VII as a function of calcium concentration. A, wild-type sorcin in buffer containing 2mM EGTA and 12, 20, 25 and 40 μM $CaCl_2$ (from bottom to top). B, E53Q mutant in buffer containing 2mM EGTA and 15, 25, 40, 70, 100 and 300 μM $CaCl_2$ (from bottom to top). C, E94A mutant in buffer containing 2mM EGTA and 15, 25, 40, 70, 100, 300 and 600 μM $CaCl_2$ (from bottom to top). D, E53Q mutant in buffer containing 2mM EGTA and 15, 25, 40, 70, 100, 300 and 600 μM $CaCl_2$ (from bottom to top). E, the plateau signal at steady state (R_{eq}) is plotted as a function of total calcium concentration. Wild-type (● and ○), E53Q (■ and □). E94A (▲) and E124A (◊ and ♦) sorcin. Filled and empty symbols refer to data obtained with two different chips.

3.2 D-HELIX SITE-SPECIFIC MUTANTS (W99G, W105G)

3.2.1 CLONING, EXPRESSION AND PURIFICATION

The sorcin site-specific variants W99G and W105G were obtained as detailed under Materials and Methods. In these variants the two Trp residues located in the D-helix were replaced in the sorcin c-DNA with a glycine residue. The length and purity of the genes were checked by electrophoresis on 1% agarose gel in TBE: the final DNA products have the expected length of 620 base pairs. The DNA fragments were sequenced to verify the introduction of the desired mutation and were inserted into a recombinant plasmid suitable for protein expression (Pet22).

The recombinant plasmids were used to transform competent *E. coli* BL21(DE3) cells, as described under Materials and Methods. The recombinant proteins were expressed and purified according to the same purification procedure used for the native protein (see Materials and Methods) which exploits the occurrence of a significant Ca^{2+}-induced conformational change that leads to interaction with membrane proteins. Both the W99G and W105G variants undergo the calcium induced activation albeit at higher concentrations than wt sorcin.

The expression levels of the site-specific mutants are somewhat lower than those of native sorcin.

3.2.2 STRUCTURAL CHARACTERIZATION

The tendency to aggregate and precipitate upon Ca^{2+}-binding, which limits the experimental conditions that can be used for the measurement of the Ca^{2+}-bound protein spectra is particularly marked in the W105G mutant.

Possible structural changes relative to the wild-type protein were monitored by means of CD and fluorescence spectroscopy and by analytical ultracentrifugation.

The folding of the mutated apoproteins is essentially unaltered with respect to wild-type sorcin as indicated by the far UV CD spectra (fig. 26) and points to a similar α-helical content, i. e. 60% for wt sorcin and 58% for both W99G and W105G.

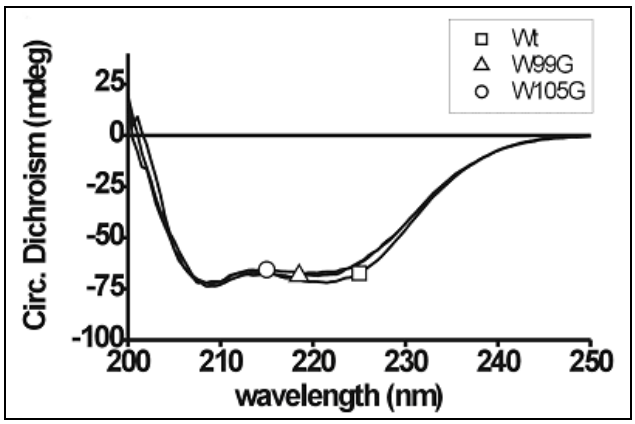

Fig. 26 – Spectroscopic characterization of wt sorcin and its W99G and W105G vartiants. Wt (□), W99G (○), W105G (Δ) sorcin. Far-UV CD spectra in 5 mM Tris-HCl pH 7.5 and 20°C, protein concentration: 18μM.

Support for the similarity of tertiary-quaternary structure was gained from the similarity of the weight-average molecular mass (M_W) calculated from sedimentation velocity experiments (35000 Da for wild-type sorcin, 36500 Da for W99G, and 34700 Da for W105G).

The occurrence of structural perturbations that are localized to the environment of the tryptophan residues and of other aromatic side chains is indicated by the near UV-CD (fig. 27) and fluorescence emission spectra (fig. 28) of the mutated proteins.

The near UV CD spectrum of native sorcin is negative and shows two sharp bands (262-268 nm) attributed to phenylalanines, a weaker band (283 nm) due to tyrosyl residues and an intense well-resolved peak (292 nm) due to tryptophan residues. The near-UV CD spectrum of the W105G mutant is similar to that of the wt protein, although the ellipticity is less negative, while in the W99G spectrum the ellipticity is positive in the 272-292 region as in the case of Ca^{2+}-bound wt sorcin.

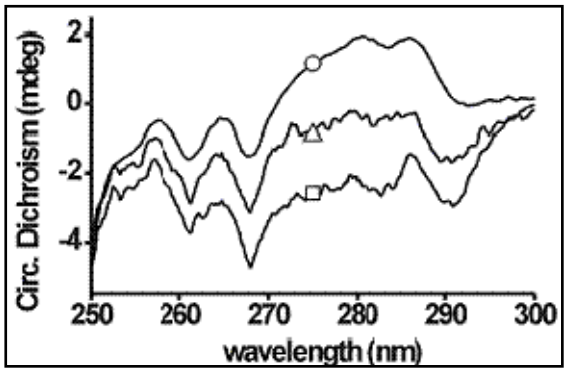

Fig. 27 – Near-UV CD spectra of Wt (□), W99G (○), W105G (Δ) sorcin in 100mM Tris-HCl pH 7.5, 2 mM EGTA and 20°C; protein concentration: 30μM.

The fluorescence emission spectrum of the native sorcin displays a broad peak with a maximum at 338 nm, upon excitation at 280 nm. The fluorescence emission spectra of the two sorcin variants display a decrease of the intrinsic fluorescence, since most of the aromatic contribution at 280 nm is due to tryptophan residues. The emission peak of W99G is blue-shifted by 2 nm relative to wt sorcin, whereas the emission peak of W105 is red shifted by the same amount. Interestingly, in 285-300 nm region the spectra of the two mutants are not additive, an indication that mutation of W99 and of W105 alters the microenvironment of the other chromophore.

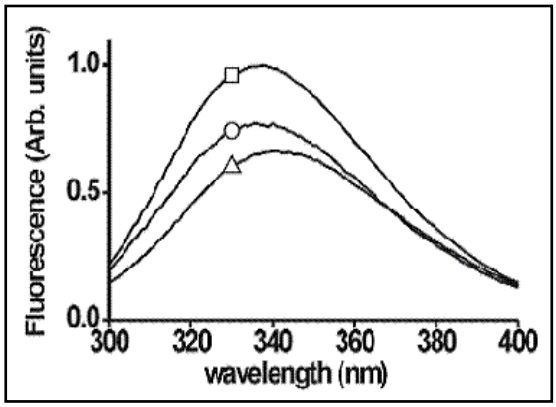

Fig. 28 – Fluorescence emission spectra of Wt (□), W99G (○), W105G (Δ) sorcin in 100 mM Tris-HCl pH 7.5 and 25°C, protein concentration: 4 μM, excitation wavelength: 280nm, slit width: 0.5nm.

3.2.3 FUNCTIONAL CHARACTERIZATION

3.2.3.1 Determination of calcium affinity

As in the case of the site-specific mutants E53Q, E94A and E124A, the affinity for calcium of the W99G and W105G variants could not be determined in direct fluorescence experiments, but was estimated by means of indirect fluorescence titrations in the presence of the fluorescent chelator Quin2. The results obtained at pH 7.5 are presented in Fig. 29 in terms of the degree of Quin 2 saturation as a function of total calcium concentration. The Ca^{2+} affinity of the W99G and W105G variants is practically unaltered relative to wt sorcin and can be fitted likewise with two Ca^{2+} binding constants in the micromolar range [K_1= (0.5 ± 0.2) x 10^{-6}M and K_2 ~10^{-5}M] using a dissociation constant for the chelator of 60 nM. The K_1 value is better defined than K_2; the value of the latter binding constant is at the resolution limits of the technique under the conditions used.

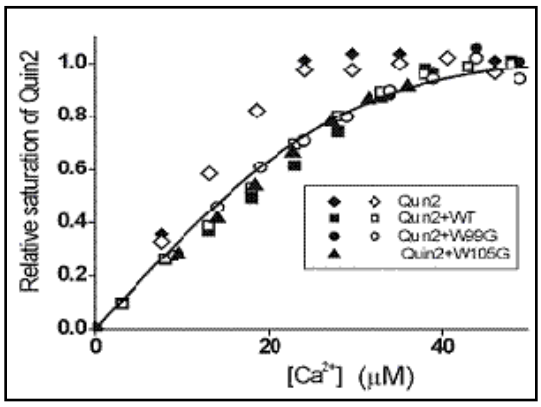

Fig. 29 – Fluorescence titration of wild type sorcin and its W99G and W105G variants with calcium in the presence of the calcium chelator Quin2. The relative saturation of Quin2 is plotted as a function of total calcium concentration. WT (□, ■), W99G (○, ●), and W105G (▲) sorcin at a concentration of 25 μM were titrated with calcium in the presence of 25 μM Quin2 in 0.1 M Tris-HCl at pH 7.5 and 25°C. The titrations of Quin2 alone (◊, ♦) are also shown. Filled and empty symbols refer to data obtained in two different titrations.

3.2.3.2 Interaction with annexin VII monitored in immunoblot and Surface Plasmon Resonance (SPR) experiments.

To establish whether W99G and W105G are able to interact with annexin VII immunoblot experiments were performed, first. The results presented in Fig. 30 indicate that binding of annexin VII to W99G is significant when the total calcium concentration is 10 μM and that comparable binding to W105G is observed only when the cation concentration is increased to 75 μM.

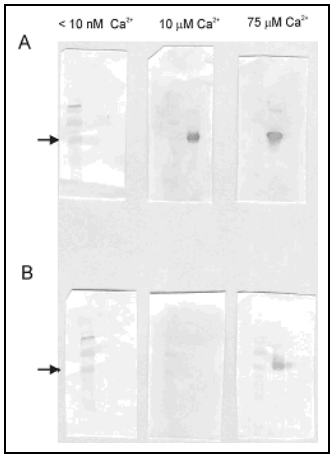

Fig. 30 – Interaction of the W99G and W105G sorcin variants with annexin VII. The variants were subjected to SDS-PAGE and transferred to PVDF membranes which were incubated with annexin VII in the presence of <10 nM, 10 or 75 μM CaCl2 (from left to right) and subsequently with anti-annexin monoclonal antibody. A, W99G. B, W105G. Lane 1: molecular mass markers (46, 30, 21.5, 14.3, 6.5 and 3.4 kDa); lane 2: sorcin variant. The arrows indicate the band corresponding to sorcin (Mr 21.5 kDa).

In SPR experiments was studied the effect of the mutation on the sorcin-annexin VII interaction in a quantitative manner. The experiments were carried out as a function of both Ca^{2+} and protein concentration.

At constant protein and calcium concentration the plateau signal at steady-state (R_{eq}) obtained with wild-type sorcin and W99G are very similar (Fig. 31 A).

When the experiments are performed as a function of calcium concentration at constant protein concentration, the R_{eq} values increase with increase in calcium concentration (Fig. 31 B). The R_{eq} values of W99G resemble those of wt sorcin at < 40 μM calcium, but are slightly lower at higher calcium concentrations. In contrast, the R_{eq} values obtained with W105G are significantly lower with respect to wt sorcin at all the Ca^{2+} concentrations investigated. At 50 μM calcium, for example, the R_{eq} values correspond to 385 for wt sorcin, 287 for W99G, and 79 for W105G. Thus, the experiments show that the affinity for the annexin VII N-terminus decreases in the order wild-type sorcin ≥ W99G > W105G.

A further series of experiments was performed as a function of protein concentration at a constant calcium concentration of 20 μM (Fig. 31 C). These experiments have allowed the assessment of the apparent dissociation constant, K_D, for each protein by Scatchard analysis of the ratio R_{eq}/C versus R_{eq}. The analysis yields apparent K_D values, at 20 μM calcium, of 1.9 μM for wt sorcin, 2.0 μM for W99G. and 12.6 μM for W105G.

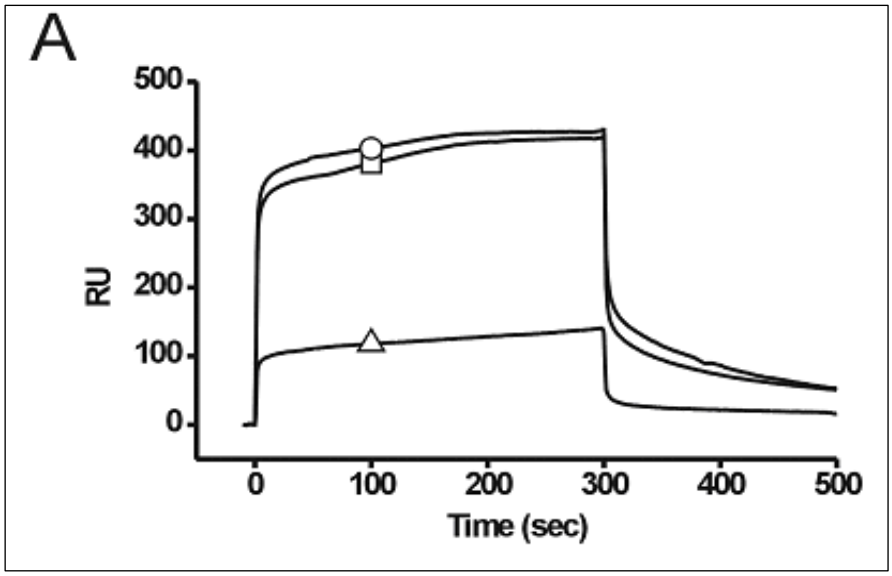

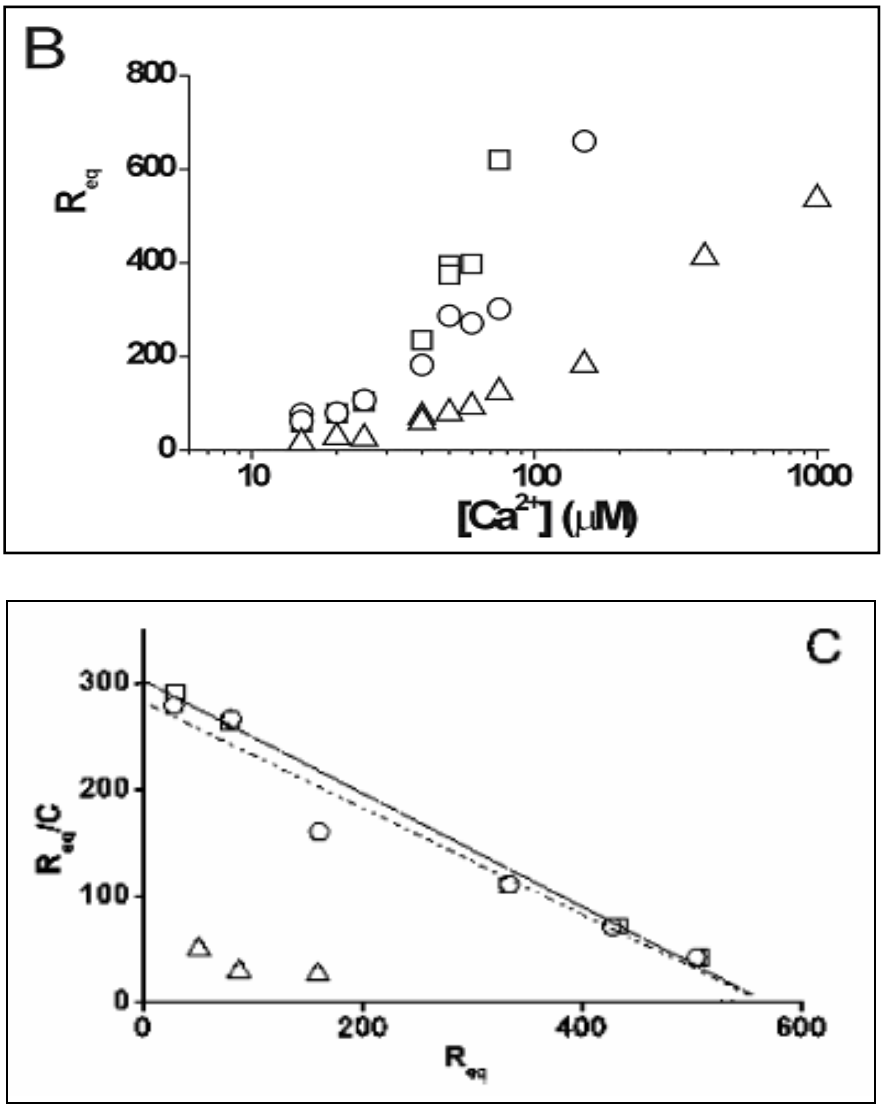

Fig. 31 – Binding of wt sorcin and its W99G and W105G variants to the immobilized N-terminal peptide of annexin VII at different Ca^{2+} concentrations. Wt (□), W99G (○) and W105G (Δ) sorcin. A, sensorgrams of 6 μM sorcin injected at time zero onto a chip containing the immobilized N-terminal annexin VII peptide. The increase in RU relative to base line indicates complex formation; the plateau region represents the steady-state phase of the interaction, whereas the decrease in RU represents sorcin dissociation from the immobilized peptide after injection of buffer (10 mM HEPES, 0.15 M NaCl, 20 μM $CaCl_2$, 0.005% surfactant P20 at pH 7.4). Temperature, 25°C. B, the plateau signal at steady state (R_{eq}) is plotted as a function of total Ca^{2+} concentration. Sorcin concentration, 1 μM in 10 mM HEPES, 0.15 M NaCl, 0.005% surfactant P20 at pH 7.4. Temperature, 25 °C. C, the plateau signal at steady state (R_{eq}) measured at different sorcin concentrations (C) is plotted as a function of R_{eq}/C; buffer: 10 mM HEPES, 0.15 M NaCl, 20 μM $CaCl_2$, 0.005% surfactant P20 at pH 7.4.

3.2.3.3 Effect on the activity of the ryanodine receptor in isolated cardiomyocytes

The interaction of sorcin and its D-helix variants W99G and W105G with RyR was monitored by measuring the effect on the RyR-activated Ca^{2+} release process which manifests itself in Ca^{2+} sparks.

The protocol used to introduce recombinant protein into permeabilized myocytes is shown in Fig. 32 A. After the exposure to β-escin for 30 s, the myocytes were superfused with a mock intracellular solution for 30 s before superfusing with 3 μM sorcin, or sorcin variants, for 2 min. After superfusion, sparks were monitored for 10-12 min in the absence of flow. Sample line-scan records that display the transient increases in intracellular Ca^{2+} concentration characteristic of Ca^{2+} sparks are presented in Fig. 32 B. Spark frequency progressively decreases by 20-25% over 10-12 min and the inclusion of sorcin in the perfusion solution causes a more marked decrease in spark frequency, reaching a steady state after 8-10 min (Fig. 32 C).

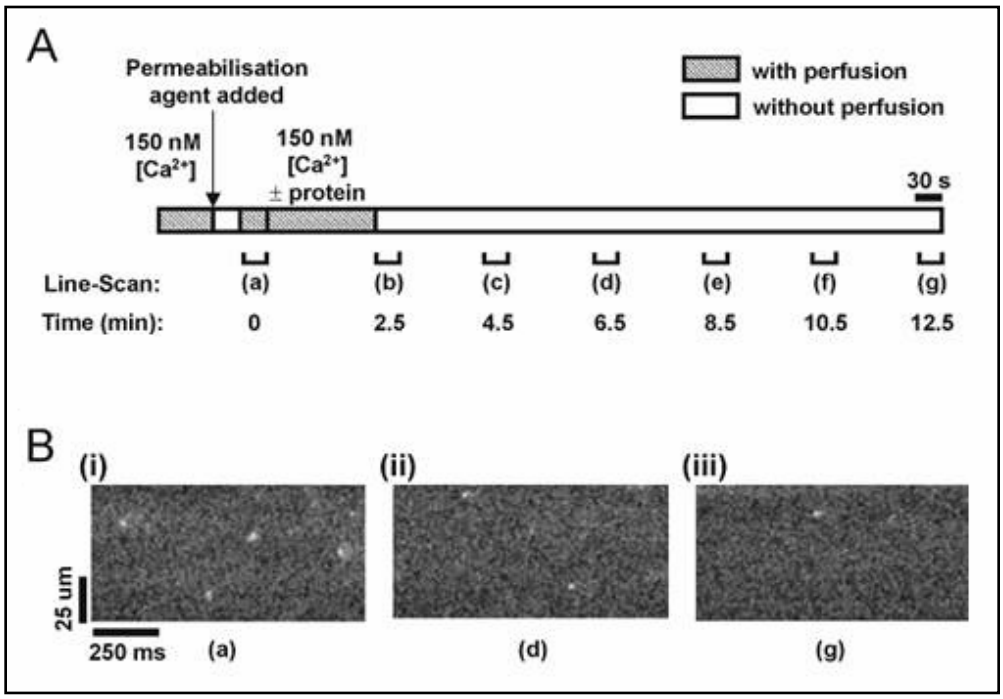

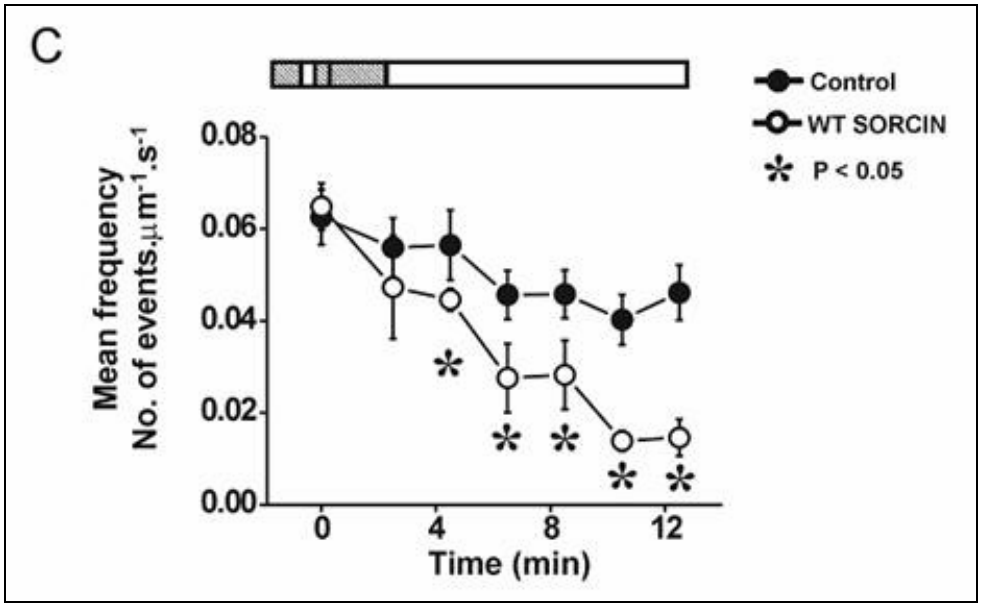

Fig. 32 – Ca^{2+} spark protocol. A, the experimental protocol used to introduce recombinant protein to permeabilised myocytes. B, sample line-scans: 0 (a) 6 (d) and 12 min (g) after permeabilization. C, the mean spark frequency at various times after permeabilisation. Steady state values were measured at 10-12 mins of incubation with the recombinant protein.

The effect of W99G and W105G on RyR activity was compared to that of wt sorcin by analysing the spark characteristics after incubation with each protein for 10 min; the spark parameters were compared with those observed after incubation for the same time with a solution of the identical composition without the protein. (Fig. 33) The inhibitory effect of sorcin on RyR manifests itself in the significant reduction not only of the mean values of Ca^{2+} spark frequency, but also of spark width, spark peak and spark duration compared to the control spark parameters (Fig. 33 A).

The two site-specific mutants have a contrasting effect: W99G behaves in a manner similar to wt sorcin pointing to the occurrence of interaction (Fig. 33 B), while, in the presence of the W105G mutant, the Ca^{2+} spark parameters are close to those of the control cardiomyocytes (Fig. 33 C).

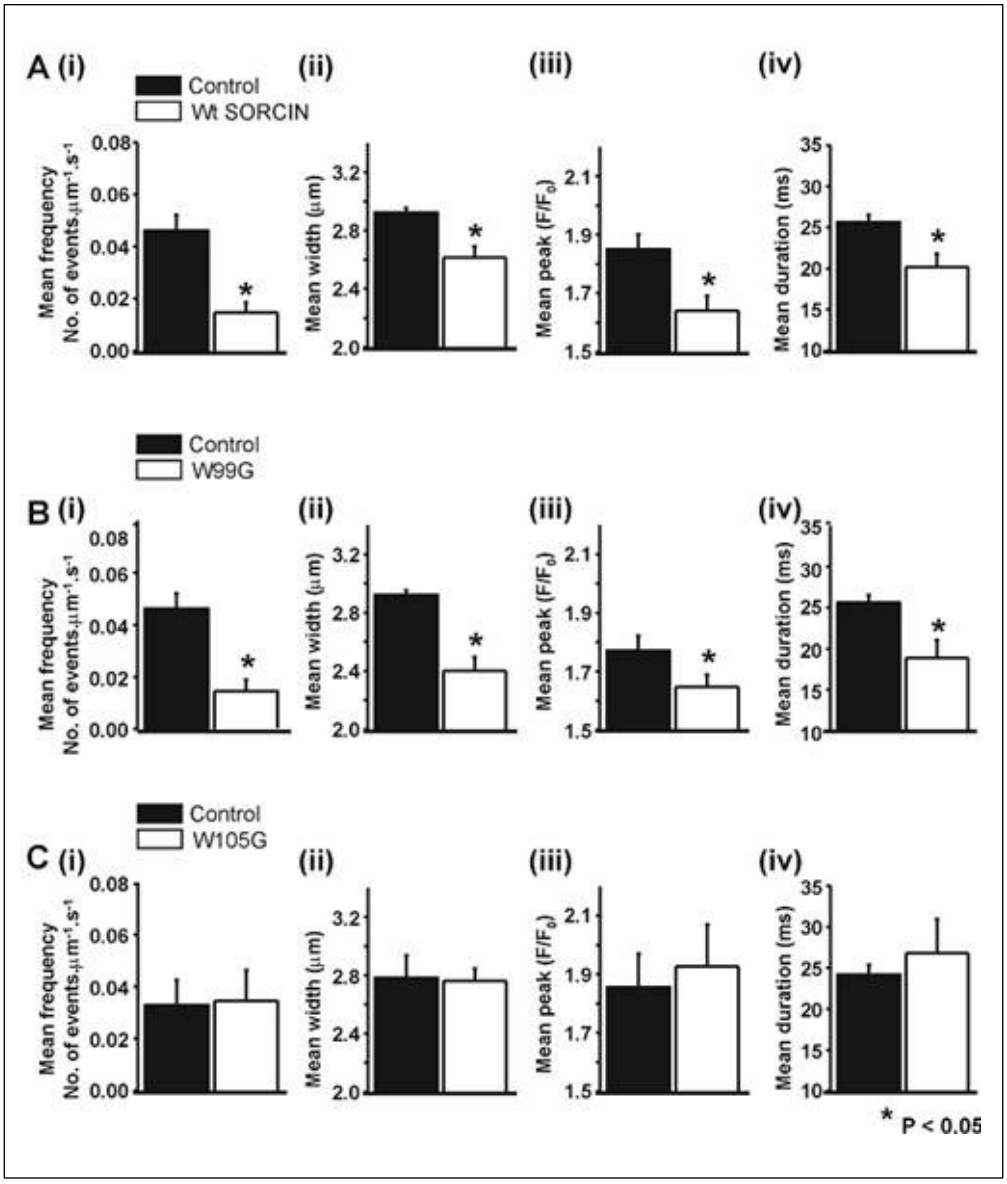

Fig. 33 – Effect of wt sorcin, W99G and W105G on Ca^{2+} spark properties. Mean ± SEM values for: (i) spark frequency; (ii) spark width (full width half maximal); (iii) peak F/F_o; (iv) spark duration (full width half maximal). A, control group, n = 4 cells; 636 events; sorcin, n = 4 cells, 176 events. B, control group, n = 5 cells, 795 events; W99G group, n = 5 cells, 200 events. C, control group, n = 4 cells, 630events; W105G group, n = 4 cells, 592 events. * $P < 0.05$.

4. DISCUSSION

Sorcin shares with the other members of the PEF family the ability to translocate from cytosol to membranes upon binding of calcium. In turn, the change in subcellular localization is exploited for the transmission of Ca^{2+}-triggered biochemical signals to a variety of target proteins that have been identified in the cell types where the protein is expressed constitutively.

The molecular mechanism underlying the activation process is still elusive also because the available PEF proteins X-ray crystal structures reveal only limited and subtle changes between the Ca^{2+}-free and Ca^{2+}-bound forms (Blanchard et al., 1997; Lin et al., 1997; Jia et al., 2000; Strobl et al., 2000). Therefore, the information of the occurrence of Ca^{2+} binding needs not only to be transmitted from the functional EF-hands but also to be amplified into a structurally significant conformational change.

To address these aspects of sorcin structure and function, the functionally relevant EF-hands have been identified first. In sorcin, EF4 and EF5 are non canonical and diverge from the canonical EF-hands in terms of length and sequence of the loop; these sites therefore are unlikely to bind calcium at micromolar concentrations and likely have a structural role. According to the protein sequence, only the EF1, EF2 and EF3 sites are potentially able of binding calcium at these physiological concentrations. A comparison of their sequence predicts that the EF3-hand should be endowed with the highest affinity for the metal. Thus, the unusual EF1 site lacks an acidic residue in the metal coordination positions and has a gap in position Y of the Ca^{2+} binding loop; EF2 should have a lower affinity for calcium relative to EF3 due to substitution of the canonical aspartate in position –X by a glycine residue. However, these sequenced-based arguments do not allow one to predict how different the Ca^{2+} affinities of these sites will be.

Titration of sorcin with calcium in the analytical ultracentrifuge shows that the binding of two Ca^{2+}/monomer suffices to trigger the functionally relevant conformational change. When the levels of Ca^{2+} exceed 2 equiv/monomer, the absorbance at 280 nm decreases abruptly due to formation of aggregates. In fact, the Ca^{2+}-induced conformational change leads to exposure of hydrophobic surfaces and to sorcin precipitation in the absence of molecular targets (Zamparelli et al., 2000).

The two physiologically relevant EF-hands were identified by site-directed mutagenesis of the conserved glutamate in position –Z

in the EF1, EF2 and EF3 sites. Only those mutations involving a physiologically relevant site are expected to alter the functional properties of the mutant significantly relative to the wt protein provided that only the properties of the mutated site are influenced. This approach has been applied successfully for example in the case of m-calpain mutants (Dutt et al., 2000).

The far and near UV CD spectra used as structural markers to characterize the E53Q, E94A and E124A mutants, where EF1, EF2 and EF3 are mutated respectively, indicate that the global fold and the environment of the aromatic residues are essentially unperturbed relative to wt sorcin (Fig. 21). The only exception concerns the environment of tyrosine and tryptophan residues in the E124A mutant, as manifest in the near UV CD spectrum. Thus, the tyrosine band at 283 nm has a significantly smaller amplitude than in the native protein (Fig. 21). This change has been attributed to disruption of the network of hydrogen bonding and hydrophobic interactions that in Ca^{2+}-free sorcin comprises the Glu124 carboxylate, the D-helix with the two Trp residues (99 and 105), and the aromatic ring of Tyr67 located on the loop connecting EF1 to EF2 (Ilari et al., 2002). The observation that the Glu 124 carboxylate is not solvent exposed conforms to the behaviour of the –Z ligand in regulatory proteins (Xie et al., 2001). In turn, the Tyr67-OH is hydrogen bonded to Asp113 which occupies the X position in the EF3 Ca^{2+}- binding loop. Tyr67, due to this hydrogen bonding interaction, should contribute significantly to the strength of the tyrosine CD band. Thus, removal of E124 and disruption of the interaction network should decrease the band amplitude as is indeed observed in the E124A mutant. The concomitant decrease in the tryptophan band at 292 nm has functional implications because it suggests that the loss of the hydrogen-bonding interactions established at the EF3 Ca^{2+} binding loop by Asp113 and Glu124 is sensed also by Trp99 and Trp105 located on the long and rigid D-helix that connects EF3 to EF2. On this basis, the D-helix appears capable of transferring the structural perturbations originating in the EF3 Ca^{2+}-binding loop far from the site of mutation. In turn, this far reaching effect of the Glu124 mutation points to EF3 as the ideal trigger of the pathway that leads from Ca^{2+} binding to sorcin activation. However, for this picture to be true EF3 should be endowed with the highest affinity for Ca^{2+}.

The fluorescence titration data in the presence of Quin2 show that it is the case (Fig. 22). The overall affinity for Ca^{2+} follows the order wild-type sorcin > E53Q > E94A > E124A, indicating that disruption

of the EF3 site has the largest effect on this property of the protein. Disruption of the EF2 and EF1 hands has progressively smaller effects.

The immunoblot data likewise point to a major functional role of EF3: the E124 mutant requires a significantly higher calcium concentration (500 μM) than wild-type sorcin, E53Q and E94A for interaction with the binding partners annexin VII and RyR which bind to the N- and C-terminal sorcin domains, respectively (Fig. 23-24). Disruption of the EF3 site therefore has the largest effect on the ability of sorcin to interact with its molecular targets. The extent of the functional impairment was estimated by means of SPR experiments that assess directly the interaction of wt sorcin and the various EF-hand mutants with the immobilized N-terminal peptide of annexin VII. As shown by Verzili et al. (2000), this peptide provides a suitable model to monitor complex formation between the whole protein and sorcin. At all calcium concentrations investigated, the amount of complex formed decreases in the same order as calcium affinity, namely wt sorcin > E53Q > E94A > E124A. At about 18 μM Ca^{2+}, wt sorcin appears to have an apparent K_D of 300 nM while the E53Q, E94A and E124A mutants require a 5- 30-, and 250-fold increase in Ca^{2+} concentration, respectively, to interact with the immobilized annexin VII peptide with similar K_D values.

The functional picture that emerges is that EF3 is the major player in sorcin activation. It has the highest affinity for calcium and can trigger a Ca^{2+}-dependent conformational change by means of the hydrogen-bonding interactions established by Asp113 and Glu124 in the Ca^{2+} binding loop. This conformational change, though limited in extent, reaches EF2 and the EF1-EF2 loop and results in the reorganization of the hydrophobic core around the D helix. It may be recalled that the long D helix provides the structural coupling between the two physiological EF hands. The behaviour of the 90-198 sorcin fragment, which lacks EF1 and EF2, binds Ca^{2+} with decreased affinity, and is unable to translocate to membranes (Zamparelli et al., 2000) likewise suggests that integrity of the transmission pathway is a prerequisite for sorcin activation.

To validate these ideas concerning the role of the D-helix in sorcin activation, W99 and W105, the only two Trp residues of the polypeptide chain, located differently on the D-helix, were used to advantage. Thus, W99 lies near EF2 and faces solvent, whereas W105 lies near EF3, faces the protein core and establishes a large number of interactions with other residues of the D- and G-helices and of the loop between EF1 and EF2. The assessment of the Ca^{2+} affinity of the W99G and W105G mutants was hampered by the strong tendency of the Ca^{2+}-bound forms,

in particular of W105G, to aggregate and/or precipitate in the absence of protein targets. However, the indirect fluorescence titration experiments show that, under the experimental conditions tested, the Ca^{2+} affinity of both W99G and W105G is unaltered respect to wt sorcin (Fig. 29).

The efficiency of the information transfer mechanism was established by assessing the interaction of W99G and W105G with annexin VII, a target of the sorcin N-terminal domain, in immunoblot and SPR experiments. The interaction with annexin VII is unaltered by the W99G mutation, but is compromised significantly (7 fold) when W105 is substituted (Fig. 31). Since the Ca^{2+} affinity of W105G is unchanged relative to wt sorcin, the impairment in the interaction has to be attributed to an alteration of the information transfer process via the D-helix.

The interaction of the two tryptophan mutants with RyR, involving the sorcin C-terminal domain, was assessed in isolated cardiomyocytes by analysis of the Ca^{2+} spark parameters. In the control experiments with native sorcin (Fig. 32), over 10-12 min Ca^{2+} spark frequency displays a small but significant decrease that may reflect the balance of several factors, including (i) a change in the Ca^{2+} content of the SR immediately after permeabilization of the cardiomyocytes and (ii) minor changes in concentration of low-molecular weight modulators of RyR2 activity, e.g. ATP, Mg^{2+}, H^{+}. The decreased frequency, amplitude, duration and width of the Ca^{2+} sparks by wt sorcin are consistent with previous reports on heart cells (Lokuta et al., 1997; Seidler et al., 2003; Farrell et al., 2003). These studies proved that sorcin reduces the open time of the channel, an effect that would reduce the duration of the Ca^{2+} spark and thus the width and amplitude.

The two sorcin-variants W99G and W105G behave as follows: W99G decreases Ca^{2+} spark frequency very similarly to wt sorcin, whereas W105G has no significant effects on any of the Ca^{2+} spark parameters. This effect could be explained in terms of an alteration of the sorcin-RyR2 interaction surface that weakens the interaction itself. Despite this alteration, the information about Ca^{2+} binding to EF3 does reach the N-terminal domain as shown by the ability of W105G to interact with annexin VII, albeit with a lower Ca^{2+} sensitivity than wt sorcin.

In conclusion, the behavior of the site-specific tryptophan mutants provide experimental support to the proposal that the interaction network around the D-helix is central to the Ca^{2+}-induced sorcin activation mechanism. The conformational changes that take place at EF3 upon Ca^{2+} binding are amplified by the D-helix which thereby acts as a trigger of sorcin activation.

At this point, a discussion of the data obtained in the present thesis in a general framework is in order.

The role of EF3 and of the D-helix in sorcin activation indicated by the behaviour of the mutants finds a physiological confirmation in the discovery of a spontaneous mutation in the human protein, namely F112L, which is thought to account for an inherited form of hypertrophic cardiomyopathy and hypertension (Rueda et al., 2006). This mutation involves F112 located on the D helix at the beginning of the EF3 Ca^{2+}-binding loop. Unpublished studies by Mohiddin et al. show that transgenic mice expressing F112L sorcin targeted to the heart have a normal lifespan and reproductive ability, although their hearts are dilated with thinned ventricular walls. The effects on RyR and calcium sparks appear to be dependent on the ability of sorcin to interact with RyR2 more than on its bulk structure or electrical charge. In fact, Rueda et al (2006) showed that, except for Ca^{2+} spark duration, all other parameters in cells perfused with F112L-sorcin are significantly different from those obtained in the presence of wt-sorcin, but resemble closely those obtained in the absence of sorcin. This mutation in an essential region of the protein therefore suffices to impair the interaction with the calcium channel and to alter the cardiac functions in a significant manner. In general terms, the data on the F112L variant provide further support to the contention that sorcin plays an important role in the excitation-contraction process and in particular in the relaxation phase after muscle contraction. Thus, in cardiac muscle the main sorcin targets are RyR2, which triggers the release from calcium stores and thereby activates contraction (Beers 2002), NCX, that restabilises the resting levels of calcium after muscle contraction by exchanging this metal with Na^{+} (Maack et al., 2005), and SERCA, which is responsible for Ca^{2+} re-uptake by the SR after muscle contraction (Matsumoto et al., 2005). Sorcin reduces the activity of RyR and increases the activity of NCX and SERCA. Hence, its net effect is to terminate calcium induced calcium release during the relaxation process after muscle contraction.

Lastly, the role played by the D helix in sorcin activation may be applicable to all PEF proteins given the D helix conservation and the fact that the EF3 site is endowed with the highest Ca^{2+} affinity in most members of the family. As in the case of sorcin, the subtle changes that occur upon calcium binding may be amplified by the hydrophobic core around the D-helix and transferred from EF3 to the rest of the molecule resulting in protein activation.

5. REFERENCES

André, I., Linse, S. (2002)
"Measurement of Ca^{2+}-binding constants of proteins and presentation of the CaLigator software.", *Anal Biochem*., **305**, 195-205.

Arthur, J. S., Elce, J. S., Hegadorn, C., Williams, K. e Greer, P. A. (2000)
"Disruption of the murine calpain small subunit gene, Capn4: calpain is essential for embryonic development but not for cell growth and division", *Mol. Cell. Biol.*, **20**, 4474-81.

Bassani JW, Bassani RA, Bers DM. (1994)
"Relaxation in rabbit and rat cardiac cells: species-dependent differences in cellular mechanisms.", *J. Physiol*., **476,** 279-93.

Bers, D. M. (2001)
"Excitation-Contraction and cardiac contractile force" *edz 2* (Kluwer Academic, Dordrecht, Netherlands)

Bers, D. M. (2002)
"Cardiac excitation-contraxtion coupling.", *Nature,* **415,** 198-204.

Bers DM, Despa S. (2006)
"Cardiac myocytes Ca^{2+} and Na^{+} regulation in normal and failing hearts.", *J. Pharmacol Sci.,* **100,** 315-22.

Blanchard, H., Grochulski, P., Li, Y., Arthur, J. S. C., Davies, P. L., Elce, J. S. and Cygler, M. (1997)
"Structure of a calpain Ca^{2+}-binding domain reveals a novel EF-hand and Ca^{2+}-induced conformational changes", *Nat. Struct. Biol.,* **4,** 532-538.

Bryant, D. T. W. (1985)
"Quin 2: the dissociation constant of its Ca^{2+} and Mg^{2+} complexes and its use in a fluorimetric method for determining the dissociation of Ca^{2+}-protein complexes", *Biochem. J.,* **226**, 613-616.

Brownawell, A. M. and Creutz, C. E. (1997)
"Calcium dependent binding of sorcin to the N-terminal domain of synexin (Annexin VII)", *J. Biol. Chem.,* **272,** 22182-22190.

Carafoli, E. (2005)
"Calcium- a universal carrier of biological signals Delivered on 3 July 2003 at the Special FEBS Meeting in Brussels.", *FEBS J.,* **272**, 1073-1083.

Carson, M. (1997)
Ribbons. *Methods Enzymol.,* **277,** 493-505

Clemen, C., Hofmann, A., Zamparelli, C. and Noegel, A. J. (1999)
"Expression and localisation of annexin VII (synexin) isoforms in differentiating myoblasts", *J. Muscle Res. Cell Motil.,* **20**, 669-79.

Dutt, P., Arthur, J. S., Grochulski, P., Cygler, M., Elce, J. S. (2000)
"Roles of individual EF-hands in the activation of m-calpain by calcium", *Biochem. J.,* **348**, 37-43.

Edelhoch, H. (1967)
"Spectroscopic determination of tryptophan and tyrosine in proteins", *Biochemistry,* **6***,* 1948-1954.

Farrell, E. F. , Antaramian A., Rueda, A., Gomez, A. M. (2003)
"Sorcin inhibits calcium release and modulates excitation-contraction coupling in the heart", *J. Biological Chem.,* **278**, 34660-34666.

Flaherty, KM, Zozulya, S., Stryer, L., Mckay DB (1993)
"Three-dimensional structure of recoverin, a calcium sensor in vision.", *Cell,* **75**, 709-716.

Finn, B. Z., Eveans, J., Drakenberg, T., Waltho, J. P., Thulin, E. and Forsén, S. (1995)
"Calcium-induced structural changes and domain autonomy in calmodulin", *Nat. Struct. Biol.,* **2**, 777-783.

Franzini-Armstrong C, Protasi F, Ramesh V. (1999)
"Shape, size, and distribution of Ca(2+) release units and couplons in skeletal and cardiac muscles.", *Biophys J*., **77**, 1528-39.

Fruen BR, Bardy JM, Byrem TM, Strasburg GM, Louis CF. (2000)
"Differential Ca(2+) sensitivity of skeletal and cardiac muscle ryanodine receptors in the presence of calmodulin.", *Am J. Physiol Cell Physiol*., **279,** 724-33.

Gracy, K. N., Clarke, C. L., Meyers, M. B. and Pickel, V. M. (1999)
"N-methyl-D-aspartate receptor 1 in the caudate-putamen nucleus: ultrastructural localization and co-expression with sorcin, a 22,000 mol. wt calcium binding protein", *Neuroscience*, **90**, 107-117.

Graham-Siegenthaler, K., Gauthier, S., Davies, P. L. and Elce, J. S. (1994)
"Active recombinant rat calpain II. Bacterially produced large and small subunits associate both in vivo and in vitro", *J. Biol. Chem.,* **269**, 30457-60.

Gros, P., Ben Neriah, Y., Croop, J. M. and Housman, D. E. (1986)
"Isolation and expression of a complementary DNA that confers multidrug resistance", *Nature,* **323**, 728-731.

Hamada, H., Okochi, E., Oh-hara, T. and Tsuruo, T. (1988)
"Purification of the M_r 22,000 calcium-binding protein (sorcin) associated with multidrug resistance and its detection with monoclonal antibodies", *Canc. Res*., **48**, 3173-3178.

Heizmann, C. W. and Hunziker, W. (1991)
"Intracellular calcium-binding proteins: more sites than insights", *TIBS,* **16**, 98-103.

Herzberg, O., James, M. N. (1988)
"Refined crystal structure of troponin C from turkey skeletal muscle at 2,0 Å resolution", *J. Mol. Biol.,* **203**, 761-779.

Higuchi R, Krummel B, Saiki RK. (1988)
"A general method of in vitro preparation and specific mutagenesis of DNA fragments: study of protein and DNA interactions.", *Nucleic Acids Res*., **16,** 7351-67.

Hinata M, Kimura J. (2004)
"Forefront of Na+/Ca2+ exchanger studies: stoichiometry of cardiac Na+/Ca2+exchanger;3:1or4:1?"*J Pharmacol Sci*., **96**, 15-8.

Ilari, A., Johnson, K. A., Nastopoulos, V., Verzili, D., Zamparelli, C., Colotti, G., Tsernoglou, D. and Chiancone, E. (2002)
"The crystal structure of the sorcin calcium binding domain provides a model of Ca^{2+}-dependent processes in the full-length protein", *J. Mol. Biol.,* **317**, 447-458.

Ikura, M. (1996)
"Calcium binding and conformational response in EF- hand proteins", *TIBS,* **21**, 14-17.

Jia, J., Han, Q., Borregaard, N., Lollike, K. and Cygler, M. (2000)
"Crystal Structure of Human Grancalcin, a Member of the Penta-EF-Hand Protein Family", *J. Mol. Biol.,* **300**, 1271-1281.

Jia, J., Tarabykina, S., Hansen, C., Berchtold, M. and Cygler, M. (2001)
"Structure of Apoptosis-Linked Protein ALG-2: Insights into Ca^{2+}-Induced Changes in Penta-EF-Hand Proteins", *Structure,* **9**, 267-275.

Kawasaki, H. e Kretsinger, R. (1994)
"Calcium-binding proteins 1: EF-hands", *Protein Profile,* **1**, 343-349.

Kitaura, Y., Watanabe, M., Satoh, H., Kawai, T., Hitomi, K. and Maki, M. (1999)
"Peflin, a Novel Member of the Five-EF-hand-Protein Family, Is Similar to the Apoptosis-Linked Gene 2 (ALG-2) Protein but Possesses Nonapeptide Repeats in the N-Terminal Hydrophobic Region", *Biochem. Biophys. Res. Commun.,* **263**, 68-75.

Kitaura, Y., Satoh, H., Takahashi, H., Shibata, H. and Maki, M. (2002)
"Both ALG-2 and Peflin, Penta-EF-hand (PEF) Proteins, Are Stabilized by Dimerization through Their Fifth EF-Hand Regions", *Arch. Biochem. Biophys.,* **399**, 12-18.

Koch, G., Smith, M., Twntyman, P. and Wright, K. (1986)
"Identification of a novel calcium-binding protein (CP_{22}) in multidrug-resistant murine and hamster cells", *FEBS Lett*., **195**, 275-279.

Kretsinger, R. H. and Nockolds, C. E. (1973)
"Carp muscle calcium-binding protein. Structure determination and general description", *J. Biol. Chem*., **2**, 3313-3326.

Kretsinger RH, Rudnick SE, Weissman LJ. (1986)
"Crystal structure of calmodulin.", *J. Inorg. Biochem*., **28,** 289-302.

Laemmli, U. K. (1970)
"Cleavage of structural proteins during the assembly of the head of bacteriophage T4", *Nature (London),* **227**,680-685.

Langer GA, Peskoff A. (1996)
"Calcium concentration and movement in the dyadic cleft space of the cardiac ventricular cell.", *Biophys. J.,* **70**, 1169-82.

Lewit-Bentley, A. and Réty, S. (2000)
"EF calcium-binding proteins", *Current Opinion in Structural Biology,* **10**, 637-643.

Lin, G., Chattopadhyay, D., Maki, M., Wang, K. K. W., Carson, M., Jin, L., Yuen, P., Takano, E., Hatanaka, M., DeLucas, L. J. and Narayana, S. V. L. (1997)
"Crystal structure of calcium bound domain VI of calpain at 1.9 Å resolution and its role in enzyme assembly, regulation and inhibitor binding", *Nat. Struct. Biol.,* **4**, 539-546.

Linse, S. and Forsén, S. (1995)
"Determinants that govern high affinity calcium binding", *Adv. Second Messenger Phosphoprotein Res*., **30**, 89-151.

Lo, K., Zhang, Q., Li, M., Zhang, M. (1999)
"Apoptosis-linked gene product ALG-2 is a new member of the calpain small subunit subfamily of Ca^{2+}-binding proteins", *Biochemistry*, **38***,* 7498-7508.

Lokuta, A. J., Meyers, M. B., Sander, P. R., Fishmann, G. I. and Valdivia, H. H. (1997)
"Modulation of cardiac ryanodine receptors by sorcin", *J. Biol. Chem.,* **272**, 25333-25338.

Lollike, K., Johnsen, A. H., Durussel, I., Borregaard, N. and Cox, J. A. (2001)
"Biochemical characterization of the penta-EF-hand protein grancalcin and identification of l-plastin as a binding partner", *J. Biol. Chem.,* **276**, 17762-17769.

Maack, C., Ganesan, A., Sidor, A., O'Rourke, B. (2005)
"Cardiac sodium-calcium exchanger is regulated by allosteric calcium and exchanger inhibitory peptide at distinct sites.", *Circ. Res.,* **96,** 91-99.

Maki, M., Narayana, SV. and Hitomi, K. (1997)
"A growing family of the Ca^{2+}-binding proteins with five EF-hand motifs", *Biochem. J*., **328**, 718-720.

Maki, M., Yamaguchi, K., Kitaura, Y., Satoh, H. and Hitomi, K. (1998)
"Calcium-induced exposure of a hydrofobic surface of mouse ALG-2, which is a member of the penta-EF-hand protein family", *J. Biochem. (Tokio),* **124**, 1170-7.

Marx SO, Reiken S, Hisamatsu Y, Jayaraman T, Burkhoff D, Rosemblit N, Marks AR. (2000)
"PKA phosphorylation dissociates FKBP12.6 from the calcium release channel (ryanodine receptor): defective regulation in failing hearts.", *Cell*., **101,**365-76.

Marx SO, Reiken S, Hisamatsu Y, Gaburjakova M, Gaburjakova J, Yang YM, Rosemblit N, Marks AR. (2001)
"Phosphorylation-dependent regulation of ryanodine receptors: a novel role for leucine/isoleucine zippers.", *J. Cell Biol*., **153,** 699-708.

Matsumoto, T., Hisamatsu, Y., Ohkusa, T., Inoue, N., Sato, T., Suzuki, S., Ikeda, Y., Matsuzaki, M. (2005)
"Sorcin interacts with sarcoplasmic reticulum Ca^{2+}-ATPase and modulates excitation-contraction coupling in the heart.", *Basic Res. Cardiol.,* **100,** 250-262.

Meyers, M. B. and Biedler, J. (1981)
"Increased synthesis of a low molecular weight protein in vincristine-resistant cells", *Biochem. Biophys. Res.Commun*., **99**, 228-235.

Meyers, M. B., Splenger, B. A., Chang, T.D., Melera, P. W. and Biedler, J. L. (1985)
"Gene amplification- associated cytogenetic aberrations and protein changes in vincristine -resistant Chinese hamster, mouse and human cells*",* *J. Cell Biol.,* **100**, 588-597.

Meyers, M. B., Schneider, K. A., Spengler, B. A., Chand, T. D. and Biedler, J. L. (1987)
"Sorcin (V 19), a soluble acidic calcium-binding protein overproduced in multidrug-resistant cells", *Biochem. Pharm*., **36**, 2373-2380.

Meyers, M. B., Zamparelli, C., Verzili, D., Dicker, A. P., Blanck, T. J. J. and Chiancone E. (1995a)
"Calcium-dependent translocation of sorcin to membranes: functional relevance in contractile tissue", *FEBS Lett*., **357**, 230-234.

Meyers, M. B., Virginia, M. P., Shen, S. S., Sharma, V. K., Scotto, W. and Fishman, G. I. (1995b)
"Association of sorcin with the cardiac ryanodine receptor", *J. Biol. Chem*., **270**, 26411-26418.

Meyer, S. L., Bozyczko-Coyne, D., Mallya, S. K., Spais, C. M., Bihovsky, R., Kaywooya, J. K., Lang, D. M., Scott, R. W. and Siman, R. (1996)
"Biologically active monomeric and heterodimeric recombinant human calpain I produced using the baculovirus expression system", *Biochem. J.,* **314,** 511-9.

Meyers, M. B., Puri, T. S., Chien, A. J., Gao, T., Hsu, P.-H., Hosey, M. M. and Fishman, G. I. (1998)
"Sorcin associates with pore-forming subunit of voltage-dependent L-type Ca^{2+} channels", *J. Biol. Chem.,* **273**, 18930-18935.

Missotten, M., Nichols, A., Rieger, K. and Sadoul, R. (1999)
"A novel mouse protein undergoing calcium-dependet interaction with the apoptosis-linked-gene 2 (ALG-2) protein", *Cell Death Differ.,* **6**, 124-9.

Nelson, M. R. and Chazin, W. J. (1998)
"Structures of EF-hand Ca^{2+}-binding proteins: Diversity in the organization, packing and response to Ca^{2+} Binding", *BioMetals,* **11**, 297-318.

Pack-Chung, E., Meyers, M. B., Pettingell, W. P., Moir, R. D., Brownawell, A. M., Cheng, I., Tanzi, R. E. and Kim, T. W. (2000)
"Presenilin 2 interacts with sorcin, a modulator of the ryanodine receptor", *J. Biol. Chem.,* **275**, 14440-14445.

Polotskaja, A. V., Gudgov, A. V. and Kopnin, B. P. (1983)
"Overproduction of specific polypeptides in Djungarian hamster and mouse cells resistant to colchicine and adriablastin", *Bull. Exp. Biol. Med*., **9**, 95-96.

Roberts, D., Meyers, M. B., Biedler, J. L. and Wiggins, L. (1989)
"Association of sorcin with drug resistance in L1210 cells", *Cancer Chemoter. Pharmacol*., **19**, 123-130.

Rueda, A., Song, M., Toro, L., Stefani, E., Valdivia, H. H. (2006)
"Sorcin modulation of Ca^{2+} sparks in rat vascular smooth muscle cells", *J. Physiol.*, **576**, 887-901.

Saito, A., Seiler, S., Chu, A., Fleischer, S. (1984)
"Preparation and morphology of sarcoplasmic reticulum terminal cisternae from rabbit skeletal muscle.", *J. Cell Biol.,* **99,** 875-85**.**

Salzer, U., Hinterdorfer, P., Hunger, U., Borken, C. e Proaska, R. (2002)
"Ca^{++}-dependent vesicle release from erytrocytes involves stomatin-speficic lipid rafts, synexin (annexin VII), and sorcin.", *Blood*, **99**, 2569-77.

Scriven DR, Dan P, Moore ED. (2000)
"Distribution of proteins implicated in excitation-contraction coupling in rat ventricular myocytes.", *Biophys J.,* **79,** 2682-91.

Seidler, T., Miller, S.L.W., Loughrey, C. M., Kania, A., Burow, A., Kettlewell, S., Teucher, N., Wagner, S., Kogler, H., Meyers, M., Hasenfuss, G., Smith, G.L. (2003)
"Effects of adenovirus-mediated sorcin overexpression on excitation-contraction in isolated rabbit cardiomyocytes.", *Circ. Res.,* **93,** 132-139.

Silva, J. J. R. and Wiliams, R. J. P. (1991)
"The biological chemistry of the elements", *Oxford University press*, 268-298.

Smith, G. L., Elliott, E. E., Kettlewell, S., Currie, S., Quinn, F. R. (2006)
"Na^{+}/Ca^{2+} exchanger expression and function in a rabbit model of myocardial infarction", *J. Cardiovasc. Electrophysiol.*, **17,** S57-S63.

Strobl, S., Fernandez-Catalan, C., Braun, M., Huber, R., Masumoto, H., Nakagawa, K., Irie, A., Sorimachi, H., Bourenkov, G., Bartunik, H., Suzuki, K., and Bode, W (2000)
"The crystal structure of calcium-free human m-calpain suggests an electrostatic switch mechanism for activation by calcium", *Proc. Natl. Acad. Sci.U.S.A.,* **97,** 588-592.

Subramanian, L., Crabb, J. W., Cox, J., Drussel, I., Walker, T. M., Van Ginkel, P. R., Bhattacharya, S., Dellaria, J. M., Palczewski, K., Polans, A. S. (2004)
"Ca^{2+} binding to EF hands 1 and 3 is essential for the interaction of apoptosis-linked gene-2 with Alix/AIP1 in ocular melanoma" *Biochemistry,* **43,** 11175-86

Takeda, T., Asahi, M., Yamaguchi, O., Hikoso, S., Nakayama, H., Kusakari, Y., Kawai, M., Hongo, K., Higuchi, Y., Kashiwase, K., Watanabe, T., Taniike, M., Nakai, A., Nishida, K., Kurihara, S., Donoviel, D. B., Bernstein, A., Tomita, T., Iwatsubo, T., Hori, M., Otsu, K. (2005)
"Presenilin 2 regulates the systolic function of heart by modulating Ca^{2+} signalling.", *FASEB J.,* **19**, 2069-71.

Teahan, C. G., Totty, N. F. and Segal, A. W. (1992)
"Isolation and characterization of grancalcin, a novel E-F hand calcium-binding protein from human neutrophils", *Biochem. J.,* **286,** 549-554.

Trafford W, Diaz ME, Negretti N, Eisner DA. (1997)
"Enhanced Ca^{2+} current and decreased Ca^{2+} efflux restore sarcoplasmic reticulum Ca^{2+} content after depletion.", *Circ Res.,* **81**, 477-84.

Tsigelny I., Shindyalov IN, Bourne PE, Sudhof TC, Taylor P. (2000)
"Common EF-hand motifs in cholinesterases and neuroligins suggest a role for Ca^{2+}-binding in cell surface associations", *Protein Sci.,* **9**, 180-185.

Van der Bliek, A. M., Meyers, M. B., Biedler, J. L., Hes, E. and Borst, P. (1986)
"A 22-kd protein (sorcin / V19) encoded by an amplified gene in multidrug-resistant cells, is homologous to the calcium binding light chain of calpain", *EMBO J.,* **5,** 3201-3208.

Van der Bliek, A. M., Baas, F., Van der Velde-Koerts, T., Biedler, J. L., Meyers, M. B., Ozols, R. F., Hamilton, T. C., Joenie, H. and Borst, P. (1988)
"Genes amplified and ovexpressed in human multidrug-resistant cell lines", *Cancer Res.,* **48**, 5927-5932.

Verzili, D., Zamparelli, C., Mattei, B., Noegel, A. A., Chiancone, E. (2000)
"The sorcin-annexin VII calcium-dependent interaction requires the sorcin N-terminal domain", *FEBS lett.*, **471**, 197-200.

Vito, P., Lacanà, E. and D'Amadio, L. (1996)
"Interfering with apoptosis: Ca^{2+}-binding protein ALG-2 and Alzheimer's disease gene ALG-3", *Science*, **271**, 521-525.

Vito, P., Pellegrini, L., Guiet, C. and D'Adamio, L. (1999)
"Cloning of AIP1, a novel protein that associates with the apoptosis-linked gene ALG-2 in a Ca^{2+}-dependent reaction", *J. Biol. Chem.,* **274,** 1533-40.

Wang, S. L. , Tam, M. F., Ho, Y. S., Pai, S. H. and Kao, M. C. (1995)
"Isolation and molecular cloning of human sorcin a calcium binding protein in vincristine-resistant H0B1 lymphoma cells", *Biochim. Biophys. Acta,* **1260**, 285-293.

Xie, X., Dwyer, M. D., Swenson, L., Parker, M. H. e Botfiel, M. C. (2001)
"Crystal structure of calcium-free human sorcin: A member of the penta-EF-hand protein family", *Protein Science,* **10**, 2419-2425.

Yoshizawa, T., Sorimachi, H., Tomioka, S., Ishiura, S. and Suzuki, K. (1995)
"A catalytic subunit of calpain possesses full proteolytic activity", *FEBS Lett.,* **358**, 101-3.

Zamparelli, C., Ilari, A., Verzili, D., Vecchini, P., Chiancone, E. (1997)
"Calcium and pH-linked oligomerization of sorcin causing translocation from cytosol to membranes", *FEBS Lett.*, **409,** 1-6.

Zamparelli, C., Ilari, A., Verzili, D., Giangiacomo, L., Colotti, G., Pascarella, S. and Chiancone, E. (2000)
"Structure-function relationships in sorcin, a member of the penta EF-hand family. Interaction of sorcin fragments with the ryanodine receptor and an Escherichia coli model system", *Biochemistry*, **39,** 658-66.

Zhang, M., Taraka, T. e Ikura, M. (1995)
"Calcium-induced conformational transition revealed by the solution structure of apocalmodulin", *Nat. Struct. Biol.,* **2**, 758-767.

6. ATTACHMENTS

- **Mella M.,** Colotti G., Zamparelli C., Verzili D., Ilari A. e E. Chiancone (2003)

"Information transfer in the penta-EF-hand protein sorcin does not operate via the canonical structural/functional pairing. A study with site-specific mutants."
J. Biol. Chem. 278(27), 24921-8

- Colotti G., Zamparelli C., Verzili D., **Mella M**., Loughrey CM, Smith GL, Chiancone E (2006)

"The W105G and W99G sorcin mutants dimostrate the role of the D helix in the Ca^{2+}-dependent interaction with annexin VII and the cardiac ryanodine receptor"
Biochemistry 45 (41), 12519-12529

THE JOURNAL OF BIOLOGICAL CHEMISTRY
© 2003 by The American Society for Biochemistry and Molecular Biology, Inc.
Vol. 278, No. 27, Issue of July 4, pp. 24921–24928, 2003
Printed in U.S.A.

Information Transfer in the Penta-EF-hand Protein Sorcin Does Not Operate via the Canonical Structural/Functional Pairing

A STUDY WITH SITE-SPECIFIC MUTANTS*

Received for publication, December 30, 2002, and in revised form, March 28, 2003
Published, JBC Papers in Press, April 22, 2003, DOI 10.1074/jbc.M213276200

Manuela Mella, Gianni Colotti, Carlotta Zamparelli, Daniela Verzili, Andrea Ilari, and Emilia Chiancone‡

From the Consiglio Nazionale delle Ricerche Institute of Molecular Biology and Pathology, Department of Biochemical Sciences A. Rossi Fanelli, University of Rome La Sapienza, 00185 Rome, Italy

Sorcin is a typical penta-EF-hand protein that participates in Ca^{2+}-regulated processes by translocating reversibly from cytosol to membranes, where it interacts with different target proteins in different tissues. Binding of two Ca^{2+}/monomer triggers translocation, although EF1, EF2, and EF3 are potentially able to bind calcium at micromolar concentrations. To identify the functional pair, the conserved bidentate -Z glutamate in these EF-hands was mutated to yield E53Q-, E94A-, and E124A-sorcin, respectively. Limited structural perturbations occur only in E124A-sorcin due to involvement of Glu-124 in a network of interactions that comprise the long D helix connecting EF3 to EF2. The overall affinity for Ca^{2+} and for two sorcin targets, annexin VII and the ryanodine receptor, follows the order wild-type > E53Q- > E94A- > E124A-sorcin, indicating that disruption of EF3 has the largest functional impact and that disruption of EF2 and EF1 has progressively smaller effects. Based on this experimental evidence, EF3 and EF2, which are not paired in the canonical manner, are the functional EF-hands. Sorcin is proposed to be activated upon Ca^{2+} binding to EF3 and transmission of the conformational change at Glu-124 via the D helix to EF2 and from there to EF1 via the canonical structural/functional pairing. This mechanism may be applicable to all penta-EF-hand proteins.

Sorcin is a member of the penta EF-hand (PEF)[1] family, a small group of Ca^{2+} binding proteins that comprises the large and small calpain subunits (1, 2), grancalcin (3), ALG-2 (4), and peflin (5). All these proteins bind to cell membranes through a Ca^{2+}-dependent interaction with protein targets that permits transduction of various Ca^{2+}-mediated signals. Sorcin is thought to participate in different Ca^{2+}-triggered biochemical cascades since different target proteins have been identified in the cell types where the protein is expressed constitutively, namely the ryanodine receptor (Ryr) and the α_1 subunit of L-type calcium channels in muscle cells (6, 7), presenilin 2 in human brain (8), and annexin VII in adrenal medulla (9), differentiating myocytes (10) and red blood cells (11).

The EF-hand, a structural motif characterized by a helix-loop-helix structure, is used by a large number of proteins to bind Ca^{2+} with high affinity. In the "canonical" motif, Ca^{2+} is coordinated by a 12-amino-acid-long interhelical loop sequence with pentagonal bipyramidal symmetry. In this arrangement, four conserved side chains provide the five equatorial ligands (Y, Z, -Y, -Z) since the glutamate residue in position -Z establishes a bidentate interaction with the metal. The two apical ligands are furnished by the side chain of an acidic group (X) and by a water molecule (-X). Changes in the loop sequence occur such that the EF-hands may not bind Ca^{2+} or may not be recognized in the protein primary structure. In the PEF family, the extensively modified EF4 and EF5 loops do not bind Ca^{2+}, and the N-terminal motif designated EF1 was not recognized by sequence analysis since the loop is one amino acid shorter than the canonical one. The existence of the EF1 hand was revealed only by the x-ray crystal structure of the calpain subunits, the family prototype (1, 2).

In a typical manner, EF-hands occur in pairs that are coupled structurally and functionally. The structural association takes place through a short two-stranded β sheet arrangement that gives rise to stable domains. Moreover, binding of Ca^{2+} elicits a change from a "closed" to an "open" conformation that leads to exposure of hydrophobic surfaces for target interaction. In the PEF family, all the EF-hands are clustered in the C-terminal domain that is characterized by a very similar, compact fold in all the proteins, as exemplified by the sorcin structure depicted in Fig. 1. The EF1-EF2 and EF3-EF4 pairs are associated in the canonical manner, although EF5 is unpaired in the monomer but interacts with the same motif of a second monomer in the native form of the molecule, a dimeric assemblage (2, 12–14). An intriguing peculiarity of the Ca^{2+} binding domain is the unusual presence of two long (six turns) α-helices that are shared by EF2 and EF3 (D helix) and by EF4 and EF5 (G helix). At least in principle, this direct structural link between the two canonical EF-hand pairs may represent the natural means for transferring functional information between them. The compact structure of the C-terminal Ca^{2+} binding domain contrasts the flexibility of the N-terminal domain, which is of variable length in the different PEF proteins but is always rich in glycine and proline residues. Because of its nature, the N-terminal domain is not visible in the available x-ray crystal structures of the whole proteins, namely those of sorcin (15), grancalcin (13, 16), and calpain (17, 18).

* This work was supported by the Consiglio Nazionale delle Ricerche Target Project Biotechnology (to E. C.), by local grants from the Ministero dell'Istruzione Università e Ricerca (to E. C. and C. Z.), and by a special grant for the Centro di Eccellenza Biologia e Medicina Molecolare (to E. C.). The costs of publication of this article were defrayed in part by the payment of page charges. This article must therefore be hereby marked "*advertisement*" in accordance with 18 U.S.C. Section 1734 solely to indicate this fact.

This paper is dedicated to the memory of Eraldo Antonini, beloved and unforgettable master, deceased prematurely 20 years ago, on March 19, 1983.

‡ To whom correspondence should be addressed. Tel.: 39-06-49910761; Fax: 39-06-4440062; E-mail: emilia.chiancone@uniroma1.it.

[1] The abbreviations used are: PEF, penta EF-hand; Ryr, ryanodine receptor; PVDF, polyvinylidene difluoride; SPR, surface plasmon resonance; RU, resonance units.

The present understanding of the relationships between structure and function in the PEF family is far from complete. The x-ray structures show that three EF sites are potentially able to bind Ca^{2+} in the physiological range of concentrations, namely the unusual EF1 motif and EF2 and EF3, whose structural features resemble those of EF-hands in regulatory Ca^{2+}-binding proteins. However, binding of only two Ca^{2+}/monomer suffices to trigger the conformational change that exposes hydrophobic regions and leads to interaction with the respective targets (3, 19, 20). The available data indicate that functional coupling does not involve the same EF-hands in the different proteins, suggesting that despite the high structural similarity there is no common mode of information transfer within the PEF family. Furthermore, the mechanism of communication between Ca^{2+}-binding sites has not been elucidated. In sorcin, the characterization of a protein fragment (90–198) lacking the first two EF-hands pointed to EF1 and EF2 as the physiological pair (19). In grancalcin, EF1 and EF3 that are not linked structurally are coupled functionally; EF2 is unable to bind Ca^{2+} due to the presence of alanine in place of the canonical, bidentate -Z glutamate (3). In ALG-2, studies with site-specific mutants indicate that, as in grancalcin, the EF1 and EF3 motifs form the functionally relevant Ca^{2+} binding pair (4), whereas in calpain all the first three EF hands contribute to Ca^{2+} binding, with EF3 having the highest affinity (2).

The molecular mechanism that triggers the Ca^{2+}-signaling process and leads to a change in the subcellular localization of PEF proteins through the specific interaction with protein targets is still obscure. The Ca^{2+}-induced conformational changes manifest in the x-ray crystal structures are unexpectedly small and are limited to the EF1 region (1, 2, 13, 17), and it is not known how these small changes are amplified to the extent required for target protein interaction.

In the present work sorcin was used to address these aspects of the structure-function relationships in PEF proteins. Sorcin and its isolated Ca^{2+} binding domain have been characterized extensively in solution (19, 21–23). Moreover, a model for the Ca^{2+}-dependent processes in the full-length protein has been proposed on the basis of the x-ray crystal structure of the Ca^{2+} binding domain (12). Ca^{2+} binding is thought to weaken the interactions between the N- and C-terminal domains, thereby permitting their reorientation, which in turn facilitates interaction with the target proteins at or near membranes. It is relevant in this connection that sorcin has the ability to interact with its partners by means of both the N- and C-terminal domain, as exemplified by annexin VII and the ryanodine receptor, respectively (23, 19).

Site-specific mutants of EF1, EF2, and EF3 have been designed in which the canonical glutamate in the -Z position was changed into Gln or Ala. The respective mutant proteins, E53Q, E94A, E124A, have been characterized by determining their structural properties in solution and their affinity for Ca^{2+}. Thereafter, the effect of the site-specific mutation on the capacity to interact with annexin VII and the ryanodine receptor was assessed. Substitution of the -Z glutamate in the first three EF-hands produces structural alterations of very limited extent. They can be appreciated only in the E124A mutant due to the involvement of Glu-124 in a network of hydrogen bonding and hydrophobic interactions that comprise the D helix. All the substitutions introduced affect the Ca^{2+} binding properties of sorcin. The effect is largest when EF3 is modified and decreases in the order EF2 and EF1. These findings indicate that EF3 and EF2 represent the functional pair and suggest that binding of Ca^{2+} to EF3 is the first step in sorcin activation. It is conceivable that Ca^{2+} binding at the EF3 site changes the conformation of Glu-124 and that this change is transmitted to EF2 via the long D helix. The subsequent step in the pathway could occur in the conventional manner by taking advantage of the canonical structural coupling between EF2 and EF1. This unusual mode of functional linkage may be operative in all PEF proteins given their high structural similarity and, hence, may represent a general property of the family.

MATERIALS AND METHODS

Cloning of Sorcin Mutants—The cDNA of Chinese hamster ovary sorcin, kindly provided by Dr. M. B. Meyers, was amplified by PCR using two oligonucleotides, one of which was designed to generate a novel *Nde*I restriction site at the 5′ end at the place of *Nco*I without altering the sequence within the gene. The amplified DNA thus obtained was digested with the restriction enzymes *Nde*I and *Hin*dIII and was inserted subsequently in a pET22 expression vector (Novagen, Madison, WI) that had been digested with the same enzymes. Site-directed mutagenesis was carried out by the PCR overlap extension mutagenesis method according to Higuchi *et al.* (24) using the proof-reading enzyme *Pfu* DNA polymerase to avoid the addition of 3′-over-hanging residues by *Taq* polymerase. The following oligonucleotides were used: N forward, 5′-GCGAAATTAATACGACTCACTATAGGG-3′; C reverse, 5′-CAAGCTTTTAGACGGTCATGACAC-3′; E53Q forward, 5′-CAAATTGATGCTGATCAGTTGCAGAGATGTCTAAC-3′; E53Q reverse, 5′-GTTAGACATCTCTGCAACTGATCAGCATCAATTTG-3′; E94A forward, 5′-CACCATGGGATTCAATGCATTTAAAGAGCTC-3′; E94A reverse: 5′-GAGCTCTTTAAATGCATTGAATCCCATGGTG-3′; E124A forward, 5′-GGAACGGTGGATCCCCAGGCACTGCAGAAG-GCTCTG-3′; E124A reverse, 5′-CGTCAGAGCCTTCTGCAGTGCCTG-GGGATCCACCGT-3′. The complete mutated genes were digested with *Nde*I and *Hin*dIII and cloned into a pET22 expression vector.

Expression and Purification of Wild-type Sorcin and Its Mutants—Chinese hamster ovary recombinant sorcin was expressed in *Escherichia coli* BL21 (DE3) cells and was purified as previously described (21). The protein concentration was determined spectrophotometrically at 280 nm using a molar extinction coefficient on a monomer basis of 29,400 (21). The same purification procedure and the same extinction coefficient were used for the mutant proteins.

Circular Dichroism Spectra—CD spectra were recorded on a Jasco J-710 spectropolarimeter in the far UV (195–240 nm) and in the near UV (250–320 nm) region. The experiments at pH 7.5 were carried out at 20 °C in 5 mM Tris-HCl buffer, and those at pH 6.0 were carried out in 0.1 M sodium acetate buffer at 40 °C. The α-helical content was calculated from the ellipticity value at 222 nm according to Chou and Fasman (25).

Determination of Ca^{2+} Affinity—Indirect titrations were carried out in a Fluoromax spectrofluorimeter in 0.1 M Tris-HCl buffer at pH 7.5 and 25 °C in the presence of the fluorescent calcium chelator Quin2, according to Bryant (26). The excitation wavelength was 339 nm (slit width, 0.5 nm); the increment of emission intensity due to calcium binding to Quin2 was followed at 492 nm. Special care was taken to reduce Ca^{2+} contamination to 0.5–1.0 μM by treating the protein solutions and the glassware with Chelex 100, as recommended by André and Linse (27). For each mutant four sets of independent experiments were carried out, which included control titrations of Quin2 alone and of native sorcin. At the end of each titration, the fluorescence intensity corresponding to zero free Ca^{2+} concentration was determined by the addition of 5 mM EGTA. The fluorescence intensity of Quin2 at high calcium concentrations was taken as the higher asymptote. To estimate the Ca^{2+} affinity constants of native sorcin and its mutants, each experimental set was fitted with the program CaLigator (27); the choice between one and two binding constants was made on the basis of the χ^2 values.

Interaction of Wild-type Sorcin and Its Mutants with Annexin VII in Overlay Assay Experiments—Aliquots of purified wild-type sorcin and of the mutants were subjected to electrophoresis on a 15% polyacrylamide gel under denaturing conditions (28) and transferred to polyvinyl difluoride membranes (PVDF, Problott, Applied Biosystems, Foster City, CA) in transfer buffer (25 mM Tris-HCl, 192 mM glycine, 20% methanol, pH 8.3) for 45 min at 100 mA (29). For Western blotting analysis, the PVDF membranes were incubated at room temperature with annexin VII (5 μg/ml) in 1% gelatin in TBST buffer (20 mM Tris-HCl, 0.5 M NaCl, 0.05% Tween 20, pH 7.5) containing 10 μM or 500 μM $CaCl_2$. Subsequently, the membranes were incubated with anti-annexin VII polyclonal antibody (dilution 1:3000) in 1% gelatin in TBST buffer. The blots were developed by incubation with alkaline phosphatase conjugate monoclonal anti-mouse IgG (Sigma) in 1% gelatin in TBST. Control experiments ruled out the existence of cross-reactivity

between sorcin and its mutants and the anti-annexin VII antibody (data not shown).

Interaction of Wild-type Sorcin and Its Mutants with Annexin VII in Surface Plasmon Resonance (SPR) Measurements—SPR experiments were carried out using a BIACORE X system (Biacore AB, Uppsala, Sweden). Two N-terminal peptides of annexin VII were synthesized by Sigma-Genosys (Cambridge, UK), to improve the peptide solubility and binding to the sensor chip, three lysine residues were added to the first 20 amino acids of annexin VII (MSYPGYPPTGYPPPPGYPPA). Peptide P1 contained three lysine residues at the N terminus of the sequence, whereas peptide P2 contained three lysine residues at the C-terminal end. The peptide purity was checked by matrix-assisted laser desorption ionization time-of-flight mass spectrometry. The calculated isoelectric point of both P1 and P2 is 9.90, based on the program pI-tool (30).

The sensor chips (CM5, Biacore AB) were activated chemically by injection of 35 μl of a 1:1 mixture of *N*-hydroxysuccinimide (50 mM) and *N*-ethyl-*N*′-(3-dimethylaminopropyl)carbodiimide (200 mM) at a flow rate of 5 μl/min. The N-terminal peptides of annexin VII were immobilized on the activated sensor chip via amine coupling. The reaction was carried out in 20 mM sodium acetate at pH 6.0, and the remaining ester groups were blocked by injecting 1 M ethanolamine hydrochloride (35 μl). In control experiments, the sensor chip was treated as described above in the absence of peptide. The interaction of the immobilized annexin VII peptides with wild-type sorcin and its mutants was detected through mass concentration-dependent changes of the refractive index on the sensor chip surface. The changes in the observed SPR signal are expressed as resonance units (RU). Typically, a response change of 1000 RU corresponds to a change in the surface concentration on the sensor chip of about 1 ng of protein per mm^2 (40). The experiments were carried out at 25 °C in 10 mM HEPES, pH 7.4, 0.15 M NaCl, and 0.005% surfactant P-20 (HBS-P buffer), treated with Chelex 100 to eliminate contaminating calcium, and degassed. For the experiments as a function of Ca^{2+} concentration, calcium chloride or EGTA were added to the buffer. Measurements were performed at a flow rate of 20 μl/min with an immobilization level of the annexin VII N-terminal peptides corresponding to 200–1200 RU. Values of the plateau signal at steady state (R_{eq}) were calculated from kinetic evaluation of the sensorgrams using the BIAevaluation 3.0 software. Scatchard analysis of the dependence of R_{eq} on the concentration of wt sorcin was also performed to assess the equilibrium dissociation constant at 25 μM Ca^{2+}. The amine coupling kit, the surfactant P-20, and the CM-5 sensor chip were purchased from Biacore AB; all the other reagents were high purity grade.

Interaction of Wild-type Sorcin and Its Mutants with the Ryanodine Receptor—Aliquots of purified wild-type sorcin, EF1, EF2, and EF3 sorcin mutants were transferred to PVDF membranes as described above for the sorcin-annexin VII interaction. Incubation of the membranes with terminal cisternae vesicles from rabbit skeletal muscle enriched in Ryr (5 μg/ml) was likewise carried out in TBST buffer containing 10 μM or 500 μM $CaCl_2$ as described above. The blots were incubated with an anti-Ryr monoclonal antibody (INALCO) and were developed by incubation with alkaline phosphatase conjugate monoclonal anti-mouse IgG. Control experiments ruled out the existence of cross-reactivity between sorcin and its mutants and the anti-Ryr antibody (data not shown).

RESULTS

Structural Characterization of the Site-specific Sorcin Mutants—Far and near UV CD spectroscopy was used to assess the possible occurrence of structural changes in the mutated apoproteins. The experiments were carried out at pH 7.5 and at pH 6.0 since the x-ray crystal structure of the Ca^{2+} binding domain was obtained at the latter pH value (12). Although sorcin operates in a medium containing about 1 mM Mg^{2+}, this cation was not included in the buffers used throughout this study since previous work showed that Mg^{2+} has no effect on the structural and functional properties of the protein (21). The far UV CD spectra of all the site-specific mutants under study are indistinguishable from those of native sorcin both at pH 6.0 and at pH 7.5 (data not shown).

In the near UV CD region the spectrum of wild-type sorcin is negative and is characterized by two sharp bands at 262 and 268 nm attributed to phenylalanines, by a weaker band at 283 nm due to the tyrosyl fine structure (0–0 transition), and by a fairly intense, well resolved peak at 292 nm due to tryptophan residues (22). The two tryptophan residues, Trp-99 and Trp-105, which are located on the D helix (Fig. 1, *B* and *C*), both contribute to the observed signal. However, the contribution of Trp-99 is likely to be smaller since this residue is more exposed to solvent than Trp-105 (12). The spectra of the mutant proteins are very similar to those of wild-type sorcin at both pH values with the exception of E124A, albeit only over the wavelength range 272–300 nm (Fig. 2). Thus, in the E124A mutant, the phenylalanine bands are unchanged, whereas the bands of

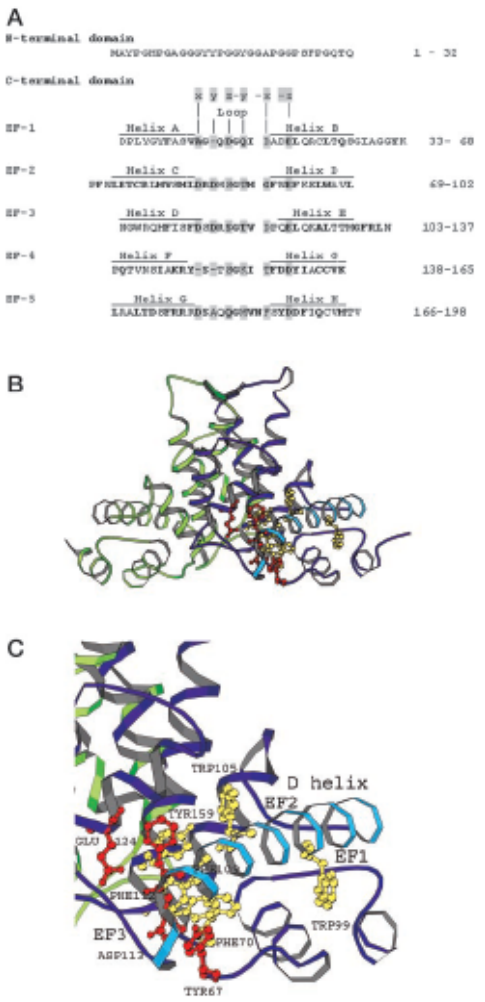

FIG. 1. Structure of sorcin. *A*, amino acid sequence. The residues conserved in all members of the PEF family are in *bold*; the residues in the Ca^{2+}-coordinating positions are in *gray*. *B*, x-ray structure of the sorcin Ca^{2+} binding domain (Protein Data Bank code 1GJY; Ref. 12). *C*, blow-up of the D helix (*pale blue*) and of the structural elements that take part in the proposed signal transduction mechanism. The residues involved in hydrogen bonding (Tyr-67–Asp-113, Glu-124–Phe-112) are in *red*, and those forming the hydrophobic core (Phe-70, Trp-99, Trp-105, Tyr-159) around the D helix are in *yellow*. The EF-hands (EF1-EF3) are also indicated. The picture is depicted in MOLSCRIPT (39).

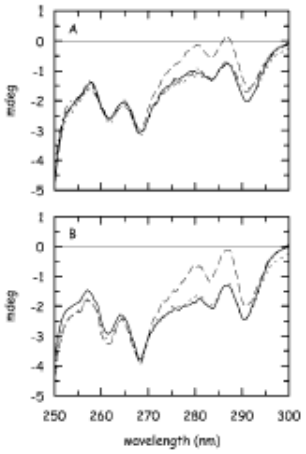

FIG. 2. Near UV circular dichroism spectra of wild-type sorcin and of the E53Q, E94A, and E124A mutants. Wild-type sorcin (——), E53Q (·····), E94A (—), and E124A (– –) were at a concentration of 50 μM. *A*, 0.1 M sodium acetate buffer, pH 6.0, 40 °C. *B*, 0.1 M Tris-HCl buffer, pH 7.5, 25 °C.

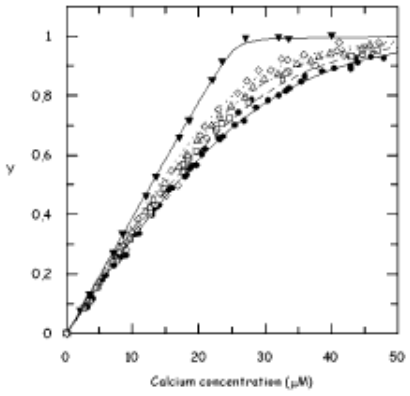

FIG. 3. Fluorescence titration of wild-type sorcin and of the E53Q, E94A, and E124A mutants with calcium in the presence of the calcium chelator Quin2. The degree of saturation of Quin2 (y) is plotted as a function of total calcium concentration. Wild-type sorcin (●), E53Q (□), E94A (△), and E124A (◇) at a concentration of 25 μM were titrated with calcium in the presence of 25 μM Quin2 in 0.1 M Tris-HCl at pH 7.5 and 25 °C. The titration of Quin2 alone (▼) is also shown. Four sets of independent titrations were carried out for native sorcin and for each mutant.

tyrosine and tryptophan residues occur at the same wavelength as in the wild-type protein at both pH values but have a smaller amplitude. The difference is particularly significant for the tyrosine contribution.

Sorcin precipitates upon binding of 2 Ca^{2+}/monomer in the absence of target proteins due to the exposure of hydrophobic surfaces (22). The same phenomenon was observed also for the site-specific mutants under study. Therefore, the effect of calcium on the near UV CD spectra was not studied.

Calcium Affinity of the Site-specific Sorcin Mutants—As for the wild-type protein (19), the affinity for calcium could not be determined in direct fluorescence experiments since the fluorescence intensity is practically unchanged upon binding of 2 eq of Ca^{2+}/monomer, and higher amounts of calcium lead to precipitation.

Calcium affinity was assessed in indirect fluorescence titration experiments in the presence of the calcium chelator Quin2. The results obtained at pH 7.5 are presented in Fig. 3 in terms of the degree of saturation of Quin2 as a function of total calcium concentration. Simple inspection of the data indicates that in the mutants calcium affinity decreases with respect to the wild-type protein in the order E53Q > E94A > E124A.

An important consequence of the occurrence of precipitation upon saturation of sorcin with 2 eq of Ca^{2+}/monomer is that higher Ca^{2+}/protein ratios cannot be scrutinized. Hence, one cannot establish whether more than two high affinity Ca^{2+}-binding sites are present on the sorcin molecule and is forced to analyze the titration data in terms of a two-site model. In the framework of this minimum scheme and on the basis of the statistical parameters obtained from the fitting procedure, the behavior of the wild-type protein can be described with two apparent dissociation constants in the micromolar range, namely $K_1 = 0.42 \pm 0.05 \times 10^{-6}$ M and $K_2 = 6.3 \pm 4.1 \times 10^{-6}$ M, using a dissociation constant for the chelator of 60 nM at pH 7.4, 20 °C (31). On the other hand the binding profiles of the mutants can be fitted satisfactorily by a single binding constant corresponding to $0.48 \pm 0.13 \times 10^{-6}$ M in E53Q, $0.71 \pm 0.14 \times 10^{-6}$ M in E94A, and $1.10 \pm 0.27 \times 10^{-6}$ M in E124A. For the mutants the second constant cannot be determined with accuracy because it is below the resolution limits of the technique under the experimental conditions used (about 1×10^{-5} M).

If one assumes that the site-specific mutations studied introduce local structural perturbations, the observed changes in Ca^{2+} affinity can be taken to indicate that glutamic acid in the -Z position of the EF3 hand is more important than the corresponding residue of the EF2 and of the EF1 hands in determining the Ca^{2+}-dependent conformational change that permits interaction with the target proteins. To prove this contention, binding of the mutant proteins with two physiological sorcin partners was assessed, namely annexin VII and Ryr, which are known to interact with the N- and C-terminal sorcin domains, respectively (23, 19).

Interaction of Wild-type Sorcin and Its Site-specific Mutants with Annexin VII and the Ryanodine Receptor in Immunoblot Experiments—In a first set of experiments wild-type sorcin and its mutants were transferred to PVDF membranes and incubated with annexin VII at pH 7.5 in buffer containing 10 or 500 μM calcium. Polyclonal anti-annexin VII antisera were used to detect complex formation. At the lower calcium concentration, wild-type sorcin and the E53Q and the E94A mutant appear to interact similarly with annexin VII, whereas no interaction occurs in the case of the E124A mutant. At the higher calcium concentration (500 μM) all the proteins interact with annexin VII in a similar manner (Fig. 4).

A second set of experiments was carried out to test the interaction with Ryr under the same experimental conditions. Wild-type sorcin and its mutants were blotted on PVDF membranes and incubated with Ryr-enriched terminal cisternae vesicles from rabbit skeletal muscle, and monoclonal anti-Ryr antibodies were used to detect complex formation. In accordance with the results obtained with annexin VII, at about 10 μM calcium native sorcin, the E53Q and the E94A mutants form a complex with the ryanodine receptor, whereas no interaction occurs in the case of E124A. At the higher calcium concentration, sorcin and the mutants all interact to a similar extent with Ryr (Fig. 5). It should be mentioned that no inter-

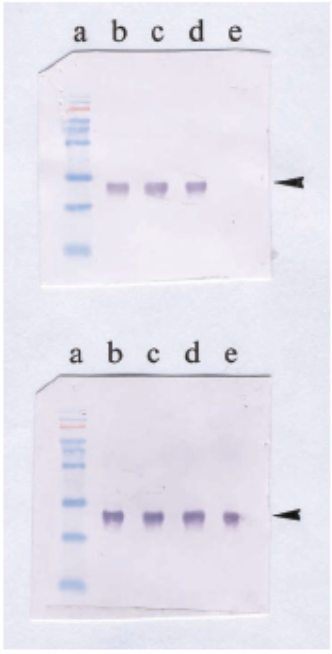

FIG. 4. Interaction of wild-type sorcin and of the E53Q, E94A, and E124A mutants with annexin VII in the presence of 10 μM (*upper panel*) or 500 μM $CaCl_2$ (*lower panel*). *a*, molecular weight markers (180, 130, 100, 73, 54, 50, 35, 24, 16, and 10 kDa). *b*, wild-type sorcin; *c*, E53Q; *d*, E94A; *e*, E124A subjected to SDS-PAGE (28) and transferred to PVDF membranes (29). The PVDF membranes were incubated with annexin VII in buffer containing 10 μM (*upper panel*) or 500 μM $CaCl_2$ (*lower panel*) and subsequently with anti-annexin VII polyclonal antibody. The *arrows* indicate the band corresponding to sorcin (M_r 21.5 kDa).

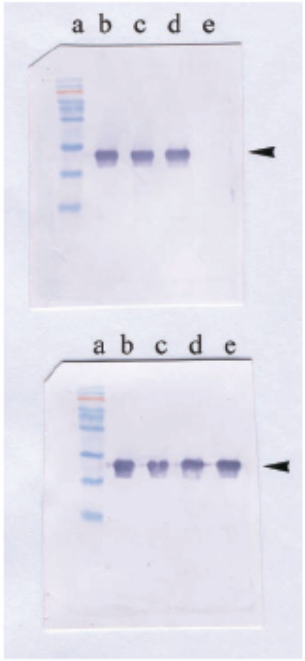

FIG. 5. Interaction of wild-type sorcin and of the E53Q, E94A, and E124A mutants with the ryanodine receptor in the presence of 10 μM (*upper panel*) or 500 μM $CaCl_2$ (*lower panel*). *a*, molecular weight markers (180, 130, 100, 73, 54, 50, 35, 24, 16, and 10 kDa); *b*, wild-type sorcin; *c*, E53Q; *d*, E94A; *e*, E124A subjected to SDS-PAGE (28) and transferred to PVDF membranes (29). The PVDF membranes were incubated with terminal cisternae vesicles from rabbit skeletal muscle enriched in ryanodine receptor in buffer containing 10 μM (*upper panel*) or 500 μM $CaCl_2$ (*lower panel*) and subsequently with anti-Ryr monoclonal antibody. The *arrows* indicate the band corresponding to sorcin (M_r 21.5 kDa).

action of sorcin and its mutants with annexin VII or with Ryr was observed in control experiments carried out in EGTA-containing buffer (data not shown).

Interaction of Wild-type Sorcin and Its Site-specific Mutants with the N-terminal Peptide of Annexin VII in SPR Experiments—SPR was used to obtain quantitative information on the interaction between sorcin and annexin VII, which is known to involve the N-terminal domains of both proteins (9, 23).

During the course of previous experiments, the lifetime of chips with immobilized annexin VII was found to be limited to a few days (23). To increase the chip stability, the use of a synthetic peptide corresponding to the annexin VII N terminus (amino acids 1–20) was explored. The use of the annexin N terminus has a further advantage. Because this peptide does not bind Ca^{2+}, a simplified experimental picture is obtained by annulling the contribution of Ca^{2+} binding to the target protein. The peptide was rendered soluble by introducing three lysine residues before amino acid 1 (peptide P1) or at the end of the sequence (peptide P2). Both P1 and P2 are immobilized efficiently on CM5 chips and react similarly with wild-type sorcin in the presence of calcium at micromolar concentrations, although P1 yields consistently higher RU values. Like immobilized full-length annexin VII (23), the immobilized peptides regain full binding activity after treatment with EGTA-containing buffer, which leads to complete dissociation of bound sorcin. Verzili *et al.* (23) established that at pH 7.5 and 6 μM calcium the interaction of immobilized full-length annexin VII with sorcin is significant (K_D = 0.63 μM). Under similar conditions, the immobilized P1 peptide yields apparent K_D values in the order of 1 μM, in good agreement with the results obtained with the full-length protein. The P1 peptide, therefore, was chosen for the systematic study of the interaction with sorcin and its mutants.

The Ca^{2+} dependence of the interaction with the N-terminal peptide of annexin VII was assessed at constant (300 nM) concentration of native or mutant sorcin. Typically, the sensorgrams display three phases (Fig. 6); the initial increase in RU from the base line corresponds to association of sorcin or its mutants to the immobilized annexin peptide, the plateau region represents the steady-state phase of the interaction, where the rate of sorcin association to the immobilized peptide is balanced by the rate of its dissociation from the complex, and the decrease in RU corresponds to the dissociation phase during buffer flow at the end of the sample injection. Simple inspection of the sensorgrams depicted in Fig. 6, *A–D*, shows that in the mutants both k_{on} and k_{off} increase with respect to

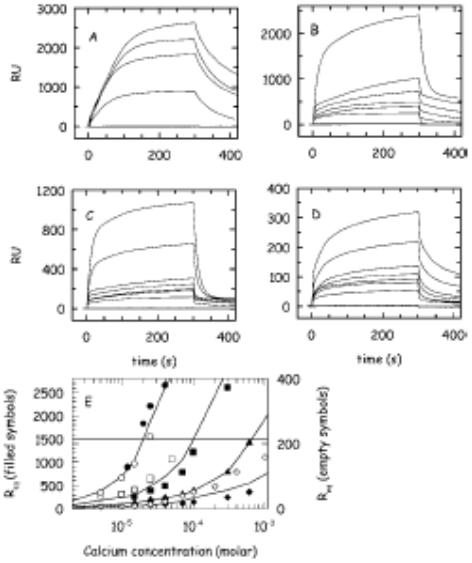

FIG. 6. SPR experiments on the binding of sorcin or its E53Q, E94A, and E124A mutants to the immobilized N-terminal peptide of annexin VII as a function of calcium concentration. In the sensorgrams (*A–D*) wild-type sorcin or its mutants at a concentration of 300 nM were injected at time 0 onto the chip containing the immobilized N-terminal annexin VII peptide. The increase in RU relative to the base line indicates complex formation; the plateau represents the steady-state phase of the interaction, whereas the decrease in RU represents the dissociation of sorcin from the immobilized annexin VII peptide attendant injection of buffer (10 mM HEPES, 0.15 M NaCl, 0.005% surfactant P20 at pH 7.4) at 25 °C. *A*, wild-type sorcin in buffer containing 2 mM EGTA and 12, 20, 25, and 40 μM $CaCl_2$ (from *bottom* to *top*). *B*, E53Q mutant in buffer containing 2 mM EGTA, 15, 25, 40, 70, 100, and 300 μM $CaCl_2$ (from *bottom* to *top*). *C*, E94A mutant in buffer containing 2 mM EGTA and 15, 25, 40, 70, 100, 300, and 600 μM $CaCl_2$ (from *bottom* to *top*). *D*, E124A mutant in buffer containing 2 mM EGTA and 15, 25, 40, 70, 100, 300, and 600 μM $CaCl_2$ (from *bottom* to *top*). *E*, the plateau signal at steady state (R_{eq}) is plotted as a function of total calcium concentration. Wild-type (● and ○), E53Q (■ and □), E94A (▲), and E124A (♦ and ◇) sorcin. *Filled* and *empty symbols* refer to data obtained with two different chips.

native sorcin, whereas the RU values in the plateau region and, hence, the amount of bound analyte decrease at any given calcium concentration. Moreover, for each protein the R_{eq} values increase when the calcium concentration in the medium increases. Fig. 6*E* summarizes the R_{eq} values obtained from the data depicted in Fig. 6, *A–D*, and in another independent set of experiments. The R_{eq} values show that the affinity for the annexin N terminus decreases in the order wt sorcin > E53Q > E94A > E124A.

A quantitative estimate of the equilibrium dissociation constant could be obtained only for wt sorcin by measuring the dependence of the R_{eq} values on sorcin concentration at constant Ca^{2+} (25 μM). Scatchard analysis of the data yielded an asymptotic value of about 3000 RU, corresponding to saturation of the immobilized annexin VII N-terminal peptide with wt sorcin, and an apparent K_D value of about 45 nM describing this interaction (data not shown). Under these experimental conditions, the R_{eq} values for the mutants are much lower than for wt sorcin, pointing to much higher dissociation equilibrium constants, such that the K_D values could not be assessed with accuracy. However, if the same asymptotic value of 3000 RU is assumed for wt sorcin and its mutants, the data of Fig. 6*E* can be used to estimate the strength of the sorcin-annexin peptide interaction. In fact, the sorcin concentration that yields an R_{eq} value of 1500, *i.e.* 50% saturation of the immobilized annexin peptide, corresponds to the K_D value. The existence of a linkage between the immobilized peptide-sorcin equilibrium and the binding of Ca^{2+} demands that the lower the affinity of the sorcin mutant for the immobilized annexin VII peptide, the higher the Ca^{2+} concentration has to be to achieve the same R_{eq} value. On this basis, an apparent K_D of about 300 nM is obtained at about 18 μM Ca^{2+} for native sorcin and at increasingly higher Ca^{2+} concentrations for the EF1, EF2, and EF3 mutants, namely 100 μM for E53Q, 600 μM for E94A, and about 5 mM for E124A.

DISCUSSION

The present data provide insight into the molecular details of the events that start with the Ca^{2+} binding step, lead to activation of sorcin, and ultimately result in its interaction with protein targets at or near cell membranes. The behavior of the three site-specific sorcin mutants studied shows that the EF3 hand is the site endowed with the highest affinity for Ca^{2+}. Because the structurally associated EF4 site is defective and does not bind the metal, the typical EF-hand structural/functional pairing cannot operate (32). It is conceivable that information of Ca^{2+} binding to EF3 is transferred to the rest of the molecule by taking advantage of the specific hydrogen-bonding interactions established by the EF3 Ca^{2+} binding loop and of the long D helix that connects EF3 to EF2. The proposed mechanism may be applicable to all members of the PEF family since these structural properties are common to all these proteins.

In sorcin, only the first three EF-hands are potentially capable of binding Ca^{2+} at micromolar concentrations. In EF4, the loop is non-canonical (only 11 residues long), the metal-coordinating residue in position Y is lacking, and the bidentate -Z glutamic acid is substituted by the shorter aspartic acid. EF5 is likewise defective since the loop is two residues shorter than in canonical EF-hands and there is no glutamic acid in position -Z. A comparison of the sequences of EF1 through EF3 predicts that the EF3-hand should be endowed with the highest affinity for calcium due to the presence of four acidic residues in the metal coordination positions. Indeed, EF3 is the most conserved EF-hand within the PEF family in terms of Ca^{2+}-coordinating ligands (33). The unusual EF1 site has a gap in the Y coordination position and lacks an acidic residue at position X. In EF2, which is canonical in term of length and similar in sequence to EF3, the affinity for Ca^{2+} should be diminished relative to EF3 by the substitution of the canonical aspartate in position -X by a glycine residue. EF1 and EF2 are associated structurally through a canonical short two-stranded β sheet arrangement in which Met-90 and Gly-91 establish hydrogen bonds with Gln-48 and Ile-49, respectively. It is of interest that a methionine residue (Met-90) can take the place of the highly conserved isoleucine and valine residues in position 8 of the EF2 Ca^{2+} binding loop without disrupting the interaction with the partner EF1, at variance with observations on calmodulin mutants (34, 35). However, these sequence-based arguments do not allow one to predict how different the Ca^{2+} affinities of the first three sites will be.

To arrive at an experimental assessment of this property, the highly conserved glutamate at position -Z has been chosen for site-specific mutagenesis in the first three Ca^{2+} binding motifs, with the expectation that removal of the bidentate coordination with the metal would abolish the capacity of the mutated site to bind Ca^{2+}, as has been observed for site-specific m-calpain

mutants (36). Accordingly, the assumption made in the interpretation of the results is that any given mutation influences the structural and functional properties of the mutated site, leaving those of the other EF motifs essentially unaltered. It follows that only those mutations involving a physiologically relevant site are expected to alter the properties of the mutant significantly relative to the native protein.

The behavior of the site-specific mutants under study supports these ideas. The structural markers used, namely the far and near UV CD spectra, indicate that in the mutant proteins both the global fold of wild-type sorcin and the environment of the aromatic residues are essentially unperturbed. The only exception concerns the environment of tyrosine and tryptophan residues in the E124A mutant as manifest in the near UV CD spectrum. In particular the tyrosine band at 283 nm has a significantly smaller amplitude than in the native protein and in the E53Q and E94A mutants (Fig. 2). The observed change can be attributed to participation of the Glu-124 carboxylate in a network of hydrogen-bonding and hydrophobic interactions that reaches Tyr-67 located on the loop connecting EF1 to EF2. In Ca^{2+}-free sorcin the Glu-124 carboxylate is not solvent-exposed, as is usually the case for the -Z ligand in regulatory Ca^{2+}-binding proteins (12, 15), but is hydrogen-bonded to Phe-112, located at the D helix C terminus (Fig. 1*C*). This phenylalanine residue is part of an extended hydrophobic core that includes Phe-70, Phe-156, Phe-159, the two Trp residues (99 and 105) on the D helix, and the aromatic ring of Tyr-67. In turn, the Tyr-67 OH group is hydrogen bonded to Asp-113 (OD2), which occupies the X position in the EF3 Ca^{2+} binding loop. Tyr-67, due to this hydrogen-bonding interaction and to coupling with the electronic π-π^* transitions of the neighboring aromatic side chains, should contribute significantly to the strength of the tyrosine CD-band (37). If this holds true, disruption of the interaction network should result in a significant decrease of the band amplitude as is indeed observed in the E124A mutant. The concomitant decrease in the tryptophan band at 292 nm is of importance for its functional implications. It indicates that the loss of the hydrogen-bonding interactions established by Asp-113 and Glu-124 of the EF3 Ca^{2+} binding loop is sensed also by Trp-99 and Trp-105, located on the long and relatively rigid D helix that connects EF3 to EF2 (Fig. 1*C*). The D helix, therefore, appears capable of transmitting the structural perturbations originating in the EF3 Ca^{2+} binding loop far from the site of mutation. This role of the D helix is reminiscent of that played in calmodulin by the long Leu-69–Phe-92 E-helix that transmits the occurrence of Ca^{2+} binding between the two Ca^{2+} binding domains. In calmodulin, alteration of a single hydrogen bond, like that established between glutamic acid (Glu-82) of the E helix with Tyr-138, has the potential to disrupt the structural coupling between the two domains (38), as observed for the E124A sorcin mutant.

The changes in the near UV CD spectrum just discussed are observed uniquely in the E124A mutant (Fig. 2). This fact taken together with the far-reaching effects of the Glu-124 mutation, points to EF3 as the ideal trigger of the pathway that leads from Ca^{2+} binding to sorcin activation. A first, qualitative indication that this view is correct is provided by the close similarity of the near UV CD spectra measured in native sorcin (22) and the isolated Ca^{2+} binding domain (data not shown) during the first stages of Ca^{2+} titrations with that of the E124A mutant. It may be envisaged that in the native protein the first metal ion is coordinated by the EF3 Ca^{2+} binding loop with loss of the H-bonds established by Asp-113 and Glu-124 just as in the E124A mutant. There is, however, another requirement for this picture to be true, namely EF3 should be endowed with the highest affinity for Ca^{2+}. The fluorescence titration data in the presence of Quin2 show that it is so (Fig. 3). The overall affinity for Ca^{2+} follows the order wild-type sorcin > E53Q > E94A > E124A, indicating that disruption of the EF3 site has the largest effect on this property of the protein. Disruption of the EF2 and EF1 sites has progressively smaller effects.

Direct evidence for the major functional role of EF3 is provided by the immunoblot and SPR experiments, which allow a measure of the interaction with physiological targets and of its Ca^{2+} dependence. Based on the immunoblot data, the E124A mutant requires a significantly higher Ca^{2+} concentration (500 μM) than wild-type sorcin or the E53Q and E94A mutants (about 10 μM) for interaction with the binding partners. Figs. 4–5 show that there is no significant difference between annexin VII and Ryr, which interact with the N- and C-terminal sorcin domains, respectively (23, 19). Importantly, all the mutants retain the capacity to be activated by Ca^{2+}, in accordance with the fact that they are all able to translocate reversibly to *E. coli* membranes at millimolar concentrations of the cation, as observed during the purification procedure.

A better estimate of the Ca^{2+} concentration required to activate the mutants is furnished by the SPR experiments that involve measurement of their interaction with the immobilized N-terminal peptide of annexin VII. This peptide provides a suitable model to monitor complex formation between the whole protein and sorcin, as indicated by the data of Brownawell and Creutz (9) and by the control experiments performed. Fig. 6 shows that at any given Ca^{2+} concentration, the amount of complex formed decreases in the order wild-type sorcin > E53Q > E94A > E124A, which parallels their affinity for Ca^{2+} (Fig. 3). In wt sorcin an apparent K_D of 300 nM is obtained at about 18 μM Ca^{2+}. The E53Q, E94A, and E124A mutants require a 5-, 30-, and 250-fold increase in Ca^{2+} concentration, respectively, to interact with the immobilized annexin VII peptide with similar K_D values. It follows that sorcin activation at micromolar Ca^{2+} concentrations requires preservation not only of the EF3 but also of the EF2 hand. On this basis EF3 and EF2 can be identified as the physiological pair.

The picture that emerges is that EF3 is the major player in sorcin functionality. It has the highest affinity for Ca^{2+} and can trigger a Ca^{2+}-dependent conformational change by means of the hydrogen-bonding interactions established by Asp-113 and Glu-124 in the Ca^{2+} binding loop. The conformational change, although limited in extent, reaches EF2 and the EF1-EF2 loop through reorganization of the hydrophobic core packing around the D helix, which comprises Phe-95 and residues LWAVL in positions 98–102, Trp-105, Ile-110, Phe-112, Phe-156, and Phe-159. The canonical pairing of EF2 and EF1 facilitates transfer of information to the latter site. Integrity of the whole transmission pathway is necessary for sorcin activation, as shown by the behavior of the 90–198 sorcin fragment, which lacks EF1 and EF2. This fragment binds Ca^{2+} with decreased affinity and is unable to translocate to membranes, a finding that suggested wrongly that EF1 and EF2 represent the physiological pair (19).

The x-ray crystal structures of native sorcin and of the sorcin binding domain support the mechanism just proposed in that the different conformations predicted by the model of sorcin activation are frozen in individual monomers. This implies that the energies involved in the Ca^{2+}-induced rearrangements of the sorcin molecule are balanced by the lattice energies. In the structure of the whole molecule (15), the D helix and the loop connecting EF1 to EF2 have slightly different conformations in the two monomers forming the dimer. In one monomer Tyr-67 is hydrogen-bonded to Asp-113, and the D helix is rather straight, whereas in the other monomer the hydrogen bond is missing, the phenol moiety points toward the solvent, and the

D helix is slightly bent. In the structure of the sorcin Ca^{2+} binding domain (12), which has a tetramer in the asymmetric unit, monomers belonging to different dimers display relevant differences that are concentrated in the EF3 Ca^{2+} binding loop, in the D helix, and in the loop connecting EF3 to EF4. It is of interest that the EF3-EF4 loop interacts with the N-terminal peptide in the model proposed by Ilari *et al.* (12), which depicts the interaction between the C- and the N-terminal domains.

The very minor conformational changes that differentiate the x-ray crystal structures of the Ca^{2+}-free and Ca^{2+}-bound forms of calpain (1, 2) and grancalcin (3, 13) are likewise consistent with the mechanism proposed. The observed changes are limited to the EF1 region. This region is linked to the flexible N-terminal domain and, hence, must amplify the Ca^{2+}-induced conformational changes just described to bring about the exposure of hydrophobic residues for interaction with the binding partners. As a matter of fact, the mechanism proposed may be applicable to all members of the PEF family since they share the structural/functional elements necessary for sorcin activation. Thus, EF3 is the Ca^{2+}-binding site with the highest affinity for the metal, the -Z glutamate and Y aspartate residues in the EF3 Ca^{2+}-binding loop are not solvent-exposed but are involved in hydrogen-bonding interactions with other amino acids, and the hydrophobic core around the D helix, whose packing rearrangement provides the driving force in the sorcin signal transmission pathway, is conserved.

At this point it appears useful to speculate on the mechanism used by PEF proteins to amplify the small Ca^{2+}-induced conformational changes just discussed that occur in the Ca^{2+} binding domain to achieve target protein interaction. This requires exposure of hydrophobic patches resulting from the movement of the N- and C-terminal domains relative to each other (12). Interestingly, the loop connecting EF3 to EF4 contains a stretch of conserved residues, GFRL in sorcin and GYRL in ALG-2, that were proposed to interact with the N-terminal domain in the Ca^{2+}-free state and to become solvent-exposed upon Ca^{2+} binding (12, 14). One may speculate that these conserved residues play a role in the amplification of the Ca^{2+} signal by transmitting the conformational change to the N-terminal domain, and this may be the reason for the sequence conservation.

In conclusion, the unusual functional coupling operative in sorcin appears applicable to all PEF proteins. It may be envisaged that their activation mechanism depends on subtle changes in the packing of hydrophobic residues located around the D helix that links the site endowed with the highest affinity for Ca^{2+} to the rest of the molecule.

Acknowledgments—We thank Dr. Benedetta Mattei for invaluable help with the surface plasmon resonance experiments.

REFERENCES

1. Blanchard, H., Grochulski, P., Li, Y., Arthur, S. C., Davies, P. L., Elce, J. S., and Cygler, M. (1997) *Nat. Struct. Biol.* 4, 532–538
2. Lin, G., Chattopadhyay, D., Maki, M., Wang, K. K. W., Carson, M., Jin, L., Yu, P. W., Takano, E., Hatanaka, M., DeLucas, L. J., and Narayana, S. V. (1997) *Nat. Struct. Biol.* 4, 539–546
3. Lollike, K., Johnsen, A. H., Durussel, I., Borregaard, N., and Cox, A. (2001) *J. Biol. Chem.* 276, 17762–17769
4. Lo, K. W.-H., Zhang, Q., Li, M., and Zhang M. (1999) *Biochemistry* 38, 7498–7508
5. Kitaura, Y., Watanabe, M., Satoh, H., Kawai, T., Hitomi, K., and Maki, M. (1999) *Biochem. Biophys. Res. Commun.* 263, 68–75
6. Meyers, M. B., Puri, T. S., Chien, A. J., Gao, T., Hsu, P. H., Hosey, M. M., and Fishman, G. I. (1998) *J. Biol. Chem.* 273, 18930–18935
7. Meyers, M. B., Pickel, V. M., Sheu, S. S., Sharma, V. K., Scotto, K. W., and Fishman, G. I. (1995) *J. Biol. Chem.* 270, 26411–26418
8. Park-Chung, E., Meyers, M. B., Pettingell, W. P., Moir, R. D., Brownawell, A. M., Cheng, I., Tanzi, R. E., and Kim, T. W. (2000) *J. Biol. Chem.* 275, 14440–14445
9. Brownawell, A. M., and Creutz, C. E. (1997) *J. Biol. Chem.* 272, 22182–22190
10. Clemen, C. S., Hofmann, A., Zamparelli, C., and Noegel, A. A. (1999) *J. Muscle Res. Cell Motil.* 20, 669–679
11. Salzer, U., Hinterdorfer, P., Hunger, U., Borken, C., and Prohaska, R. (2002) *Blood* 99, 2569–2577
12. Ilari, A., Johnson, K. A., Nastopoulos, V., Verzili, D., Zamparelli, C., Colotti, G., Tsernoglou, D., and Chiancone, E. (2002) *J. Mol. Biol.* 317, 447–458
13. Jia, J., Han, Q., Borregaard, N., Lollike, K., and Cygler, M. (2000) *J. Mol. Biol.* 300, 1271–1281
14. Jia, J., Tarabykina, S., Hansen, C., Berchtold, M., and Cygler, M. (2001) *Structure (Lond.)* 9, 267–275
15. Xie, X., Dwyer, M. D., Swenson, L., Parker, M. H., and Botfield, M. C. (2001) *Protein Sci.* 10, 2419–2425
16. Jia J., Borregaard, N., Lollike, K., and Cygler, M. (2001) *Acta Crystallogr. Sect. D* 57, 1843–1849
17. Strobl, S., Fernandez-Catalan, C., Braun, M., Huber, R., Masumoto, H., Nakagawa, K., Iris, A., Sorimachi, H., Bourenkow, G., Bartunik, H., Suzuki, K., and Bode, W. (2000) *Proc. Natl. Acad. Sci. U.S.A.* 97, 588–592
18. Hosfield, C. M., Elce, J. S., Davies, L., and Jia, Z. (1999) *EMBO J.* 18, 6880–6889
19. Zamparelli, C., Ilari, A., Verzili, D., Giangiacomo, L., Colotti, G., Pascarella, S., and Chiancone, E. (2000) *Biochemistry* 39, 658–666
20. Kitaura, Y., Matsumoto, S., Satoh, H., Hitomi, K., and Maki, M. (2001) *J. Biol. Chem.* 276, 14053–14058
21. Meyers, M. B., Zamparelli, C., Verzili, D., Dicker, A. P., Blanck, T. J. J., and Chiancone, E. (1995) *FEBS Lett.* 357, 230–234
22. Zamparelli, C., Ilari, A., Verzili, D., Vecchini, P., and Chiancone, E. (1997) *FEBS Lett.* 409, 1–6
23. Verzili, D., Zamparelli, C., Mattei, B., Noegel, A. A., and Chiancone, E. (2000) *FEBS Lett.* 471, 197–200
24. Higuchi, R., Krummel, B., and Saiki, R. K. (1988) *Nucleic Acids Res.* 16, 7351–7367
25. Chou, P. Y., and Fasman, G. D. (1974) *Biochemistry* 13, 222–224
26. Bryant, D. T. W. (1985) *Biochem. J.* 228, 613–616
27. André, I., and Linse, S. (2002) *Anal. Biochem.* 305, 195–205
28. Laemmli, U. K. (1970) *Nature* 227, 680–685
29. Towbin, H., Staehelin, T., and Gordon, J. (1979) *Proc. Natl. Acad. Sci. U. S. A.* 76, 4350–4354
30. Bjellqvist, B., Hughes, G. J., Pasquali, Ch., Paquet, N., Ravier, F., Sanchez, J.-C., Fruiger, S., and Hochstrasser, D. F. (1993) *Electrophoresis* 14, 1023–1031
31. Tsien, R. Y., and Pozzan, T. (1989) *Methods Enzymol.* 172, 230–262
32. Nelson, M. R., and Chazin, W. J. (1998) *Biometals* 11, 297–318
33. Glaser, F., Pupko, T., Paz, I., Bell, R. E., Bechor-Shental, D., Martz, E., and Ben-Tal, N. (2003) *Bioinformatics* 19, 163–164
34. Jaren, O. R., Harmon, S., Chen, A. F., and Shea, M. A. (2000) *Biochemistry* 39, 6881–6890
35. Fefeu, S., Bielefsky, R. R., McCormick, J. E., Martin, S. R., Bayley, P. M., and Feeney, J. (2000) *Biochemistry* 39, 15920–15931
36. Dutt, P., Arthur, J. S. C., Grochulski, P., Cygler, M., and Elce, J. S. (2000) *Biochem. J.* 348, 37–43
37. Strickland, E. H. (1974) *CRC Crit. Rev. Biochem.* 2, 113–175
38. Sun, H., Yin, D., Coffeen, L. A., Shea, M. A., and Squier, T. C. (2001) *Biochemistry* 40, 9605–9617
39. Kraulis, P. J. (1991) *J. Appl. Crystallogr.* 24, 283–291
40. Biacore AB (1994) *BIAtechnology Handbook*, Version AB, pp. 4–5, Biacore AB, Uppsala, Sweden

Biochemistry **2006**, *45*, 12519−12529 12519

The W105G and W99G Sorcin Mutants Demonstrate the Role of the D Helix in the Ca^{2+}-Dependent Interaction with Annexin VII and the Cardiac Ryanodine Receptor†

Gianni Colotti,‡ Carlotta Zamparelli,‡ Daniela Verzili,‡ Manuela Mella,‡ Christopher M. Loughrey,§,∥ Godfrey L. Smith,§ and Emilia Chiancone*,‡

Consiglio Nazionale delle Ricerche Institute of Molecular Biology and Pathology, Department of Biochemical Sciences A. Rossi Fanelli, University of Rome La Sapienza, 00185 Rome, Italy, and Institute of Biomedical and Life Sciences, University of Glasgow, Glasgow G12 8QQ, United Kingdom

Received March 2, 2006; Revised Manuscript Received August 22, 2006

ABSTRACT: Sorcin, a 21.6 kDa two-domain penta-EF-hand (PEF) protein, when activated by Ca^{2+} binding, interacts with target proteins in a largely uncharacterized process. The two physiological EF-hands EF3 and EF2 do not belong to a structural pair but are connected by the D helix. To establish whether this helix is instrumental in sorcin activation, two D helix residues were mutated: W105, located near EF3 and involved in a network of interactions, and W99, located near EF2 and facing solvent, were substituted with glycine. Neither mutation alters calcium affinity. The interaction of the W105G and W99G mutants with annexin VII and the cardiac ryanodine receptor (RyR2), requiring the sorcin N-terminal and C-terminal domain, respectively, was studied. Surface plasmon resonance experiments show that binding of annexin VII to W99G occurs at the same Ca^{2+} concentration as that of the wild type, whereas W105G requires a significantly higher Ca^{2+} concentration. Ca^{2+} spark activity of isolated heart cells monitors the sorcin−RyR2 interaction and is unaltered by W105G but is reduced equally by W99G and the wild type. Thus, substitution of W105, via disruption of the network of D helix interactions, affects the capacity of sorcin to recognize and interact with either target at physiological Ca^{2+} concentrations, while mutation of solvent-facing W99 has little effect. The D helix appears to amplify the localized structural changes that occur at EF3 upon Ca^{2+} binding and thereby trigger a structural rearrangement that enables interaction of sorcin with its molecular targets. The same activation process may apply to other PEF proteins in view of the D helix conservation.

Sorcin (SOluble Resistance-related Calcium binding proteIN) belongs to the penta-EF-hand (PEF)[1] family, a small group of Ca^{2+}-binding proteins that comprises calpains (*1*, *2*), grancalcin (*3*), ALG-2 (*4*), and peflin (*5*). The binding of Ca^{2+} triggers the reversible translocation of all PEF proteins from the cytoplasm to cell membranes where they interact with specific target proteins and thereby participate in a variety of physiological processes. The molecular mechanism of the Ca^{2+}-linked activation process is largely unknown, although a major role has been assigned to the long and rigid D helix located in the C-terminal domain, a compact, highly conserved structure that contains the five EF-hands (*6*). The D helix is unusual in that it is shared by two EF-hands belonging to different structural pairs, namely, by EF2 and EF3, a peculiarity that pertains also to the G helix which is shared by EF4 and EF5. The latter helix has a clear structural role as it gives rise to a stable interface between two monomers together with the H helix. Upon dimer formation, the two odd EF5 motifs interact with each other and achieve the canonical structural pairing of EF-hands (*7*−*10*). In contrast to the C-terminal domain, the N-terminal domain is of variable length across the range of PEF proteins but is always rich in glycine and proline residues. Because of the flexibility that this endows, the N-terminus is not visible in most available X-ray crystal structures (*8*, *9*).

The conformational change that permits interaction of PEF proteins with targets entails exposure of hydrophobic residues and is triggered by the binding of two Ca^{2+} ions per monomer. In a recent study with site-specific sorcin variants carrying mutations at the Ca^{2+} binding loops, EF3 and EF2 have been identified as the two functional EF-hands since Ca^{2+} affinity decreases in the following order: EF3 > EF2 > EF1. Moreover, since the D helix connects the structurally distant EF3 and EF2 hands and contains an extended hydrophobic patch, it was hypothesized to be instrumental in Ca^{2+}-induced activation of sorcin (*6*). A molecular description of these processes requires an understanding of the mechanism underlying the transfer of information about

† This study was funded by the British Heart Foundation (to G.L.S.) and by the Ministero Istruzione Università e Ricerca, PRIN 2005 (to E.C.).

* To whom correspondence should be addressed: Department of Biochemical Sciences A. Rossi Fanelli, University of Rome La Sapienza, 00185 Rome, Italy. Telephone: +390649910761. Fax: +39064440062. E-mail: emilia.chiancone@uniroma1.it.

‡ Consiglio Nazionale delle Ricerche−IBPM, University of Rome La Sapienza.

§ University of Glasgow.

∥ Current address: Institute of Comparative Medicine, University of Glasgow, Glasgow G12 8QQ, United Kingdom.

[1] Abbreviations: PEF, penta-EF-hand; PVDF, polyvinyl difluoride; RyR1, skeletal muscle ryanodine receptor; RyR2, cardiac ryanodine receptor; SCBD, sorcin Ca^{2+}-binding domain; SPR, surface plasmon resonance; SR, sarcoplasmic reticulum.

10.1021/bi060416a CCC: $33.50
Published on Web 09/26/2006

A

N-terminal domain

```
MAYPGHPGAGGGYYPGGYGGAPGGPGPPGQTQ                          1-32

C-terminal domain (SCBD)
 Helix A    EF2   Helix B              Helix C    EF2
DPLYGYFASVAGQDGQIDADELQRCLTQSGIAGGYKPFNLETCRLMVSMLDRDMSGTMG     33-91

        Helix D          EF3   Helix E       Helix F
FNEFKELWAVLNGWRQHFISFDSDRSGTVDPQELQEALTTMGFRLNPQTVNSIAKR      92-147

  EF4        Helix G          EF5     Helix H
YSTSGNITFDDYIACCVKLRALTDSFRRRDGAQQGHVNYSYDDFIQCVMTV          148-198
```

B

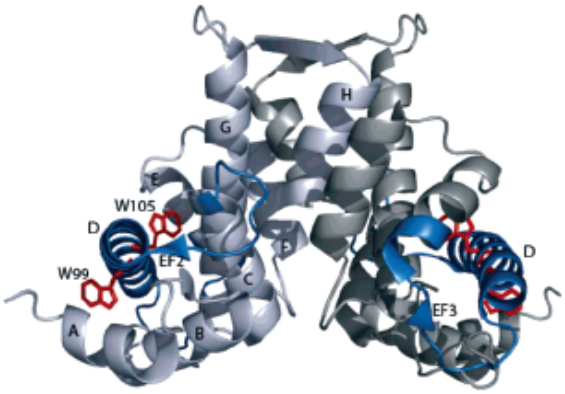

FIGURE 1: Sorcin sequence (A) and structure of the Ca^{2+}-binding domain, SCBD (B). In panel A, the 11 amino acids which interact with SCBD in the model of Ilari et al. (*7*) are in boldface. In panel B, the two monomers are depicted in different colors. The D helix and physiologically relevant EF2 and EF3 are colored blue; the two tryptophan residues, W99 and W105, are colored red. This figure was created with PYMOL (*36*).

the Ca^{2+} binding event from EF3 to the rest of the molecule and the nature of the ensuing structural rearrangements. Surprisingly, the reported Ca^{2+}-dependent changes in the crystal structures of known PEF proteins are rather subtle and are localized to the EF1−EF2 pair, close to the connection between the N- and C-terminal domains (*1*, *9*, *11*−*13*). It is not known how such small changes are amplified to the extent required for target protein interaction. In the case of sorcin, Ilari et al. (*7*) proposed an activation mechanism based on the X-ray crystal structure of the C-terminal domain (SCBD, sorcin Ca^{2+}-binding domain, corresponding to residues 33−198) that accounts for the increased hydrophobicity of the Ca^{2+}-bound protein. Ca^{2+} binding is believed to cause a series of structural rearrangements that loosens the interactions between the N- and C-terminal domains, making them available for binding the respective targets.

This work was undertaken to validate this mechanism. Experiments were designed that take advantage of the presence of the only two tryptophan residues, W99 and W105, in the D helix. As shown in Figure 1, W99 is close to the EF2 Ca^{2+}-binding loop (~4 Å), whereas W105 is close to EF3 (~7 Å). The two tryptophan residues are one and one-half helical turns apart such that the side chain of W99 lies on the outer surface of the SCBD, in contact with residues that join the two domains, whereas the W105 side chain points toward the core of the SCBD where it interacts primarily with residues of the D and G helices (*7*). The different localization of the two tryptophan residues within the D helix and the different type of interactions they establish suggest that their substitution may affect differently the functional coupling of EF3 and EF2 and the interaction with target proteins. The involvement of W105 in the network of hydrophobic and hydrogen bonding interactions is expected to render this residue of major importance for the transmission of the Ca^{2+}-dependent conformational changes. To verify this contention, site-specific mutants W99G and W105G were produced and their interaction with annexin VII and with the cardiac ryanodine receptor (RyR2) (*14*), the main Ca^{2+} channel of cardiac sarcoplasmic reticulum (SR), was studied. Previous work has shown that annexin VII and the skeletal muscle ryanodine receptor (RyR1) interact with the sorcin N-terminal and C-terminal domain, respectively (*15*, *16*); RyR2 can be taken to behave like RyR1 given their structural similarity. In the case of RyR2, the possible influence of the N-terminal domain was assessed by comparing the isolated SCBD to the wild-type protein. Additionally, EF3 site variant E124A was employed as a control since it is unable to bind Ca^{2+} at physiological

concentrations due to substitution of Glu124 in position −*Z* (*6*).

The sorcin−annexin VII interaction was studied directly by Western blot and surface plasmon resonance experiments, whereas the interaction of sorcin with RyR2 was monitored by measuring Ca^{2+} spark activity in isolated rabbit heart cells (*17*). Previous work has shown that addition of sorcin affects Ca^{2+} sparks in permeabilized myocytes (*18*, *19*). Although Ca^{2+} affinity is substantially unaltered in the two mutants with respect to the wild-type protein, substitution of W105 affects its capacity to recognize and interact with the two targets significantly, while mutation of W99 has an only small effect on sorcin function. These results support the crucial role of the D helix in sorcin activation (*6*, *7*) and in particular show that W105 is a major player in this process. Other PEF proteins are likely to use the same activation mechanism in view of the high degree of sequence conservation in the D helix (*20*).

MATERIALS AND METHODS

Cloning of the W99G and W105G Sorcin Variants. The cDNA of Chinese hamster ovary sorcin, cloned between the unique NdeI and HindIII sites of plasmid pET22 (Novagen) (*6*), was subjected to site-directed mutagenesis by the PCR overlap extension mutagenesis method, according to the method of Higuchi et al. (*21*).

The following oligonucleotides were used: Nforward, 5′-GCGAAATTAATACGACTCACTATAGGG-3′; Creverse, 5′-CAAGCTTTTAGACGGTCATGACAC-3′; W99G forward. 5′-GAATTTAAAGAGCTCGGCGCTGTGCTGAATGG-3′; W99G reverse. 5′-CCATTCAGCACAGCGCCGAGCTCTTTAAATTC-3′; W105G forward, 5′-CTGTGCTGAATGGCGGCAGACAACACTTCATC-3′; and W105G reverse, 5′-GATGAAGTGTTGTCTGCCGCCATTCAGCACAG-3′.

The PCR products that were obtained were agarose-purified, digested with NdeI and HindIII, and cloned into a pET22 expression vector (Novagen).

Expresszion and Purification of Wild-Type (wt) Sorcin and Its Variants. Chinese hamster ovary recombinant sorcin was expressed in *Escherichia coli* BL21(DE3) cells and purified as previously described (*22*). The same purification procedure was used for the site-specific mutants. Protein concentrations were determined spectrophotometrically at 280 nm. The molar extinction coefficients were calculated according to the method of Edelhoch (*23*) and were 29 400 for the wt protein, 22 640 for W99G, 22 640 for W105G, and 22 000 for SCBD.

Circular Dichroism and Fluorescence Spectra. CD spectra were recorded on a Jasco J-710 spectropolarimeter in the far-UV (200−250 nm) and near-UV (250−350 nm) regions. The experiments were carried out at 20 °C in 100 mM Tris-HCl at pH 7.5. The α-helical content was calculated from the ellipticity value at 222 nm (*24*) and with Selcon3 (srs.dl.ac.uk/VUV/CD/selcon.html).

Intrinsic fluorescence was measured in a Fluoromax spectrofluorimeter at 25 °C in 100 mM Tris-HCl at pH 7.5 using an excitation wavelength of 280 nm and a slit width of 0.5 nm. The emission signal was followed between 300 and 400 nm.

Analytical Ultracentrifugation. Sedimentation velocity experiments were carried out on a Beckman-Coulter ProteomeLab XL-I analytical ultracentrifuge at 40 000 rpm and 15 °C at a protein concentration of 1 mg/mL in 0.1 M Tris-HCl buffer at pH 7.5. The protein concentration gradient in the cells was determined by absorption scans along the centrifugation radius at 280 nm with three averages and a step resolution of 0.005 cm. Data were analyzed with SEDPHAT (sedimentation and polymer hydrodynamic analysis tool, www.analyticalultracentrifugation.com/sedphat/configurations.htm) and are expressed in terms of the weight-average molecular mass (M_w) by assuming a spherical shape of the molecule.

Determination of Ca^{2+} Affinity. Titrations based on the competitive chelator method (*25*) were carried out in 100 mM Tris-HCl at pH 7.5 and 25 °C using the fluorescent Ca^{2+} chelators Quin 2, as described in Zamparelli et al. (*26*), and Fluo-3. The excitation wavelength was 339 nm in the case of Quin 2 and 488 nm in the case of Fluo-3; the increment of emission intensity due to Ca^{2+} binding was followed for Quin 2 at 492 nm (slit width of 0.5 nm) and for Fluo-3 at 528 nm (slit width of 1 nm). The protein concentration in the experiments involving Quin 2 was 25 μM and in those with Fluo-3 was 15 μM.

Control experiments were performed on Quin 2 and on Fluo-3 alone. Special care was taken to reduce Ca^{2+} contamination to 0.5−1.0 μM by treating the protein solutions and the glassware with Chelex 100 as recommended by André and Linse (*27*). At the end of each titration, the fluorescence intensity corresponding to the nominally zero free Ca^{2+} concentration was determined by addition of 5 mM EGTA. The fluorescence intensity of Quin 2 or Fluo-3 at high Ca^{2+} concentrations was taken as the higher asymptote. The binding constants were assessed by fitting the experimental data with CaLigator (*27*) by using the [2 Ca^{2+} sites + chelator] model.

Overlay Assay Experiments. W99G and W105G were subjected to electrophoresis on a 15% polyacrylamide gel under denaturing conditions (*28*) and transferred to polyvinyl difluoride membranes (PVDF) in transfer buffer [25 mM Tris-HCl, 192 mM glycine, and 20% methanol (pH 8.3)] at 100 mA for 45 min. The PVDF membranes were incubated at room temperature with annexin VII (5 μg/mL) in 1% gelatin in TBST buffer [20 mM Tris-HCl, 0.5 M NaCl, and 0.05% Tween 20 (pH 7.5)] containing 1 mM EGTA or 10 or 75 μM $CaCl_2$ (total). Subsequently, the membranes were incubated with an anti-annexin VII monoclonal antibody kindly provided by A. Noegel (1:3000 dilution) in 1% gelatin in TBST buffer. The blots were developed by incubation for 2−5 min with alkaline phosphatase-conjugated monoclonal anti-mouse IgG in 1% gelatin in TBST. The longer incubation time was used for the blots carried out at < 10 nM calcium (i.e., in 1 mM EGTA) to exclude any interaction; under these conditions, the ovalbumin molecular mass marker band shows positive staining. Control experiments ruled out the existence of cross reactivity between the sorcin variants and the anti-annexin VII monoclonal antibody.

Surface Plasmon Resonance Measurements. Surface plasmon resonance (SPR) experiments were carried out using a BIACORE X system (BIAcore AB, Uppsala, Sweden). The N-terminal peptide of annexin VII was synthesized by SIGMA-Genosys (Cambridge, U.K.); to improve peptide

solubility and binding to the sensor chip, three lysine residues were added to the N-terminal end of the 20 first amino acids of annexin VII (MSYPGYPPTGYPPFPGYPPA). The peptide purity was checked by MALDI-TOF mass spectrometry. The calculated isoelectric point of the peptide is 9.90, determined using pI-tool (*29*).

The sensor chip (CM5, Biacore AB) was activated chemically by injection of 35 μL of a 1:1 mixture of *N*-ethyl *N*′-[3-(dimethylamino)propyl]carbodiimide (200 mM) and *N*-hydroxysuccinimide (50 mM) at a flow rate of 5 μL/min. The N-terminal peptide of annexin VII was immobilized on the activated sensor chip via amine coupling. The reaction was carried out in 20 mM sodium acetate at pH 6.0; the remaining ester groups were blocked by injecting 1 M ethanolamine hydrochloride (35 μL). In control experiments, the sensor chip was treated as described above in the absence of peptide.

The interaction of the immobilized annexin VII peptide with wild-type sorcin, SCBD, and the variants was detected through mass concentration-dependent changes in the refractive index on the sensor chip surface. The changes in the observed SPR signal are expressed as resonance units (RU). A response change of 1000 RU typically corresponds to a change in the protein concentration on the sensor chip of ~1 ng/mm^2 (*30*).

The experiments were carried out at 25 °C in 10 mM HEPES (pH 7.4), 150 mM NaCl, and 0.005% surfactant P-20. The buffer was treated with Chelex 100 to eliminate Ca^{2+} contaminations and degassed. For the experiments as a function of Ca^{2+} concentration, calcium chloride or EGTA was added to the buffer; the protein concentration was 300 nM. Measurements were performed at a flow rate of 20 μL/min with an immobilization level of the annexin VII N-terminal peptide corresponding to 100−900 RU. All measurements were repeated twice using different sensor chips. The amine coupling kit, the P-20 surfactant, and the CM-5 sensor chip were purchased from BIAcore AB, and all the other reagents were high-purity grade.

Scatchard analysis of the dependence of the SPR signal at steady state (R_{eq}) on the concentration of sorcin was performed to assess the dissociation constant. R_{eq} values were calculated from the sensorgrams using BIAevaluation version 3.0.

Measurement of Ca^{2+} Spark Characteristics in Isolated Heart Cells. An investigation of the direct effects of sorcin on Ca^{2+} sparks in intact rabbit cardiomyocytes is complicated by the parallel effects on the sarcolemmal extrusion of intracellular Ca^{2+} (*19*). For this reason, sarcolemmal fluxes are bypassed by the acute permeabilization of the sarcolemma with β-escin. Under such experimental conditions, single cardiomyocytes can be superfused using the standardized Ca^{2+} concentration and pH in the presence of ATP and creatine phosphate. Ca^{2+} spark activity is monitored by the inclusion of 10 μM Fluo-3 in the perfusing solution. In this study, isolated rabbit ventricular cardiomyocytes were initially suspended in a mock intracellular solution with the following composition: 100 mM KCl, 5 mM Na_2ATP, 10 mM Na_2CrP, 5.5 mM $MgCl_2$, 25 mM HEPES, and 1 mM K_3EGTA (pH 7.0) with no added Ca^{2+} (20−21 °C). They were then permeabilized using β-escin (0.1 mg/mL for 0.5−1 min). Confocal line-scan images of single cardiomyocytes were recorded using a BioRad Radiance 2000 confocal system. Permeabilized cells were perfused with a mock intracellular solution containing 0.05 mM EGTA. Fluo-3 (10 μM) in the perfusing solution was excited at 488 nm (Kr laser line) and measured above 515 nm using epifluorescence optics of a Nikon Eclipse inverted microscope with a 60× 1.2 NA water-immersion objective lens (Plan Apochromat, Nikon). In all experiments included in the analysis, the Ca^{2+} concentration in the test solution was 155−165 nM. Ca^{2+} sparks were quantified using an automatic detection and measurement algorithm (*19*).

RESULTS

Characterization of the W99G and W105G Variants. Binding of two Ca^{2+} ions per sorcin monomer leads to the exposure of hydrophobic surfaces that manifests itself in the tendency of the wt protein to aggregate or precipitate in the absence of protein targets. This tendency, which limits the experimental conditions that can be used for the measurement of the Ca^{2+}-bound protein spectra (*26*), is particularly marked in the W105G variant.

The attempts made so far to obtain X-ray quality crystals of the two tryptophan variants have failed. Therefore, possible structural changes relative to the wt protein were monitored by means of CD and fluorescence spectroscopy and by analytical ultracentrifugation. The folding of the mutated apoproteins is essentially unaltered with respect to that of wild-type sorcin as indicated by the similarity of the far-UV CD spectra (Figure 2A). Analysis of the spectra points to a similar α-helix content, i.e., 60% for wt sorcin and 58% for both W99G and W105G. Support for the similarity of tertiary−quaternary structure was gained from the similarity of the weight-average molecular mass values (M_w) calculated from sedimentation velocity experiments (35 000 Da for wild-type sorcin, 36 500 Da for W99G, and 34 700 Da for W105G).

The occurrence of structural perturbations that are localized to the environment of the tryptophan residues and of other aromatic side chains is indicated by the near-UV CD and fluorescence emission spectra of the mutated proteins. The near-UV CD spectrum of wt sorcin is negative and characterized by two sharp bands at 262 and 268 nm attributed to phenylalanines, by a weaker band at 283 nm due to the tyrosyl fine structure (0−0 transition), and by a fairly intense, well-resolved peak at 292 nm due to tryptophan residues. The near-UV CD spectra (Figure 2B) of W105G display the peaks characteristic of the native protein, although the ellipticity is less negative. In contrast, the ellipticity of the W99G mutant in the 272−292 nm region is positive as in the case of Ca^{2+}-bound wt sorcin. A broad peak characterizes the fluorescence emission spectrum of apo-wt sorcin with a maximum at 338 nm, upon excitation at 280 nm. The intrinsic fluorescence of the two mutants is decreased with respect to that of wt sorcin, since most of the aromatic contribution at 280 nm is due to tryptophan residues (Figure 2C). The emission peak of the W99G mutant is blue shifted by 2 nm relative to that of wt sorcin, whereas the emission peak of W105G is red shifted by the same amount. Interestingly, in the 285−300 nm region, the spectra of the two variants are not additive, an indication that substitution of W99 or W105 influences the microenvironment of the other chromophores.

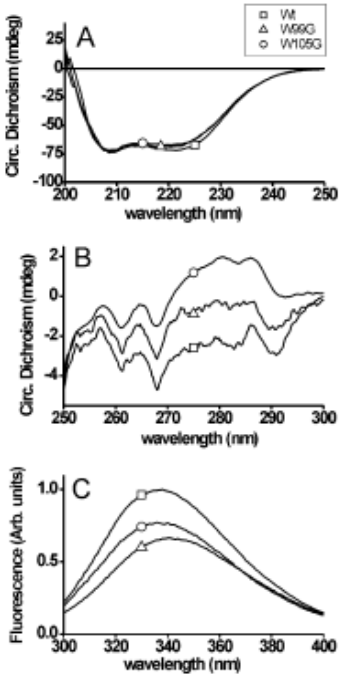

FIGURE 2: Spectroscopic characterization of wt sorcin and its W99G and W105G variants: wt (□), W99G (○), and W105G (△). (A) Far-UV CD spectra in 5 mM Tris-HCl (pH 7.5) at 20 °C with a protein concentration of 18 μM. (B) Near-UV CD spectra in 100 mM Tris-HCl (pH 7.5) and 2 mM EGTA at 20 °C with a protein concentration of 30 μM. (C) Fluorescence emission spectra in 100 mM Tris-HCl (pH 7.5) at 25 °C with a protein concentration of 4 μM, an excitation wavelength of 280 nm, and a slit width of 0.5 nm.

Sedimentation velocity experiments were used to assess the stoichiometry of Ca^{2+} binding. Solutions of 25 μM protein in Chelex-treated Tris-HCl buffer at pH 7.5 were titrated in the ultracentrifuge cell with up to 4 equiv of calcium/monomer. As for the wt protein (*16*), the $s_{20,w}$ value of W99G is always 3.2−3.3 S, although the absorbance at 280 nm decreases markedly when the level of calcium exceeds 2 equiv/monomer due to protein aggregation. W105G could not be analyzed since it precipitated out of solution even in the Chelex-treated buffer most likely due to the traces of metal leaking from the cell (Figure 3A).

The Ca^{2+} affinity of the sorcin variants was estimated by means of indirect fluorescence titration experiments in the presence of either Quin 2 or Fluo-3 as a Ca^{2+} chelator. The results obtained at pH 7.5 are presented in Figure 3B in terms of the degree of Quin 2 saturation as a function of total Ca^{2+} concentration. The data obtained with the mutants fall within the range of those measured in five different sets of experiments with wt sorcin. Accordingly, Ca^{2+} affinity is practically unaltered relative to that of wt sorcin and can be fitted with two Ca^{2+} binding constants in the micromolar

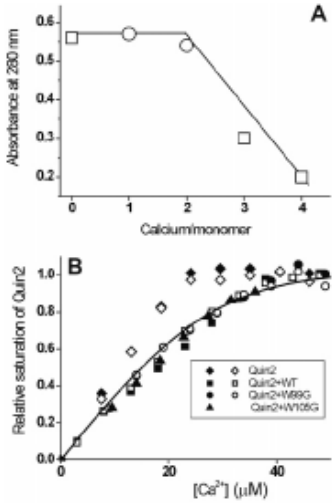

FIGURE 3: Calcium binding data. (A) Titration of W99G sorcin in the analytical ultracentrifuge. Different amounts of calcium were added just before the sedimentation velocity experiments to 15 μM protein in Chelex-treated 100 mM Tris-HCl buffer (pH 7.5). The absorbance in the plateau region is plotted as a function of the Ca^{2+}:monomer molar ratio. Different symbols refer to different experiments. (B) Fluorescence titration of wt sorcin and its W99G and W105G variants with Ca^{2+} in the presence of Quin 2. The relative saturation of Quin 2 is plotted as a function of total Ca^{2+} concentration. The wild type (□ and ■), W99G (○ and ●), and W105G (▲) sorcin at a concentration of 25 μM were titrated with Ca^{2+} in the presence of 25 μM Quin 2 in 100 mM Tris-HCl at pH 7.5 and 25 °C. Control titrations of Quin 2 alone with Ca^{2+} (◇ and ◆) are also shown.

range [$K_1 = (0.5 \pm 0.2) \times 10^{-6}$ M and $K_2 \sim 10^{-5}$ M] using a dissociation constant for the chelator of 60 nM (*25*). The K_1 value is better defined than K_2; the value of this latter binding constant is at the resolution limits of the technique under the conditions that were used. The Fluo-3 titration data are consistent with minor changes in Ca^{2+} affinity of the mutants with respect to wt sorcin (data not shown).

Interaction between the W99G and W105G Variants and Annexin VII. Overlay assay experiments were carried out first to establish whether W99G and W105G are able to recognize and interact with annexin VII. Previous data demonstrated that the sorcin−annexin VII interaction occurs via their respective N-terminal domains at micromolar Ca^{2+} concentrations (*15*, *31*). Western blot experiments indicate that binding of annexin VII to W99G is significant when the total Ca^{2+} concentration is 10 μM (Figure 4A), whereas comparable binding to W105G is observed when the cation concentration is increased to 75 μM (Figure 4B).

SPR was used to assess the effect of the mutations on the interaction between sorcin and annexin VII in a quantitative manner. At constant protein and Ca^{2+} concentrations, the steady-state signals (R_{eq}) obtained with wt sorcin and W99G are very similar and significantly higher than in the case of W105G (Figure 5A).

When the interaction is assessed as a function of Ca^{2+} concentration at a constant protein concentration, the R_{eq}

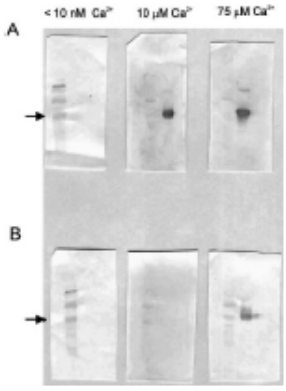

FIGURE 4: Interaction of the W99G and W105G sorcin variants with annexin VII. The variants were subjected to SDS−PAGE and transferred to PVDF membranes which were incubated with annexin VII in the presence of <10 nM, 10 μM, or 75 μM $CaCl_2$ (from left to right) and subsequently with anti-annexin monoclonal antibody. (A) W99G and (B) W105G: lane 1, molecular mass markers (46, 30, 21.5, 14.3, 6.5, and 3.4 kDa); and lane 2, sorcin variant. The arrows indicate the band corresponding to sorcin (M_r = 21.5 kDa). For buffer conditions, see Materials and Methods.

values show the expected increase with an increase in Ca^{2+} concentration (Figure 5B). The W99G variant behaves like wt sorcin at < 40 μM Ca^{2+} but yields lower R_{eq} values at higher cation concentrations, while W105G gives rise to significantly lower sensorgrams with respect to wt sorcin at all Ca^{2+} concentrations that were investigated. At 50 μM Ca^{2+}, for example, the R_{eq} values are 385 for wt sorcin, 287 for W99G, and 79 for W105G. It follows that the affinity for the annexin N-terminus decreases in the following order: wt sorcin ≥ W99G > W105G. A further series of experiments was carried out as a function of protein concentration at a constant Ca^{2+} concentration of 20 μM (Figure 5C). This type of experiment enables one to assess the apparent dissociation constant, K_D, for each protein by Scatchard analysis of the ratio R_{eq}/C versus R_{eq} (*32*). The analysis yields apparent K_D values (at 20 μM Ca^{2+}) of 1.9 μM for wt sorcin, 2.0 μM for W99G, and 12.6 μM for W105G. In this calculation, the intercept on the abscissa was considered to be the same for the three proteins since the limited number of data and the low R_{eq} values at 20 μM Ca^{2+} pertaining to the W105G mutant do not warrant a precise R_{max} determination. If one assumes that the sorcin dimer contains a single effective annexin VII binding site as suggested by Brownawell and Creutz (*31*), the analysis yields K_D values of 0.95 μM for wt sorcin, 1.0 μM for W99G, and 6.3 μM for W105G.

Effect of the W99G and W105G Variants on the Activity of the Ryanodine Receptor. The protocol used to introduce recombinant protein into permeabilized myocytes is shown in Figure 6A. After being exposed to β-escin for 30 s, the myocyte was superfused with mock intracellular solution for 30 s before superfusing with 3 μM sorcin (or sorcin variants) for 2 min to ensure that the complete bath volume (200 μL) was exchanged with the protein-containing solution. Superfusion was stopped, and sparks were monitored in the

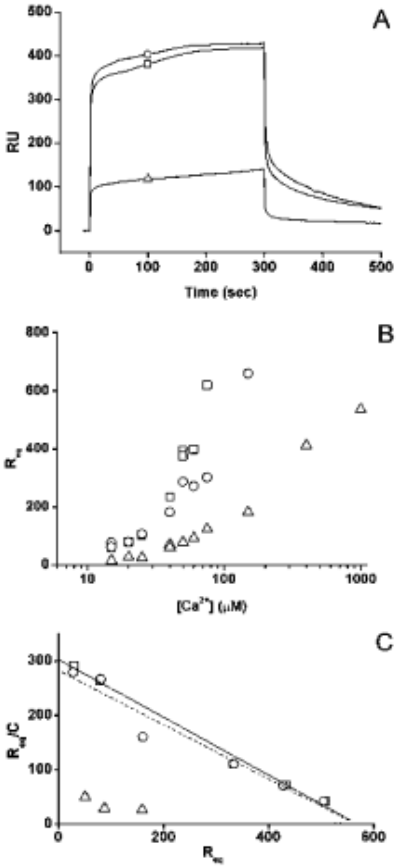

FIGURE 5: Binding of wt sorcin and its W99G and W105G variants to the immobilized N-terminal peptide of annexin VII at different Ca^{2+} concentrations: wt (□), W99G (○), and W105G (△). (A) Sensorgrams of 6 μM sorcin injected at time zero onto a chip containing the immobilized N-terminal annexin VII peptide. The increase in RU relative to baseline indicates complex formation; the plateau region represents the steady-state phase of the interaction, whereas the decrease in RU represents sorcin dissociation from the immobilized peptide after injection of buffer [10 mM HEPES, 0.15 M NaCl, 20 μM $CaCl_2$, and 0.005% surfactant P-20 (pH 7.4)]. The temperature was 25 °C. (B) The plateau signal at steady state (R_{eq}) is plotted as a function of total Ca^{2+} concentration. The sorcin concentration was 1 μM in 10 mM HEPES, 0.15 M NaCl, and 0.005% surfactant P-20 (pH 7.4). The temperature was 25 °C. (C) The plateau signal at steady state (R_{eq}) measured at different sorcin concentrations (C) is plotted as a function of R_{eq}/C. The buffer contained 10 mM HEPES, 0.15 M NaCl, 20 μM $CaCl_2$, and 0.005% surfactant P-20 (pH 7.4).

absence of flow for 10−12 min. Sample line-scan records are shown in Figure 6B showing the transient increases in intracellular Ca^{2+} concentration characteristic of Ca^{2+} sparks. Under control conditions, spark frequency progressively decreased by 20−25% over 10−12 min. As shown in Figure

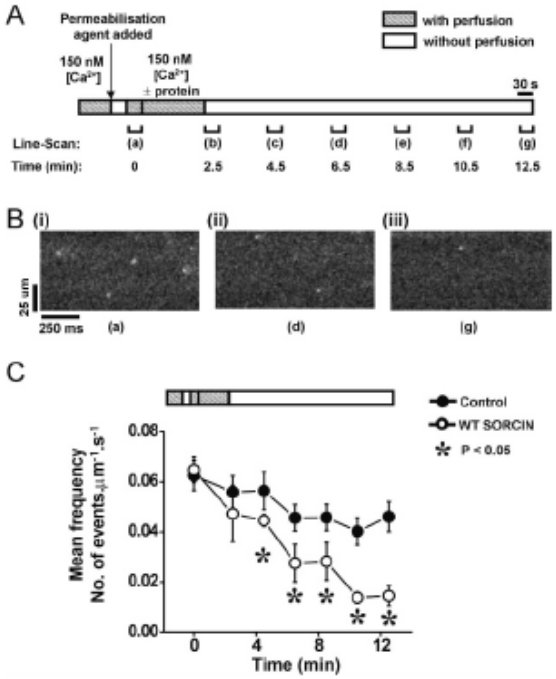

FIGURE 6: Ca^{2+} spark protocol. (A) Experimental protocol used to introduce recombinant protein into permeabilized myocytes. (B) Sample line scans 0 (a), 6 (d), and 12 min (g) after permeabilization. (C) Mean spark frequency at various times after permeabilization. Note the slow decline in spark frequency with time under control conditions. The inclusion of sorcin (3 μM) in the initial perfusing solution caused a profound decrease in frequency. Steady-state values were measured after incubation for 10−12 min with the recombinant protein.

6C, the inclusion of 3 μM sorcin in the perfusion solution caused a more marked decrease in spark frequency, reaching a steady state after 8−10 min. The difference caused by the presence of sorcin is likely to reflect the time course of entry of sorcin into the permeabilized cell. The effects of sorcin, W99G, W105G, E124A, and SCBD were studied by measuring the spark characteristics after incubation for 10 min with the protein. This activity was compared with that observed after incubation for the same time with a solution of the identical composition without the protein.

The inhibitory effect of sorcin on RyR2 activity manifests itself in the significant reduction of the mean values of Ca^{2+} spark frequency, spark width, spark peak, and spark duration compared to the control spark parameters (Figure 7A). The two tryptophan mutants have contrasting effects. W99G affects the Ca^{2+} spark parameters in a manner similar to that of the native protein (Figure 7B). In contrast, in the presence of W105G, the parameters of the Ca^{2+} sparks are close to those of the control cardiomyocytes (Figure 7C).

SCBD was used to test the possible effects of the sorcin N-terminal domain on formation of the RyR2−sorcin complex. SCBD decreases the mean values of the Ca^{2+} spark frequency and width in a manner similar to that of the full-length wt protein, while the mean duration and amplitude are not altered significantly with respect to the control cardiomyocytes (Figure 7D). The E124A mutant is unable to bind Ca^{2+} at physiological concentrations (*6*); perfusion with this mutant yields Ca^{2+} spark values very similar to those obtained under control conditions (Figure 7E).

DISCUSSION

These data provide experimental support to the model of sorcin activation that assigns a major role to the D helix which connects the two physiologically relevant sites, EF2 and EF3, and contains the only two tryptophan residues of the polypeptide chain, W99 and W105. The different location of the tryptophan residues along the D helix (W99 is ~4 Å from EF2 and W105 is ~7 Å from EF3) renders the W105G and W99G variants as selective probes of the Ca^{2+}-induced structural changes and of their functional effects. Their study therefore extends the information furnished by the mutants of the EF1, EF2, and EF3 hands studied by Mella et al. (*6*) which monitor the effect of abolishing binding of calcium to the respective EF-hand motifs.

The proposed model of sorcin activation explains an apparent paradox common to all PEF proteins: the large Ca^{2+}-dependent change in hydrophobicity would predict large conformational differences, yet only small Ca^{2+}-linked structural rearrangements limited to the EF1 region are

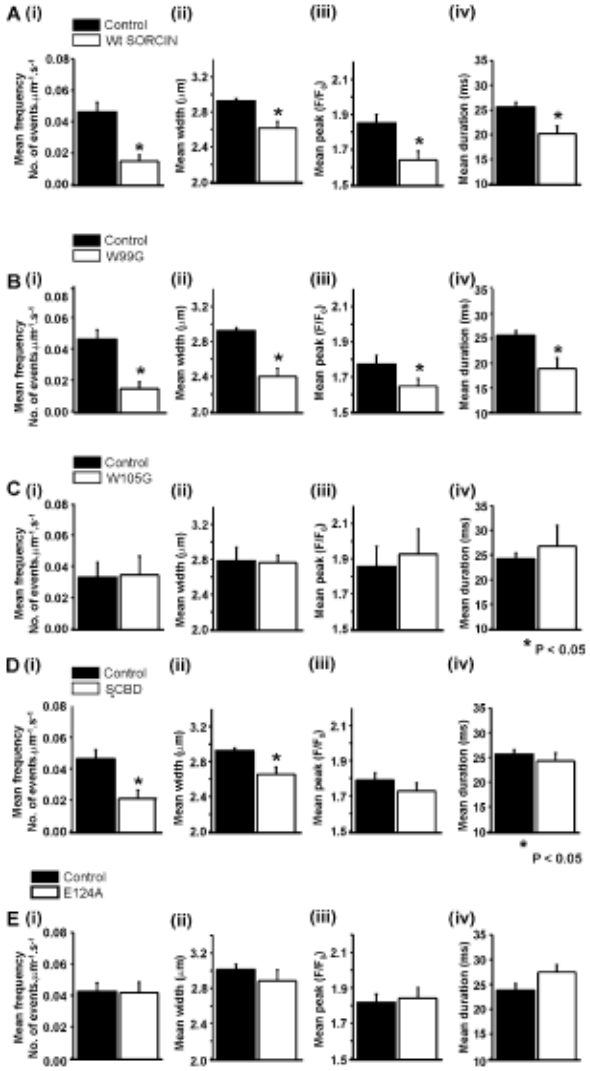

FIGURE 7: Effect of wt sorcin, of the W99G, W105G, and E124A variants, and of SCBD on Ca^{2+} spark properties. Mean values ± the standard error of the mean for (i) spark frequency, (ii) spark width (full width at half-maximum), (iii) peak F/F_0, and (iv) spark duration (full width at half-maximum). (A) Control group, $n = 4$ cells, 636 events; sorcin, $n = 4$ cells, 176 events. (B) Control group, $n = 5$ cells, 795 events; W99G group, $n = 5$ cells, 200 events. (C) Control group, $n = 4$ cells, 630 events; W105G group, $n = 4$ cells, 592 events. (D) Control group, $n = 4$ cells, 662 events; SCBD, $n = 5$ cells, 425 events. (E) Control group, $n = 7$ cells, 814 events; E124A group, $n = 7$ cells, 739 events. Asterisks indicate $P < 0.05$.

observed (*1*, *9*, *11*−*13*). On the basis of the crystal structure of SCBD, Ilari et al. (*7*) proposed that in Ca^{2+}-free sorcin the N- and C-terminal domains establish a large number of hydrophobic and hydrophilic interactions centered on the D helix. Both tryptophan residues are part of this interaction network which comprises the loop between EF1 and EF2 (Tyr67 aromatic ring) and reaches the Ca^{2+}-binding loop of EF3 where Asp113 in position X is hydrogen bonded to the Tyr67 OH group. Importantly, W99 and W105 together with other highly conserved D helix residues (Phe95, Leu98, and Phe109) give rise to a rather extended hydrophobic patch. However, whereas the W99 side chain lies on the outer surface of SCBD and establishes few van der Waals contacts with the very first residues of the domain, the W105 side

chain faces the SCBD core and establishes a large number of intradomain interactions with other residues of the D helix (Val101, Leu102, His108, and Phe109), of the EF loop (Met132 and Phe134), and of the long G helix (Tyr159, Ile160, Cys163, Val164, and Arg167).

In the SCBD model of the apoprotein which contains solely an 11-residue stretch of the N-terminus (*7*), W105 but not W99 is part of the SCBD region in contact with the N-terminal domain. The interdomain contact region comprises Val101, Leu102, Gly104, Trp105, and His108 in the D helix, Arg174 in the G helix, Met132, Gly133, Phe134, and Arg135 in the EF loop, and Gly182 in the GH loop and, therefore, many of the residues just mentioned. The possibility that W99 may be part of this contact region in the full-length protein where the N-terminal domain is 32 amino acids long cannot be excluded.

Ilari et al. (*7*) proposed that calcium binding loosens the network of interdomain interactions, rendering both domains available for target protein recognition. It follows that all the D helix residues which contact the N-terminal domain in the apoprotein may participate in the interaction with molecular targets in Ca^{2+}-bound sorcin. In principle, such interaction can be very diversified as it will depend on the specific position of a given residue in the contact region. On this basis, removal of W99, which is located near EF2 on the outer surface of SCBD and is only marginally involved in interdomain interactions, is expected to have functional ramifications very different from those of removal of W105 which faces the SCBD core near the highest-Ca^{2+} affinity EF3 site.

Ca^{2+} Binding and Association with Annexin VII. The site-specific mutations that are introduced do not alter the overall structure of wt sorcin significantly as shown by the sedimentation velocity data and far-UV CD spectra (Figure 2A), although local structural perturbations are apparent in the fluorescence emission (Figure 2C) and near-UV CD spectra (Figure 2B). However, in the absence of structural data in the crystalline state, these spectroscopic methods do not permit extrapolation to specific structural and functional features (*33*). For example, the near-UV CD spectrum of W99G resembles that of Ca^{2+}-bound wt sorcin and that of W105G resembles that of the Ca^{2+}-free form, yet both mutants require Ca^{2+} for interaction with annexin VII (Figure 5B). The absence of the negative tryptophan peak at 292 nm in the CD spectrum of W99G sorcin and its reduction in the W105G variant, just like the differences in the fine structure of the whole spectrum, point to the occurrence of specific local perturbations in the environment of aromatic residues attendant the mutations introduced. In particular, in the W99G variant, Trp105 could be more exposed to solvent than in apo-wt sorcin as is the case of the Ca^{2+}-ligated wt protein. A similar albeit smaller decrease in the tryptophan band at 292 nm was observed in the E124A variant, where the hydrogen bonding interactions established by Asp113 and Glu124 of the EF3 Ca^{2+} binding loop are lost (*6*). This similarity is indicative of similar structural rearrangements and likely is functionally relevant.

The measurements of the Ca^{2+} binding parameters are confined to a limited set of experimental conditions given the strong tendency of the Ca^{2+}-bound form of wt sorcin and in particular of W105G to aggregate and/or precipitate in the absence of protein targets. As a consequence, determination of the weaker Ca^{2+} binding constant will be particularly affected. Within these limitations, neither mutation appears to affect Ca^{2+} binding significantly (Figure 3). Thus, calcium titrations carried out in the ultracentrifugation show that the W99G variant binds two Ca^{2+} ions per monomer with an affinity similar to that of wt sorcin (*16*). The titration data obtained for the two variants in the presence of Quin 2 as the reporter dye likewise do not provide evidence for significant changes in Ca^{2+} affinity with respect to wt sorcin. The use of Fluo-3 did not improve accuracy (data not shown).

The Ca^{2+} sensitivity of annexin VII binding is unaltered by the W99G mutation but is decreased significantly (≈7 times) by the W105G mutation. In the framework of a linkage scheme, any change in the Ca^{2+} sensitivity of annexin VII binding can be attributed to a change in either calcium or target binding or both steps. In the W105G variant, since Ca^{2+} affinity is essentially unchanged relative to that of wt sorcin (Figure 3B), it is primarily the interaction with the target that is affected by the mutation. The factors that come into play are (i) impairment of information transfer via the D helix and (ii) alterations in the recognition surfaces required for sorcin N-terminal domain interaction. The latter option is unlikely since the local structural changes induced by Ca^{2+} binding and propagated via the D helix will affect mainly the relative orientation of the C- and N-terminal domains (*7*) and will only weakly alter the structure of the N-terminal domain itself.

Ca^{2+} Spark Activity. The plot of Ca^{2+} spark frequency shown in Figure 6 indicates a small but significant reduction in spark frequency over 10−12 min. The cause of these changes is unknown but may reflect the balance of several factors, including (i) a change in the Ca^{2+} content of the SR immediately after permeabilization and (ii) minor changes in concentration of low-molecular weight modulators of RyR2 activity, e.g., ATP, Mg^{2+}, H^+. The reduced frequency, amplitude, duration, and width of the Ca^{2+} spark by wt sorcin (Figure 7A) are consistent with previous reports on heart cells (*18*, *19*, *34*). Measurements on isolated RyR2 channels indicate that sorcin reduces the open time of the channel but does not affect single-channel conductance (*18*). A reduced open time would reduce the duration of the Ca^{2+} spark and therefore the amplitude and width. The effect on Ca^{2+} spark frequency may be linked to the reduced open probability of the channel at a set intracellular Ca^{2+} concentration (*18*). As with the previous work, the additional Ca^{2+} buffering attributable to sorcin is unlikely to be a complicating factor. The background Ca^{2+} buffers both in the perfusing solution and intrinsic to the permeabilized cell are present at >10 times the concentration of exogenous sorcin.

The effects of sorcin on Ca^{2+} sparks are evident at 155−165 nM Ca^{2+}, where the EF3 site is only 15% saturated. Considering local versus bulk concentration during a Ca^{2+} spark easily accounts for this apparent contradiction (*34*). Thus, within limited regions of the cytosol close to the Ca^{2+} entry and release sites, the cation concentration may rise to >10 μM and hence be sufficient to trigger the sorcin conformational changes.

The tryptophan variants have strikingly different effects on Ca^{2+} spark activity. The effects of W99G are similar in all respects to those of the wt protein and suggest that despite

the local structural changes indicated above, Ca^{2+} binding, information transfer through the D helix, and RyR2 recognition occur normally. In contrast to W99G, the W105G mutant has no significant effects on any of the Ca^{2+} spark parameters, indicating that this mutation dramatically alters either information transfer or the interaction surface with RyR2, since it does not impair Ca^{2+} binding. The ability of W105G to bind annexin VII, albeit with a lower Ca^{2+} sensitivity (Figure 5C), indicates that information about the Ca^{2+} binding event does reach the N-terminal domain and suggests that the mutation of this tryptophan affects mainly the RyR2 recognition surface. One additional explanation for differential effects of the W105G variant compared to the wt sorcin or to the W99G mutant is that the W105G variant may be phosphorylated by protein kinase A more readily than the other two proteins (*18*). The SCBD fragment, which cannot bind annexin VII, is able to interact successfully with RyR from skeletal muscle based on previous biochemical data (*16*) and on the significant reduction in Ca^{2+} spark frequency and width (Figure 7D). Interestingly, SCBD appears not to significantly affect Ca^{2+} spark peak and duration. Over the complete range of Ca^{2+} spark parameters, there is the overall impression of a weaker effect of SCBD on RyR2 activity. This may reflect a minor involvement of the N-terminal domain in the association process or simply the fact that the interaction surface is altered slightly by removal of the N-terminal domain. The E124A mutation, which disrupts coordination of Ca^{2+} at the EF3 site, ablates the ability of the variant both to bind annexin VII (*6*) and to reduce RyR2 activity (Figure 7E). This confirms that binding of Ca^{2+} to sorcin (EF3 site) is an absolute requirement for interaction with target proteins (*6*).

In conclusion, these data provide experimental support to the proposal that the interaction network around the D helix is central to the Ca^{2+}-induced activation mechanism of sorcin. The D helix acts as an amplifier of the conformational changes that take place at the EF3 loop upon Ca^{2+} binding by triggering a larger overall change that enables sorcin to interact with its target proteins. In view of the D helix conservation, it is likely that the same activation mechanism applies to all PEF proteins. Additionally, this study brings out the crucial role of Trp105 and not Trp99 in allowing sorcin to interact with RyR2. Extension of this approach to other protein targets, e.g., α_1 subunit of the L-type Ca^{2+} channel (*35*) and the cardiac Na^+/Ca^{2+} exchanger, will clarify whether this approach can be generalized to mapping the topology of the interaction of sorcin with its targets.

ACKNOWLEDGMENT

We thank Dr. Bruno Catacchio for carrying out the analytical ultracentrifuge experiments. The technical assistance of Aileen Rankin and Anne Ward is gratefully acknowledged.

REFERENCES

1. Blanchard, H., Grochulski, P., Li, Y., Arthur, S. C., Davies, P. L., Elce, J. S., and Cygler, M. (1997) Structure of a calpain Ca^{2+}-binding domain reveals a novel EF-hand and Ca^{2+}-induced conformational changes, *Nat. Struct. Biol. 4*, 532−538.
2. Lin, G. D., Chattopadhyay, D., Maki, M., Wang, K. K., Carson, M., Jin, L., Yuen, P. W., Takano, E., Hatanaka, M., DeLucas, L. J., and Narayana, S. V. (1997) Crystal structure of calcium bound domain VI of calpain at 1.9 Å resolution and its role in enzyme assembly, regulation, and inhibitor binding, *Nat. Struct. Biol. 4*, 539−547.
3. Lollike, K., Johnsen, A. H., Durussel, I., Borregaard, N., and Cox, A. (2001) Biochemical characterization of the penta-EF-hand protein grancalcin and identification of L-plastin as a binding partner, *J. Biol. Chem. 276*, 17762−17769.
4. Lo, K. W.-H., Zhang, Q., Li, M., and Zhang, M. (1999) Apoptosis-linked gene product ALG-2 is a new member of the calpain small subunit subfamily of Ca^{2+}-binding proteins, *Biochemistry 38*, 7498−7508.
5. Kitaura, Y., Matsumoto, S., Satoh, H., Hitomi, K., and Maki, M. (2001) Peflin and ALG-2, members of the penta-EF-hand protein family, form a heterodimer that dissociates in a Ca^{2+}-dependent manner, *J. Biol. Chem. 276*, 14053−14058.
6. Mella, M., Colotti, G., Zamparelli, C., Verzili, D., Ilari, A., and Chiancone, E. (2003) Information transfer in the penta-EF-hand protein sorcin does not operate via the canonical structural/functional pairing. A study with site-specific mutants, *J. Biol. Chem. 278*, 24921−24928.
7. Ilari, A., Johnson, K. A., Nastopoulos, V., Verzili, D., Zamparelli, C., Colotti, G., Tsernoglou, D., and Chiancone, E. (2002) The crystal structure of the sorcin calcium binding domain provides a model of Ca^{2+}-dependent processes in the full-length protein, *J. Mol. Biol. 317*, 447−458.
8. Xie, X., Dwyer, M. D., Swenson, L., Parker, M. H., and Botfield, M. C. (2001) Crystal structure of calcium-free human sorcin: A member of the penta-EF-hand protein family, *Protein Sci. 10*, 2419−2425.
9. Jia, J., Han, Q., Borregaard, N., Lollike, K., and Cygler, M. (2000) Crystal structure of human grancalcin, a member of the penta-EF-hand protein family, *J. Mol. Biol. 300*, 1271−1281.
10. Jia, J., Tarabykina, S., Hansen, C., Berchtold, M., and Cygler, M. (2001) Structure of apoptosis-linked protein ALG-2: Insights into Ca^{2+}-induced changes in penta-EF-hands proteins, *Structure 4*, 267−275.
11. Jia, J., Borregaard, N., Lollike, K., and Cygler, M. (2001) Structure of Ca^{2+}-loaded human grancalcin, *Acta Crystallogr. D57*, 1843−1849.
12. Strobl, S., Fernandez-Catalan, C., Braun, M., Huber, R., Masumoto, H., Nakagawa, K., Irie, A., Sorimachi, H., Bourenkow, G., Bartunik, H., Suzuki, K., and Bode, W. (2000) The crystal structure of calcium-free human m-calpain suggests an electrostatic switch mechanism for activation by calcium, *Proc. Natl. Acad. Sci. U.S.A. 97*, 588−592.
13. Hosfield, C. M., Elce, J. S., Davies, L., and Jia, Z. (1999) Crystal structure of calpain reveals the structural basis for Ca^{2+}-dependent protease activity and a novel mode of enzyme activation, *EMBO J. 18*, 6880−6889.
14. Meyers, M. B., Pickel, v. M., Shen, S.-S., Sharma, V. K., Scotto, K. W., and Fishman, G. I. (1995) Association of sorcin with the cardiac ryanodine receptor, *J. Biol. Chem. 270*, 26411−26418.
15. Verzili, D., Zamparelli, C., Mattei, B., Noegel, A. A., and Chiancone, E. (2000) The sorcin-annexin VII calcium-dependent interaction requires the sorcin N-terminal domain, *FEBS Lett. 471*, 197−200.
16. Zamparelli, C., Ilari, A., Verzili, D., Giangiacomo, L., Colotti, G., Pascarella, S., and Chiancone, E. (2000) Structure−function relationships in sorcin, a member of the penta EF-hand family. Interaction of sorcin fragments with the ryanodine receptor and an *Escherichia coli* model system, *Biochemistry 39*, 658−666.
17. Cheng, H., Lederer, W. J., and Cannel, M. B. (1993) Calcium sparks: Elementary events underlying excitation-contraction coupling in heart muscle, *Science 262*, 740−744.
18. Lokuta, C. J., Meyers, M. B., Sander, P. R., Fishman, G. I., and Valdivia, H. H. (1997) Modulation of cardiac ryanodine receptors by sorcin, *J. Biol. Chem. 272*, 25333−25338.
19. Seidler, T., Miller, S. L. W., Loughrey, C. M., Kania, A., Burow, A., Kettlewell, S., Teucher, N., Wagner, S., Kogler, H., Meyers, M. B., Hasenfuss, G., and Smith, G. L. (2003) Effects of adenovirus-mediated sorcin overexpression on excitation-contraction coupling in isolated rabbit cardiomyocytes, *Circ. Res. 93*, 132−139.
20. Maki, M., Kitaura, Y., Satoh, H., Ohkouchi, S., and Shibata, H. (2002) Structures, functions and molecular evolution of the penta-EF-hand Ca^{2+}-binding proteins, *Biochim. Biophys. Acta 1600*, 51−60.
21. Higuchi, R., Krummel, B., and Saiki, R. K. (1988) A general method of in vitro preparation and specific mutagenesis of DNA

fragments: Study of protein and DNA interactions, *Nucleic Acid Res. 16*, 7351−7367.
22. Meyers, M. B., Zamparelli, C., Verzili, D., Dicker, A. P., Blanck, T. J. J., and Chiancone, E. (1995) Calcium-dependent translocation of sorcin to membranes: Functional relevance in contractile tissue, *FEBS Lett. 357*, 230−234.
23. Edelhoch, H. (1967) Spectroscopic determination of tryptophan and tyrosine in proteins, *Biochemistry 6*, 1948−1954.
24. Chou, P. Y., and Fasman, G. D. (1974) Prediction of protein conformation, *Biochemistry 13*, 222−224.
25. Tsien, R., and Pozzan, T. (1989) Measurement of cytosolic free Ca^{2+} with Quin 2, *Methods Enzymol. 172*, 230−262.
26. Zamparelli, C., Ilari, A., Verzili, D., Vecchini, P., and Chiancone, E. (1997) Calcium- and pH-linked oligomerization of sorcin causing translocation from cytosol to membranes, *FEBS Lett. 409*, 1−6.
27. André, I., and Linse, S. (2002) Measurement of Ca^{2+}-binding constants of proteins and presentation of the CaLigator software, *Anal. Biochem. 305*, 195−205.
28. Laemmli, U. K. (1970) Cleavage of structural proteins during the assembly of the head of the bacteriophage T4, *Nature 227*, 680−685.
29. Bjellqvist, B., Hughes, G. J., Pasquali, Ch., Paquet, N., Ravier, F., Sanchez, J. C., Frutiger, S., and Hochstrasser, D. F. (1993) The focusing positions of polypeptides in immobilized pH gradients can be predicted from their amino acid sequences, *Electrophoresis 14*, 1023−1031.
30. *BIAtechnology Handbook*, version AB (1994) pp 4−5, Biacore AB, Uppsala, Sweden.
31. Brownawell, A. M., and Creutz, C. E. (1997) Calcium-dependent binding of sorcin to the N-terminal domain of synexin (annexin VII), *J. Biol. Chem. 272*, 22182−22190.
32. Schuck, P. (1997) Use of surface plasmon resonance to probe the equilibrium and dynamic aspects of interactions between biological macromolecules, *Annu. Rev. Biophys. Biomol. Struct. 26*, 541−566.
33. Strickland, E. H. (1974) Aromatic contributions to circular dichroism spectra of proteins, *CRC Crit. Rev. Biochem.*, 113−175.
34. Farrell, E. F., Antaramian, A., Rueda, A., Gomez, A. M., and Valdivia, H. H. (2003) Sorcin inhibits calcium release and modulates excitation-contraction coupling in the heart, *J. Biol. Chem. 278*, 34660−34666.
35. Meyers, M. B., Puri, T. S., Chien, A. J., Gao, T., Hsu, P.-H., Hosey, M. M., and Fishman, G. I. (1998) Sorcin associates with the pore-forming subunit of voltage-dependent L-type Ca^{2+} channels, *J. Biol. Chem. 273*, 18930−18935.
36. DeLano, W. L. (2002) *The PyMOL User's Manual*, DeLano Scientific, San Carlos, CA.

BI060416A